European Commission

JRC SCIENCE FOR POLICY REPORT

Assessment and analysis of the electromagnetic profile of prototype high-power-charging units for electric vehicles

Contribution to IEC 61851-21-2: Radiated and conducted emissions, radiated immunity and exploratory research

Pliakostathis K., Zanni M., Scholz H., Trentadue G.

2019

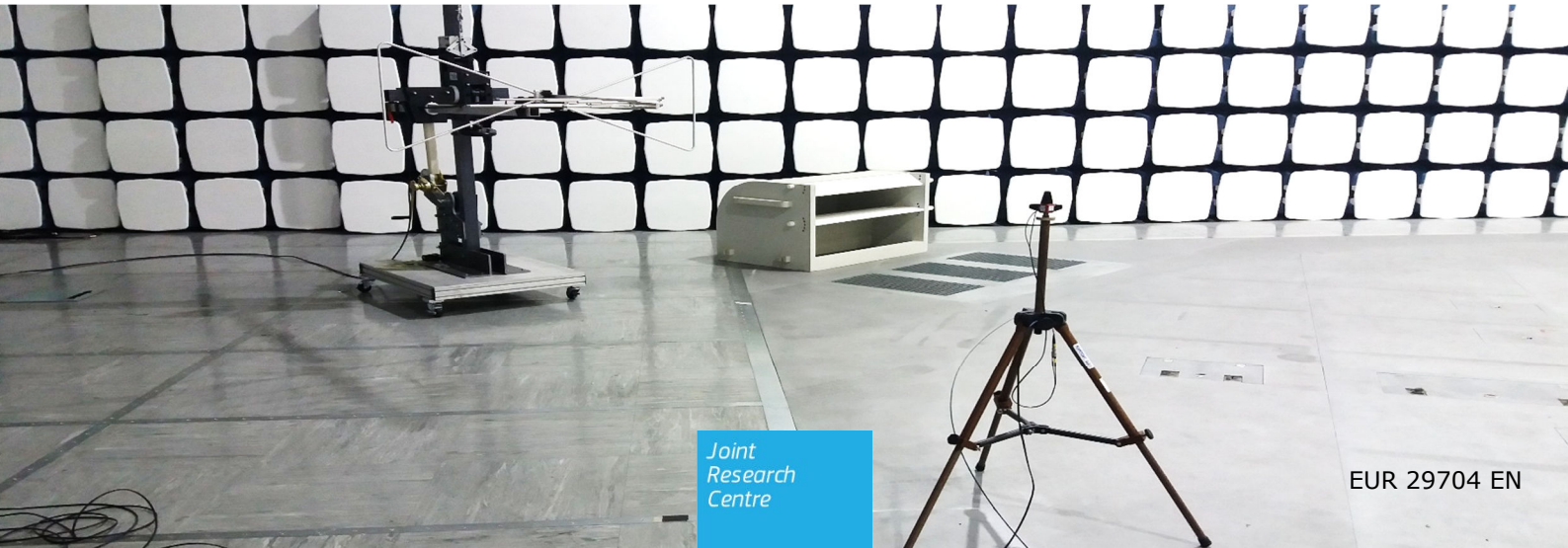

Joint Research Centre

EUR 29704 EN

EU Science Hub
https://ec.europa.eu/jrc

JRC114312

EUR 29704 EN

PDF	ISBN 978-92-76-01440-9	ISSN 1831-9424	doi:10.2760/08750
Print	ISBN 978-92-76-01441-6	ISSN 1018-5593	doi:10.2760/190062

Luxembourg: Publications Office of the European Union, 2019

How to cite this report: Pliakostathis K., Zanni M., Scholz H., Trentadue G., *Assessment and analysis of the electromagnetic profile of prototype high-power-charging units for electric vehicles: Contribution to IEC 61851-21-2: Radiated and conducted emissions, radiated immunity and exploratory research*, EUR 29704 EN, Publications Office of the European Union, Luxembourg, 2019, ISBN 978-92-76-01440-9, doi:10.2760/08750, JRC114312.

Contents

Abstract

This science for policy report discusses and analyses the electromagnetic compatibility (EMC) performance of three High-Power-Charging (HPC) columns at their standby based on IEC 61851-21-2 standard. All laboratory setups and results of the tests that are presented on this work were carried out inside V*e*LA 9 validated EMC semi-anechoic chamber (SAC) at the Joint Research Centre of the European Commission. The results of more than 150 different measured setups on radiated emissions, conducted emissions and radiated immunity are presented and discussed thoroughly. The applicable test methodologies and instrumentation used for the measurements are fully described. EMC troubleshooting techniques were also successfully carried out for some setups, while novel exploratory work, beyond IEC 61851-21-2 was also conducted. The findings and test data on this study can be a reference material to EMC engineers and contribute to the future policy making of the relevant EMC standards.

Acknowledgements

The authors are grateful to Alois Krasenbrink (JRC, C.4) and Giorgio Martini (JRC, C.4) for their support on this scientific activity, and the members of the European Microwave Signature Laboratory (EMSL, JRC) for kindly providing measurement equipment used for some parts of the laboratory tests.

Authors

Konstantinos Pliakostathis, Joint Research Centre

Marco Zanni, Joint Research Centre

Harald Scholz, Joint Research Centre

Germana Trentadue, Joint Research Centre

1 Introduction

The ever rising demand to decarbonise and electrify at global level the transport network has generated significant investments into the research and development of the underlying infrastructure. The technology that surrounds electric vehicles has reached an unprecedented level of complexity. This is due to the constant need to reach longer driving ranges, reduce battery charging times, cut down battery weight, attain improved energy efficiency through more intelligent power management systems, lower production cost and market prices, increase passenger safety and security and so on.

The success on this direction though is strongly influenced by the technological advancements of the charging infrastructure too: Manufacturers have now already developed charging systems that have demonstrated a charging power of up to 350kW, promising full battery charging within about 20 minutes to cover 400km driving range. This convenience, however, has introduced a challenge on the product design process: The EMC compliance requirement applied on these systems is challenged by the high levels of currents/voltages generated and by the fast-speed electronic circuits, which rely on pulse-type signals for their operation [1].

All these new technologies, due to the dense harmonic frequency content that they contain, have the potential to generate unwanted electromagnetic interference (EMI) [2]. This is of particular concern, especially as the number of such products, based on these new technologies, are continuously spreading across the market and interact between them in numerous ways.

The fact that high power electronics can introduce EMI issues at component or system level is not new. There are scientific reports on the literature that have identified, for example, that AC to DC converters, power inverters, high-speed microprocessors and so on can generate both conducted and radiated EMI [3-6]. Therefore, a proper EMC methodology is more than critical, especially when it comes down to the design and implementation of HPCs as they contain several of such electrical and electronic units.

1.1 Background

EMC ensures that electrical and electronic products do not generate excessive interference to the environment and at the same time it provides them a layer of extra protection against a potential dysfunction by the exposure to radiation i.e. ability of a device to retain its normal operation under the presence of external interference [7].

The environment is surrounded by a plethora of electromagnetic sources and noise. These are established due to natural phenomena, e.g. lighting discharge, however man-made technology is the major contributor to the disturbances created in the EM spectrum [8]. Broadcast transmitters for TV and radio services, mobile-phone tower systems, wireless computing (WiFi, Bluetooth, etc.), wireless equipment used by public safety organisations (police, ambulances, fire-brigade, etc.), aviation systems (aircrafts, airport radars etc.), wireless residential equipment (car alarms, wireless security cameras, etc.) and so on rely on the generation and reception of electromagnetic radiation for their functionality.

At the same time, many different type of systems and devices need to co-exist on the same environment, e.g. mobile phones next to Wi-Fi routers at workplaces, which means that each one of them needs to be designed in such a way so as to retain its normal operation under the presence of potential EMI caused by another product.

The widespread usage of wireless devices, the incorporation of fast speed digital signals into the systems, the utilisation of extremely low-voltage signals, the mixture of high-power electrical systems close to miniaturised integrated electronic components have established EMI as a very big concern during the design phase of a product.

Uncontrolled levels of EMI can force a system to fall into an error state with all the consequences arising from such a situation. EMI can be radiative, i.e. propagate into the open space or conduct through a medium, e.g. cable, or it can be coupled from one point to another through inductive or capacitive coupling, giving rise to all sort of problems, e.g. cross-coupling between adjacent wires, which manage different signals [1].

EMC test laboratories assess and validate a product for its radiative and susceptibility performance in order to ensure that it functions as expected and within the limits specified by the relevant national and international standards and regulations. On the radiated emissions testing, the product is checked against the level of the EM emissions that it generates across a given frequency band. These emissions are measured with an antenna at different polarisations, which receives the disturbances generated by the test product and it sends them to a spectrum analyser or a scanning receiver to assess their intensity against the limit across the frequency spectrum.

On the conducted emissions, the product is checked for the RF voltage noise that it generates on a conductive medium, e.g. a power-line cable used for the power supply or a multi-wire connector used for the communication signals. On this setup, a receiver is measuring the level of the RF voltages that are present on the conductors. This type of noise can be generated, for example, by the rectification stage of an AC to DC power supply system, which can then travel and affect other devices through the cabling system [1].

Immunity testing involves the exposure of the test equipment to strong radiated electric fields or to RF currents injected into the conductors connected to it. The applicable standard defines the performance criteria that the equipment meets in order to judge its level of functionality e.g. [16]. The equipment (i) remains fully functional, (ii) degrades in performance, but resumes its operation upon removal of the injected field, or (iii) requires external intervention (e.g. restarting) to restore its original condition.

All the aforementioned facts, make EMC important and an indispensable process during product development as it can affect the reliability, safety and functionality any electrical, electronic and mechanical unit, which are critical factors especially around the development of high power charging systems for vehicles.

1.2 Scope

The scope of this report is to present and discuss the EMC fingerprint of prototype HPC columns used for DC fast charging of vehicles. Specifically, the EMC performance of HPC columns on the radiated emissions, conducted emissions and radiated immunity aspect at standby is analysed. Three HPCs from established manufacturers were fully tested for this purpose. The laboratory activity focused on the impact, from the EMC perspective, that the charging columns alone had during 230VAC standby. Currently, the applicable EMC standard that regulates the charging columns is IEC 61851-21-2 [9].

A complete HPC system includes additionally a step-up power transformer (for some models) and the AC-DC rectifier sections. One (out of four delivered) HPC column required a high-voltage DC power supply from the rectifier units that was not available in the laboratory and for this reason this column was not considered during the measurement procedure. EMC results of the complete HPC systems inside VeLA 9 will be presented in the future on a separate report.

The report starts with an outline of the IEC 61851-21-2 standard, applicable to off-board charging devices for vehicles, including the definition of the maximum allowed limits set within it. This is followed by a detailed description of the laboratory setup and instruments used during the measurements. Later, the results of the radiated emissions, conducted emissions and radiated immunity of all three columns from 150 kHz to 6 GHz are presented to full extend and key findings are extracted. Then, representative EMC troubleshooting techniques are discussed for some setups and HPC configurations. The report continues with a brief discussion on measurement considerations next to a dedicated section on exploratory test methods beyond IEC 61851-21-2. At the end, conclusions on this scientific activity and suggestions for further work are quoted.

2 EMC requirements, regulation and laboratory test methods

Figure 1 shows the VeLA 9 SAC chamber, validated for radiative and immunity tests, which was used to carry out the EMC tests presented on this report. The dimensions of the SAC are 21m x 15.6m x 8m (length x width x height) and therefore the chamber can accommodate EMC pre-compliance tests for all distances up to 10m.

The test methods that were followed and applied on this report were based on IEC 61851-21-2:2016 (Ed. 1.0) [9] for the radiated emissions, conducted emissions and for the radiated immunity. Whenever there was a choice between different applicable limits due to the Class of the equipment, i.e. Class-A or Class-B, for radiated and conduced emissions, the more stringent value was set, that was *Class B*, to ensure that the Equipment under Test (EUT) fulfils the worst case situation in terms of emissions. On the immunity tests, the requirements for *environments other than residential* were considered as these expose the EUT to higher electric fields and hence, this minimised further the possibility that a malfunction could be missed during the test when the equipment was exposed to an electric field.

Figure 1: VeLA 9 semi-anechoic chamber at the Joint Research Centre of the European Commission. Receiver antenna and antenna mast are shown at the far-end of the chamber

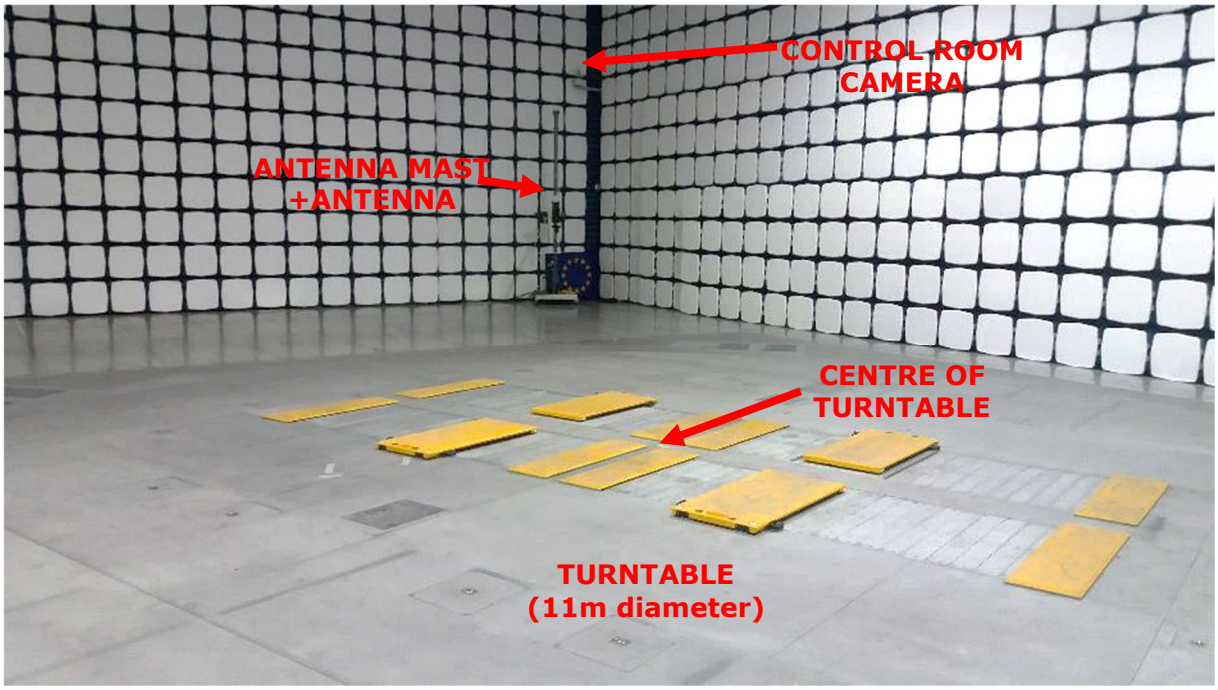

2.1 Outline of IEC 61851-21-2 standard

The EMC compliance of off-board electric vehicle charging systems is governed by IEC 61851-21-2 and it refers to chargers that provide either DC or AC power for charging a vehicle. The limits and requirements for the radiated, conducted emissions within this standard are described next.

For the radiated emissions the most commonly used distances between the antenna and the EUT is 3m or 10m, however other distances can be used provided that the corresponding limits are adjusted according to CISPR 16-1-4:2010 [10]. Vela 9 anechoic chamber permits 10m measurement distance and this was preferred over the 3m distance as the gain of an antenna varies less with respect to the EUT's length, hence minimising measurement uncertainties. However, for the radiated emission measurements between 1 GHz and 6 GHz, the 3m distance was chosen to keep the level of the noise floor close to 6 GHz further away from the limit.

Based on the above, the limits for the radiated emissions used on this report, as per IEC 61851-21-2 (Tables 18 and 19), are presented on Table 1.

Table 1: Radiated emissions limits for Class B equipment

Frequency Range (MHz)	Distance (m)	Detector type and RBW	Class B Limits (dBμV/m)
30-230	10	Quasi-peak (120kHz)	30
230-1000	10	Quasi-peak (120kHz)	37
1000 to 3000	3	Average (1MHz)	50
3000 to 6000	3	Average (1MHz)	54
1000 to 3000	3	Peak (1MHz)	70
3000 to 6000	3	Peak (1MHz)	74

The measurement time (MT) of the quasi-peak detector was set to 1s and that of the average/peak detectors to 5ms for chargers 'B' and 'C'. After a special request from the manufacturer of Charger 'A', the MT was set to 10sec and 5sec for the quasi-peak and average/peak detectors, respectively. A short discussion behind this choice is provided on Section 7 on this report.

The limits for the conducted emissions on the AC power line were defined according to Table 8 on the IEC 61851-21-2, since all chargers were supplied from a 230VAC main grid.

Table 2: Conducted emissions limits for Class B equipment for AC power line

Frequency Range (MHz)	Quasi-peak (dBμV)	Average (dBμV)
0.15 to 0.50	66 Decreasing linearly with logarithm of frequency to 56	56 Decreasing linearly with logarithm of frequency to 46
0.50 to 5.0	56	46
5.0 to 30.0	60	50

For the immunity testing, all HPCs that were tested inside the SAC were exposed to electric field strengths whose level corresponds to non-residential environments, i.e. Table 3 of IEC 61851-21-2. During these tests, the only RF power amplifier and directional coupler available in the laboratory, were operating between 800 MHz and 2 GHz, so only this frequency range was considered for the susceptibility of the EUT. The exposure field strengths according to the standard shown on Table 3.

Table 3: DC charging immunity requirements (non-residential environments)

Test applicability	Phenomenon	Basic standard	Test specification	Units
Waiting (stand-by mode)	Radiated RF field	IEC 61000-4-3 [16]	10 80-1000 80	V/m MHz % AM (1 kHz)
Waiting (stand-by mode)	Radiated RF field	IEC 61000-4-3 [16]	3 1400-2000 80	V/m MHz % AM (1 kHz)

On the above table, the field strength refers to the RMS value of an unmodulated carrier, i.e. CW signal. Hence, the peak unmodulated electric field is:

Equation 1: $E_{peak.CW} = E_{rms} \times \sqrt{2} = 10 \times \sqrt{2} = 14.1 \frac{V}{m}$ (for 80-1000MHz) and

Equation 2: $E_{peak.CW} = E_{rms} \times \sqrt{2} = 3 \times \sqrt{2} = 4.2 \frac{V}{m}$ (for 1400-2000MHz)

Then the corresponding values of the peak electric field with 80% AM modulation require the generation of peak field strength of:

Equation 3: $E_{peak.AM} = E_{peak} \times 1.8 = 14.1 \times 1.8 = 25.4 \frac{V}{m}$(for 80-1000MHz) and

Equation 4: $E_{peak.AM} = E_{peak} \times 1.8 = 4.2 \times 1.8 = 7.6 \frac{V}{m}$(for 1400-2000MHz)

The values calculated from equations 3 and 4 were the necessary peak field strengths for the exposure values required by IEC 61851-21-2 for a CW carrier when it is AM-modulated by 80%. So, effectively a 80% modulated signal produces a *peak* electric field value, which is 2.54 (√2 x 1.8) times greater than its corresponding unmodulated *rms* value. This is important to consider during immunity tests as it requires *extra power* from a RF power amplifier to handle an AM-modulated signal compared to its *unmodulated* counterpart. This extra power is hence 1.8^2=3.24 times higher, or, in terms of dB, 10xlog(3.24)=5.1 dB.

The output port of the RF amplifier and the input port of the antenna were connected with a coaxial cable of 20m. Based, on the calibration data from the manufacturer, the cables losses introduced by this cable length (on average) between 1 GHz and 2 GHz were about 3 dB, so in effect half of the output power of the amplifier was 'lost' due to the cable losses. The maximum linear power rating was 50W so, 25W at most could reach the antenna input when the amplifier was driven for maximum output power.

Considering the required power at the *antenna input port* to generate 30V/m field strength at 2m away from the antenna tip, Fig. 2, we see that this is about 25W. This means that the power rating of the RF amplifier was sufficient for our immunity tests according to IEC 61851-21-2, while the RF power amplifier retained a linear operation. Shorter distances of the antenna tip from the column would sacrifice the field uniformity, while longer distances would not produce the necessary field strength as per IEC 61851-21-2 standard.

The above theoretical calculations were verified by field strength measurements using NARDA SRM3000 for the testing of chargers 'A' and 'B', and ETS-Lindgren field-probe for the testing of charger 'C' *[N.B.: At the time of testing chargers 'A' and 'B', the software application, see Annex 2, to optically connect the field-probe to a computer for electric field monitoring purposes was not available]*.

The dwell time on the signal generator was set to 5 secs.

Figure 2: VULB antenna required input power to produce a field strength at 2m away from the antenna tip for the immunity testing (Source: ref.[11])

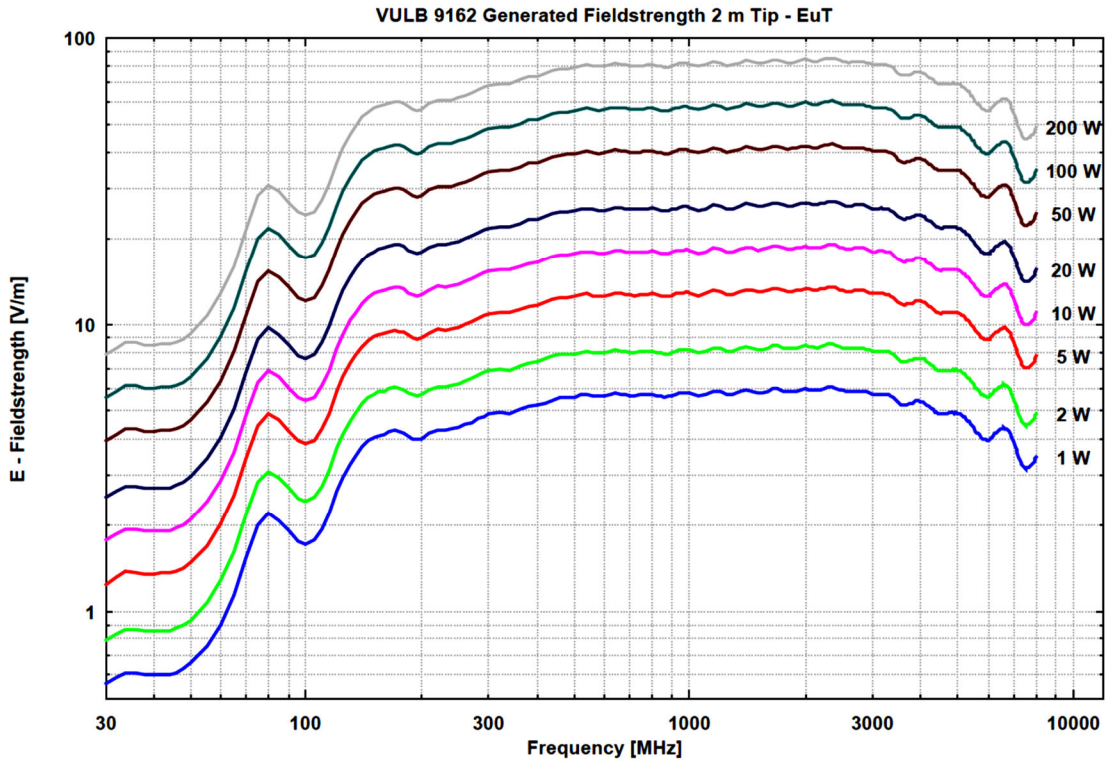

2.2 Laboratory setup and test methodology

During the measurements, the gates of the SAC were shut to eliminate any unwanted external interferences from entering the chamber or vice versa. The connection of the earth protection for each HPC was performed according to the manufacturer's requirements. For the RF grounding, a short multi-core copper cable was used to connect the column's conductive enclosure to the nearest point with the grounded SAC floor. Based on the documentation provided by the HPC suppliers at the time of the delivery of the HPC systems, RF grounding was defined for chargers 'A' and 'C' and not for Charger 'B'.

The main focus during the measurements was to investigate the radiative effect of the HPC enclosure (which includes the DC-charging cable, the display and the cabinet). For this reason the wires of the HPCs with the 230VAC grid were installed using the shortest possible cable, while ensuring that they touched the ground in order to ensure that during the radiated emissions their effect to EMI was minimised.

Prior to the execution of the measurements, the RF noise floor of the SAC on the radiated and the conducted emissions was evaluated to ensure the absence of any unwanted interference that could affect the readings on the instruments.

2.2.1 Radiated Emissions

On the radiated emissions measurements all correction factors were taken into consideration into the receiver's configuration. These were the (i) antenna factor, (ii) the cables losses between the antenna and the scanning receiver and (iii) the losses of the DC-coaxial blocker, which was used to protect the RF input circuitry of the scanning receiver. The corresponding values of the individual factors were programmed into the scanning receiver so the final result of the measured electric field that was displayed on the scanning receiver could be immediately assessed against the applicable limit. In effect, the value of the electric field strength, E, was equivalent to the following equation:

$$E\ (dB\mu V/m) = AF\ (dB/m) + L\ (dB) + R\ (dB\mu V)$$

where,

E is the actual electric-field strength (dBμV/m)

AF is the receive antenna factor (dB)

L are the (total) losses of the transmission line and the coaxial DC-blocker (dB) and

R is the reading of the EMI receiver (dBμV)

The ESR7 EMI receiver included also a pre-amplifier section whose gain was automatically calculated into the reading 'R' [12]. Hence, it was not necessary to define manually a separate correction coefficient as this was handled by the internal algorithms of the receiver.

The table below quotes the test equipment, which was used during the execution of the radiated emissions while Fig. 3 provides illustrations of the test equipment.

Table 4: Test equipment for the radiated emissions measurements

Name of equipment	**Manufacturer**	**Model**
Tri-log antenna	SCHWARZBECK	VULB 9162 (30MHz-8GHz)
EMI Test Receiver	Rohde and Schwarz	ESR7 (10Hz-7GHz)
Coaxial cables (with N-type connectors)	SSB Electronics	ECOFLEX 10
Active monopole rod antenna (for exploratory tests)	ETS-Lindgren	3301C (30Hz-50MHz)

Figure 3: Test equipment used during the radiated emissions measurements (a) Tri-Log antenna 30-8000 MHz, (b) ESR7 electromagnetic interference receiver, (c) high-quality low-loss ECOFLEX10 coaxial cables with N-type connectors

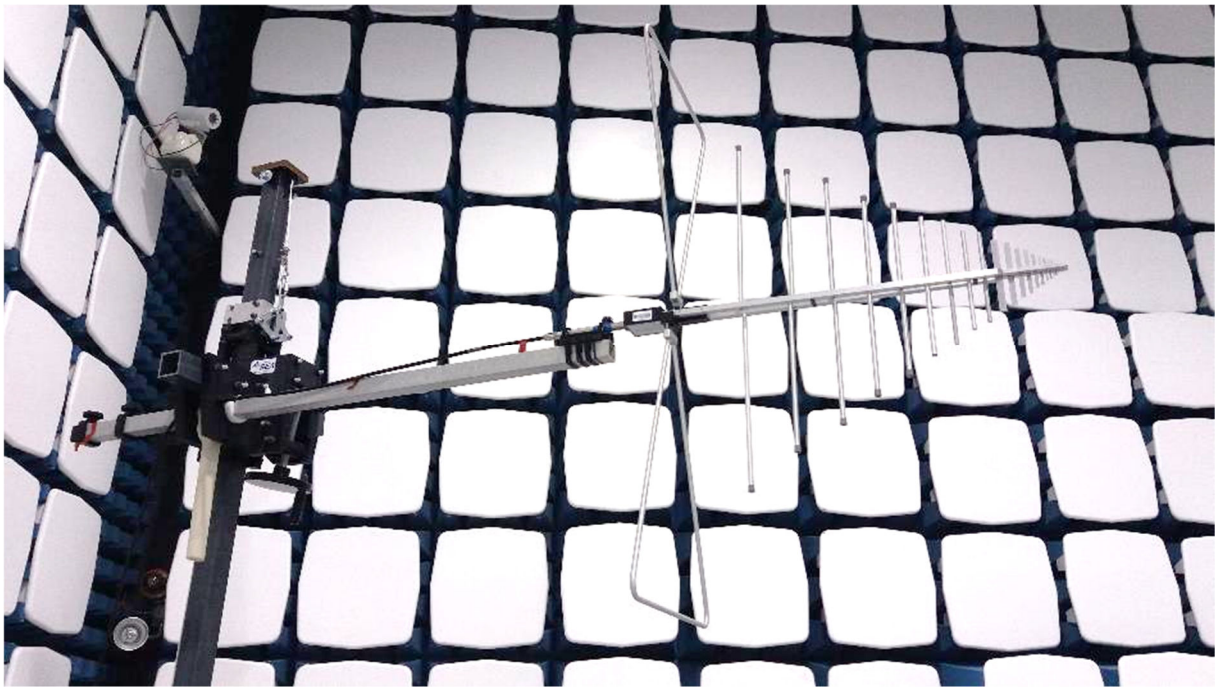

(a)

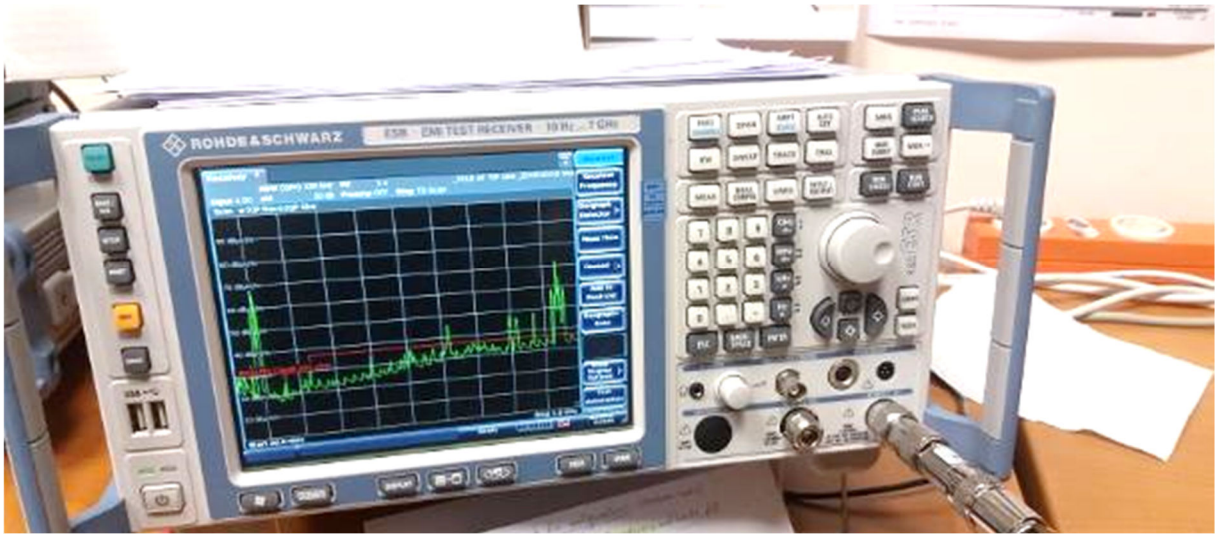

(b)

(c)

The frequency measurements of the radiated emissions between 30 MHz and 1 GHz were carried out with the antenna tip spaced d=10m away from the EUT, as per IEC 61851-21-2, while antenna height (h) scanning was taken at 1.5m, 2.0m and 3.0m to ensure that worst case emissions were not missed. The antenna height could not be set above 3.0m due to the height limit of the antenna mast, otherwise a 4m antenna height would be desirable to include on the measurements, too. The EUT, i.e. charging column, was placed at the centre of the SAC's turntable, which could rotate 360 degrees and this allowed to perform measurements on all 4 sides around the HPC enclosure while leaving the EUT and the cabling intact. This ensured that the geometry and the physical layout of the EUT was identical throughout all measurements and allowed immediate evaluation of the emissions level on the EMI receiver.

For frequency measurements between 1 GHz and 6 GHz the antenna was placed d=3.0m away from the EUT and at h=1.5m and h=2.0m (for some setups) above the ground floor, as these height values point approximately at the mid-point of the column where the HPC display is located (on average for all 3 HPCs).

All four sides of the HPCs were measured for their radiated emissions, while both vertical and horizontal polarisations were considered in combination with different antenna heights.

Exploratory research was also carried out for some HPCs by investigating the *radiated* emissions *below* 30 MHz. This was implemented with the use of an active monopole antenna, Fig. 4.

Figure 4: Active Rod Monopole antenna (ETS-Lindgren)

The following diagram illustrates the laboratory setup for the radiated emissions testing.

Figure 5: Vela 9 instrument and laboratory setup for the radiated emissions testing

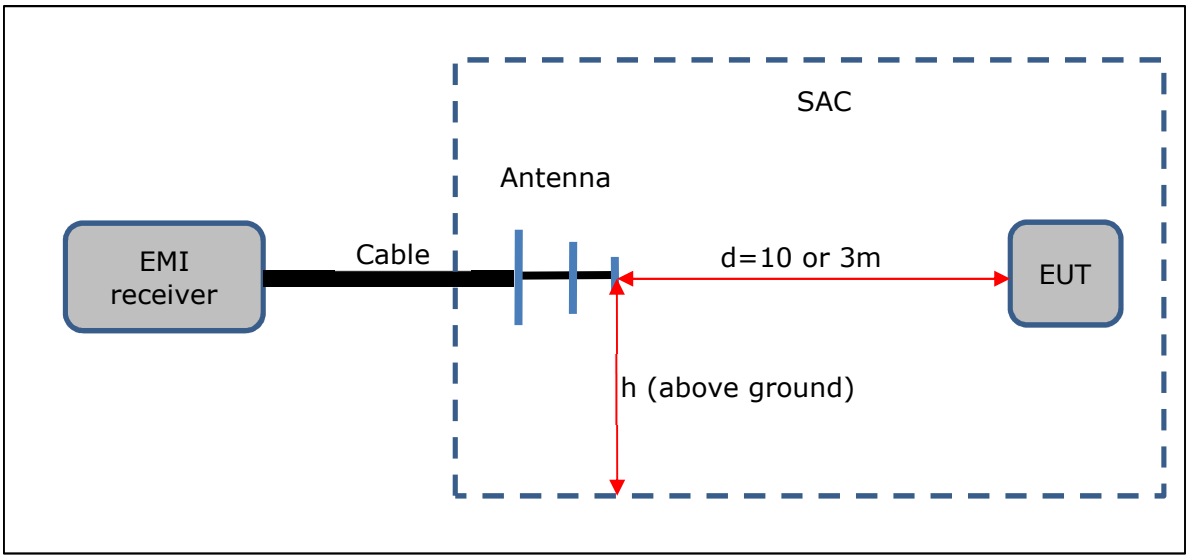

2.2.2 Conducted Emissions

VeLA 9 was equipped with two models of Line Impedance Stabilisation Networks (LISNs), which could capture the RF disturbances on the AC power lines from 150 kHz to 30 MHz as prescribed on IEC 61851-21-2. The test equipment that was used for the conducted emissions testing is quoted on table 5 and figure 6:

Table 5: Test equipment for the conducted emissions measurements

Name of equipment	**Manufacturer**	**Model**
LISN (Line Impedance Stabilisation Network)	Laplace Instruments	LISN 1600 (1-phase+N)
LISN (Line Impedance Stabilisation Network)	Rohde and Schwarz	ENV 4200 (3-phase+N)
EMI (Electromagnetic Interference) Test Receiver	Rohde and Schwarz	ESR7 (10Hz-7GHz)
Coaxial cables (with N-type connectors)	SSB Electronics	ECOFLEX 10

Figure 6: Line Impedance Stabilisation Network instrument used for the conducted emissions (a) LISN1600 (1-phase LISN) with 150 kHz high-pass filter and up to 20 dB attenuator, (b) ENV4200 (3-phase LISN) 150 kHz to 30 MHz with transient limiter

(a)

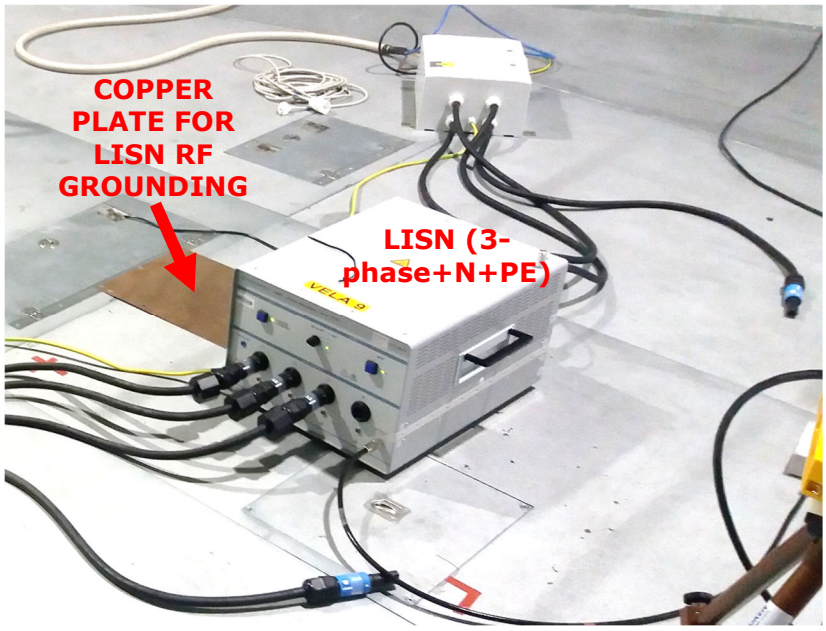

(b)

Both the phase (P) and the neutral (N) lines were assessed for the HPC columns with single phase power connection. During the tests, the HPCs were in stand-by (idle) mode with the display messages waiting for user input. For the protection of the EMI receiver, the integrated 20 dB attenuator was introduced and the 150 kHz high-pass filter was active, when the LISN1600 was used for the measurements. For HPCs, which required an AC voltage from a 3-phase power line, the ENV 4200 LISN was used for the purpose.

As in the radiated emissions, all attenuation factors of the LISN were taken into account on the EMI receiver results. The measured value of the conducted RF voltage on the instrument is expressed by the following equation:

$$V\ (dB\mu V) = L\ (dB) + R\ (dB\mu V)$$

where,

V is the conducted RF voltage (dBμV)

L are the losses of the transmission line and the attenuation factor (dB) of the LISN

R is the reading of the EMI receiver (dBμV)

For the safety of the equipment and the test operators, the ground port of the LISN was connected to the Vela 9 SAC ground with a short conductive wire/copper plate.

The next figure outlines the setup on Vela 9 for the execution of the conducted emissions testing.

Figure 7: Vela 9 laboratory and instrument setup for the conducted emissions testing

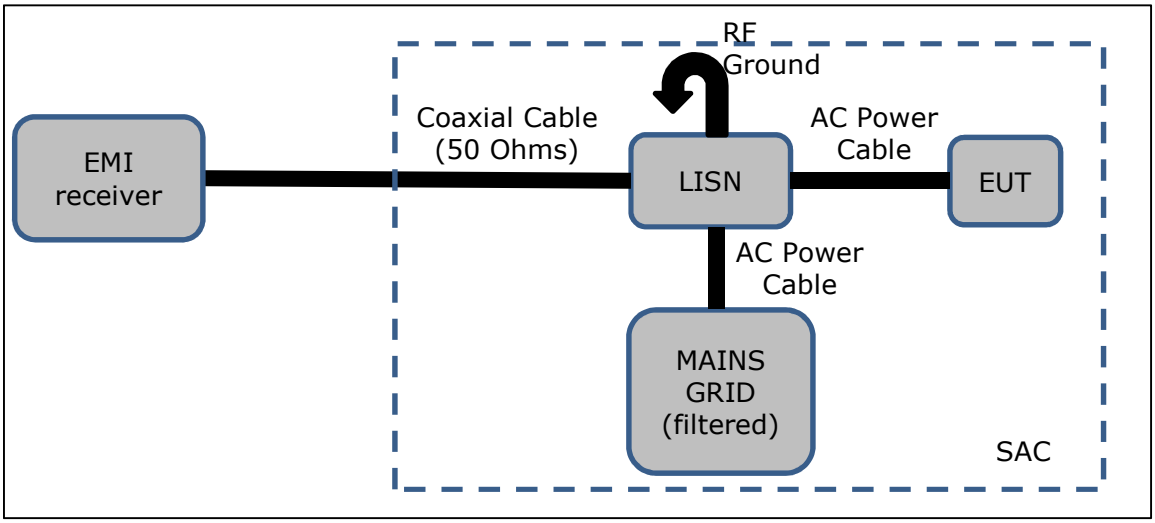

2.2.3 Radiated Immunity

The table below shows the equipment used during the immunity testing, while Fig. 8, illustrates the test equipment:

Table 6: Test equipment for the immunity (susceptibility) measurements

Name of equipment	**Manufacturer**	**Model**
Tri-log antenna	SCHWARZBECK	VULB 9162
RF solid-state power amplifier	IFI (Instruments for Industry)	S21-50
Coaxial cables (with N-type connectors)	SSB Electronics	ECOFLEX 10
Signal Generator	Rohde and Schwarz	SMB 100A
Directional Coupler	Werlatone	C5019
RF Power Meter	Rohde and Schwarz	NRVD
RF Probe (for E-field)	ETS Lindgren	HI-6005
Selective Radiation Meter	NARDA	SRM3000

Figure 8: Test equipment used for the radiated immunity tests (a) signal-generator, (b) directional coupler, (c) RF solid state power amplifier, (d) RF power meter (e) Isotropic electric field probe with optical fiber connectivity, (f) NARDA SRM3000 radiation meter

(a)

(b)

(c)

(d)

(e) (f)

During the tests, the antenna was placed 2.0m away from the EUT and 1.5m above the ground, with its main axis pointing towards the display area of the HPCs. Both horizontal and vertical polarisations were considered during the injection of the RF power to the VULB 9162 antenna, which could handle up to 100W of continuous power, way above the maximum power of the RF amplifier.

The laboratory setup for the immunity testing is illustrated on the next figure:

Figure 9: Vela 9 laboratory and instrument setup for the radiated immunity testing

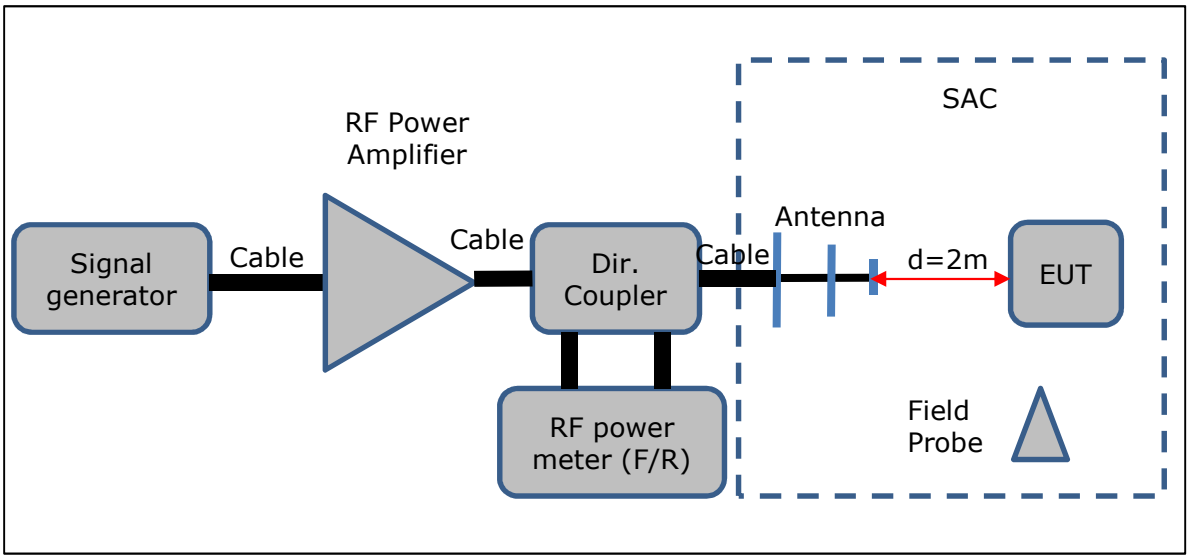

3 Radiated Emissions Testing

Prior to the start of the radiated emissions measurements, the HPCs were switched ON and they remained in ON state for at least 15 minutes to allow the settling and the warming up of the internal electric and electronic modules. The status of the messages on the HPC display were waiting for user's input (idle mode).

The results of the laboratory measurements for the radiated emissions of all three HPCs are presented on this section and for convenience they were grouped according to frequency bands:

(i) 30 – 1000 MHz and

(ii) 1 – 6 GHz

On each figure there are four plots that show the radiated emissions on each of the four sides of the charging columns. The left and right sides are referenced with respect to the display side, as shown on the next figure (Fig. 10). Parameters 'd' and 'h' indicate the distance of the antenna tip to the EUT and the height above the SAC floor, respectively.

Figure 10: Illustration of the assignment sides during the testing

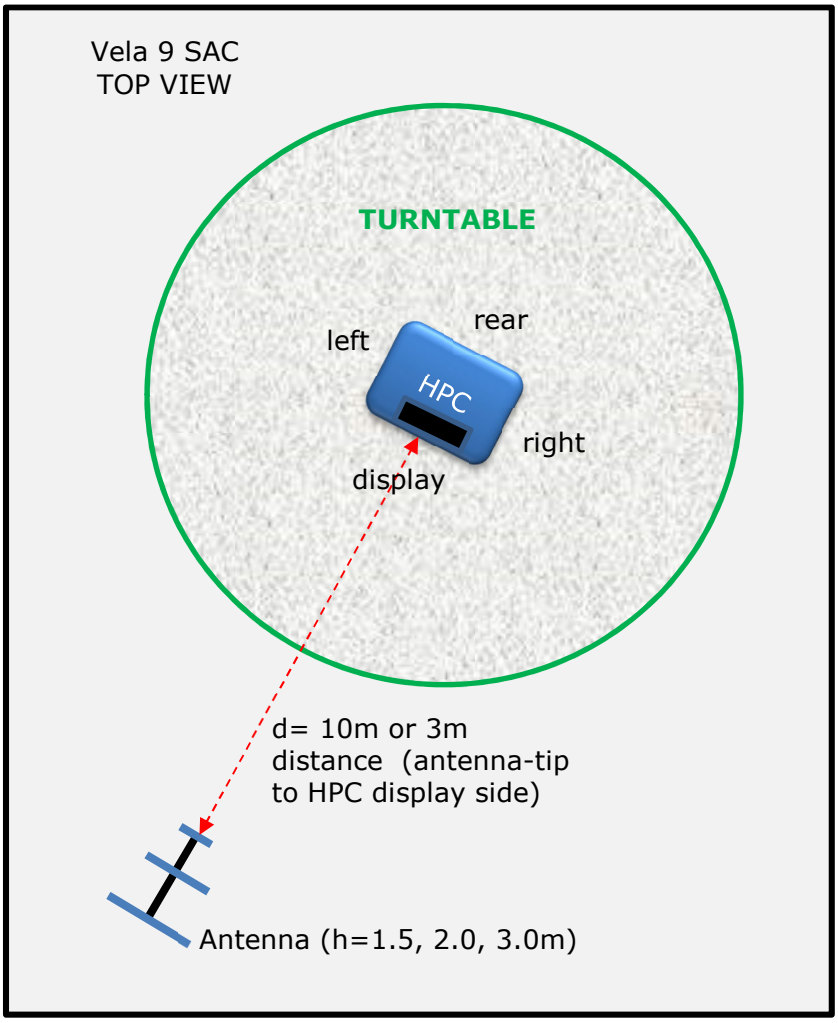

3.1 Radiated emissions 30 MHz to 1000 MHz

3.1.1 Radiated emissions for Charger 'A'

Figure 11: Charger 'A' V-pol, h=1.5m, (a) display, (b) right, (c) left, (d) rear

a.

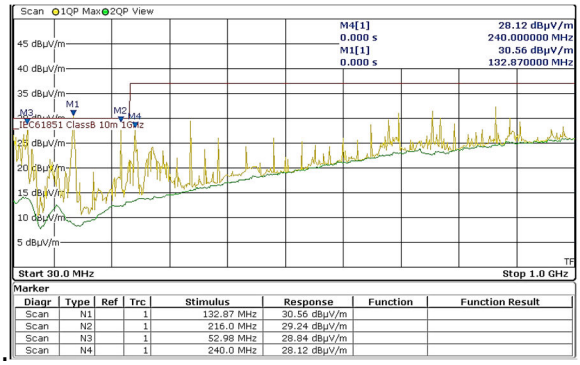

b.

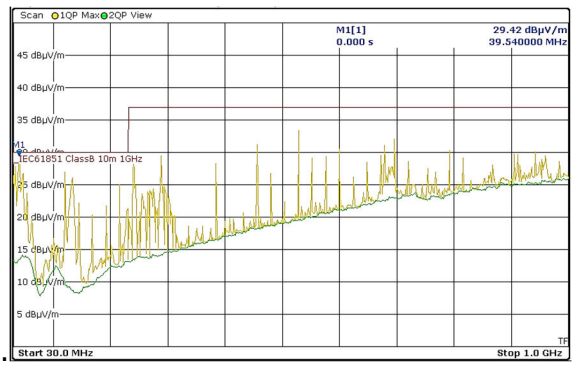

c.

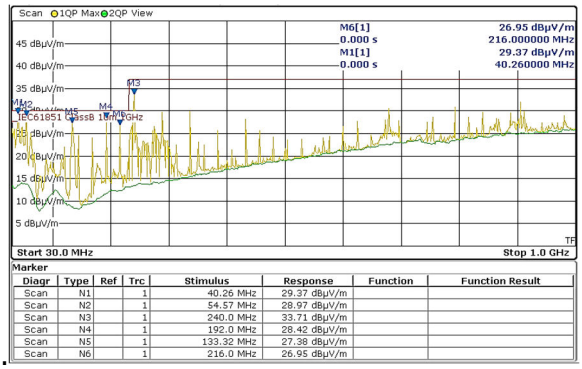

d.

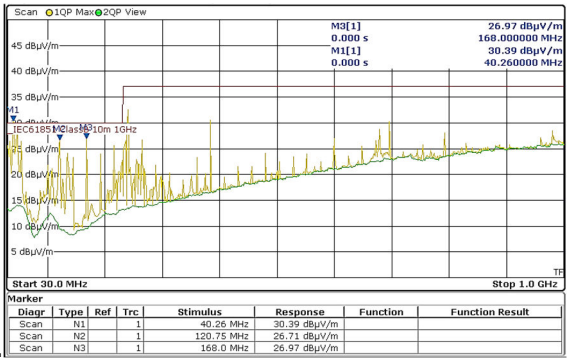

Figure 12: Charger 'A' H-pol, h=1.5m, (a) rear, (b) left, (c) display, (d) right

a.

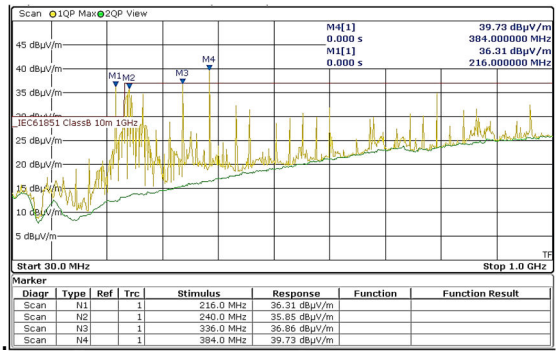

b.

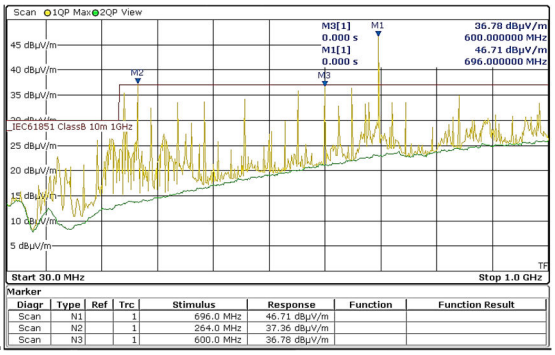

c.

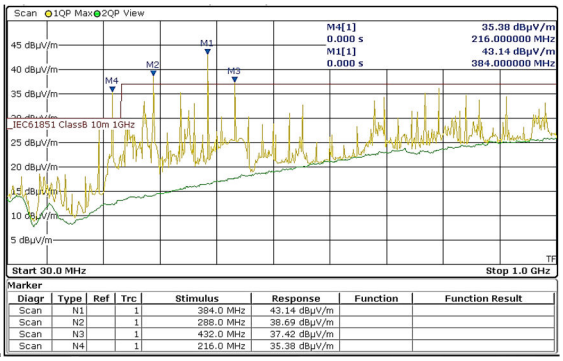

d.

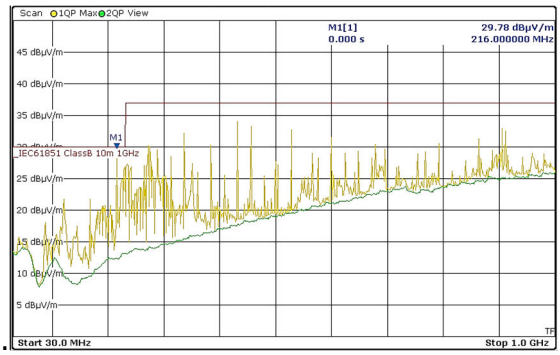

Figure 13: Charger 'A' V-pol, h=2.0m, (a) right, (b) display, (c) left, (d) rear

a.
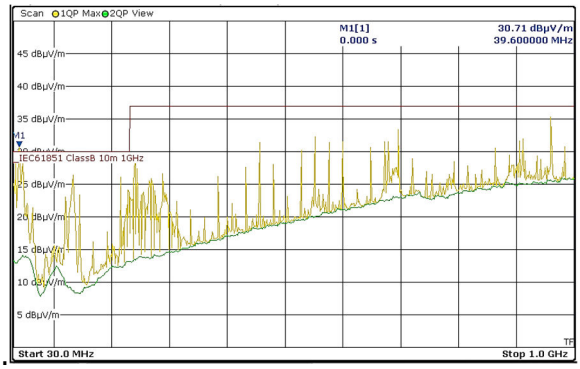

b.
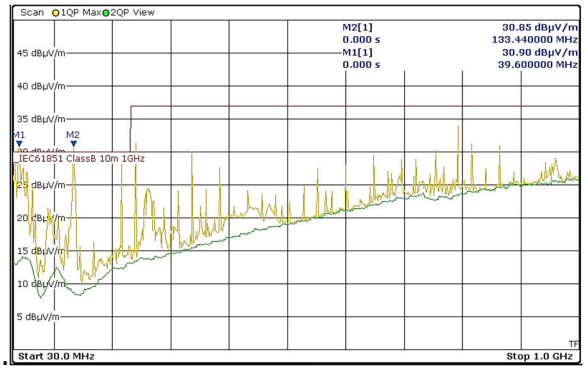

c.
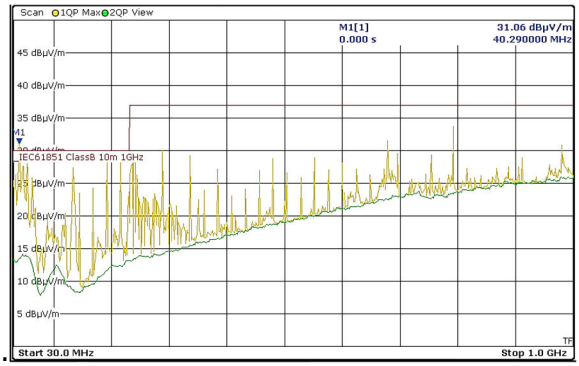

d.
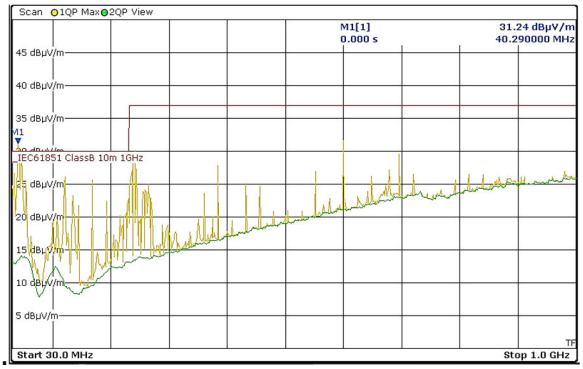

Figure 14: Charger 'A' H-pol, h=2.0m, (a) rear, (b) left, (c) display, (d) right

a.
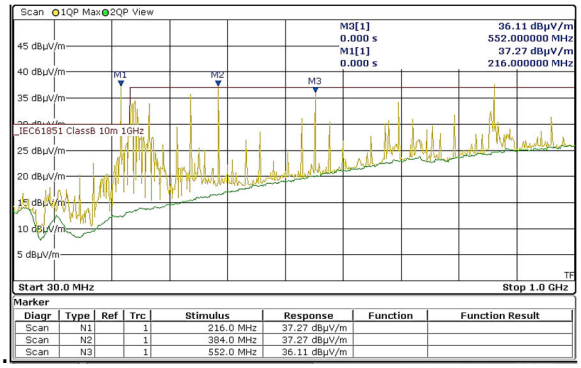

b.
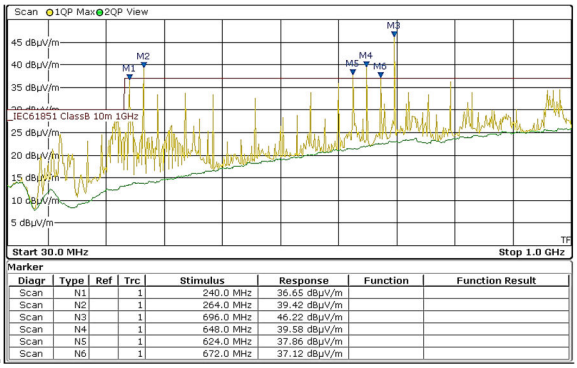

c.
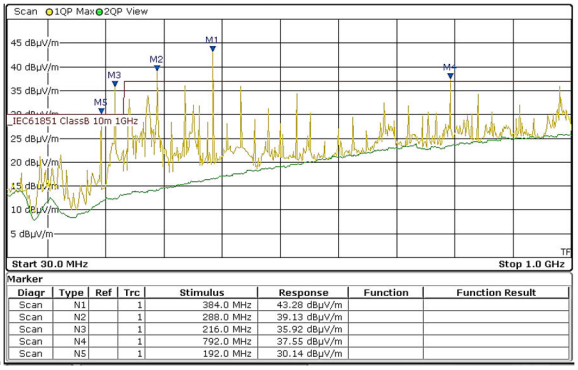

d.
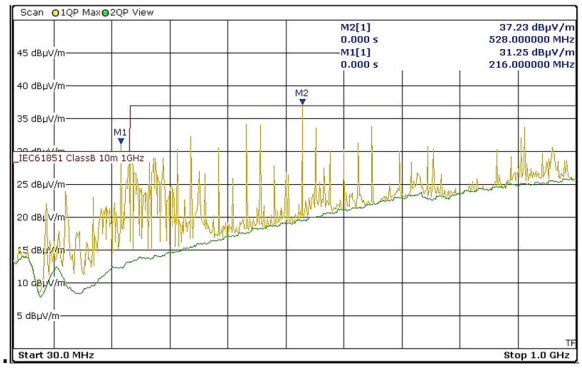

Figure 15: Charger 'A' V-pol, h=3.0m, (a) right, (b) display, (c) left, (d) rear

a.

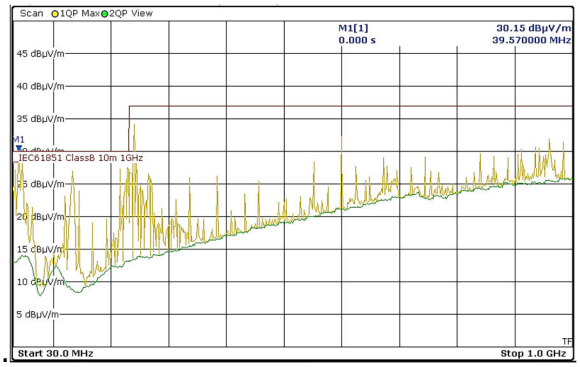

b.

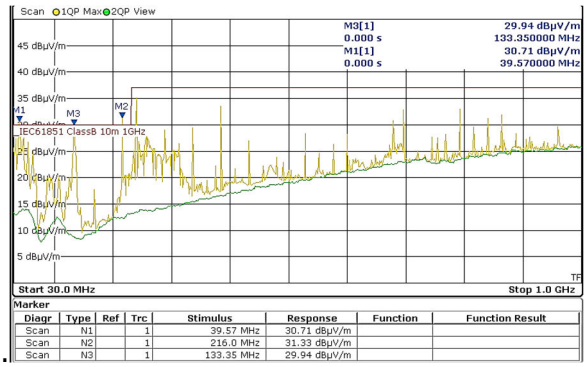

c.

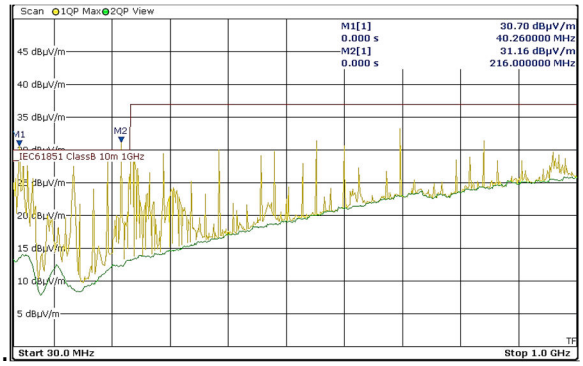

d.

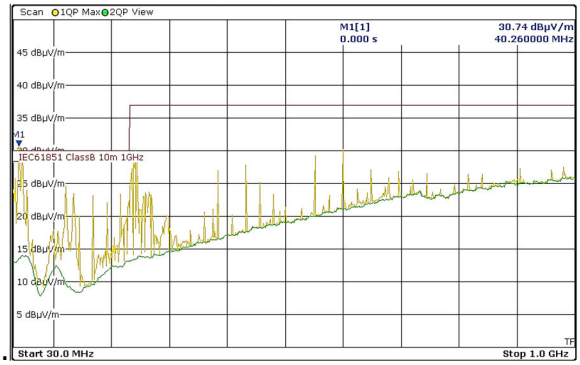

Figure 16: Charger 'A' H-pol, h=3.0m, (a) rear, (b) left, (c) display, (d) right

a.

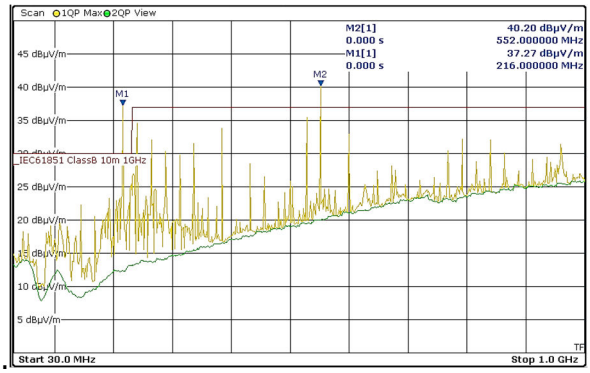

b.

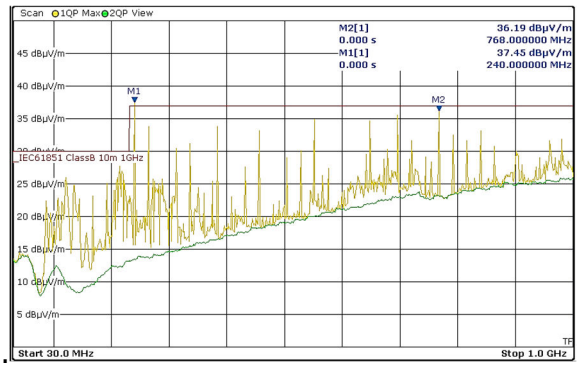

c.

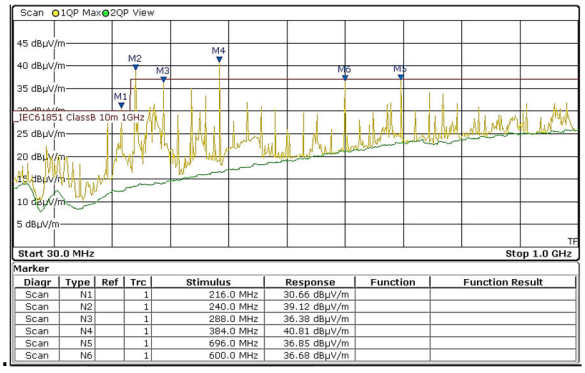

d.

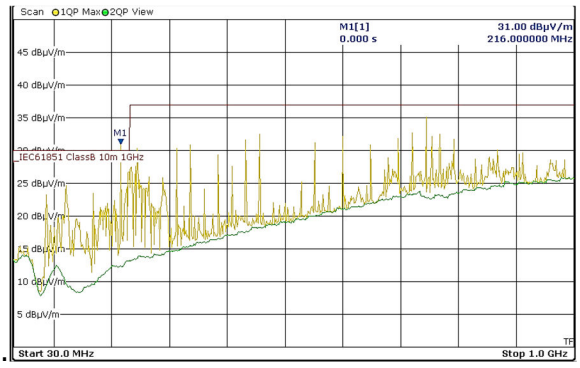

3.1.2 Radiated emissions for Charger 'B'

Figure 17: Charger 'B' V-pol, h=1.5m, (a) display, (b) right, (c) rear, (d) left

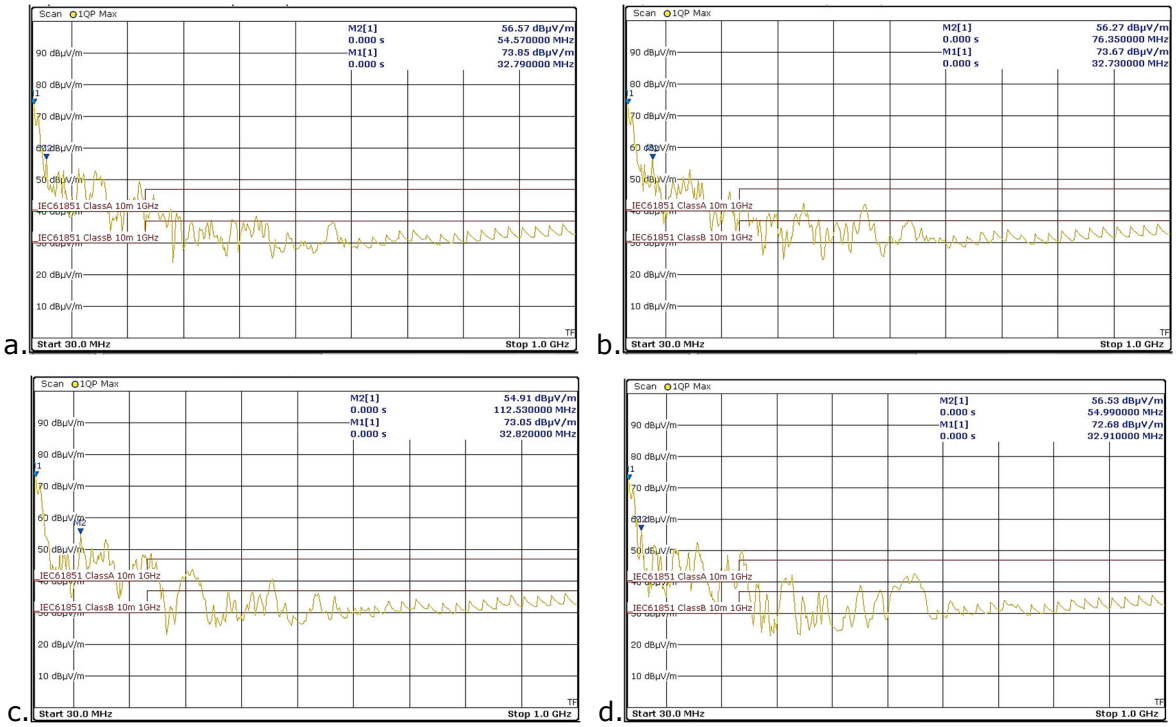

Figure 18:Charger 'B' H-pol, h=1.5m, (a) left, (b) rear, (c) right, (d) display

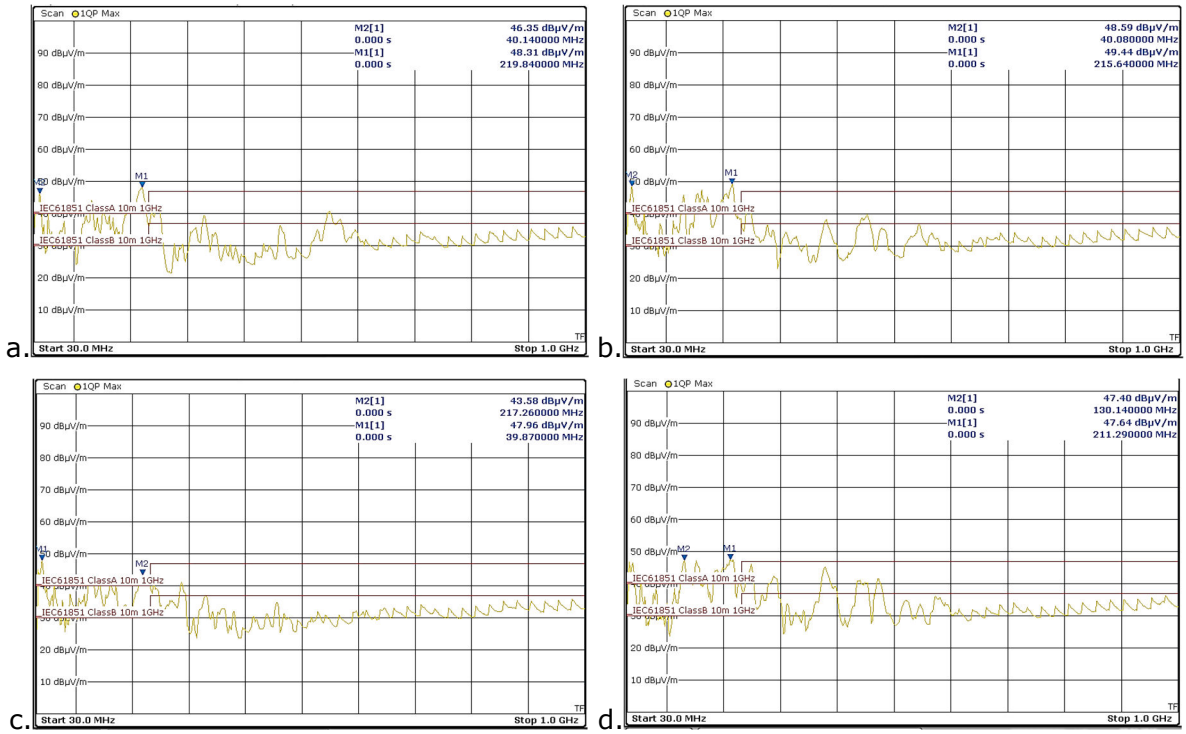

Figure 19: Charger 'B' V-pol, h=2.0m, (a) left, (b) rear, (c) right, (d) display

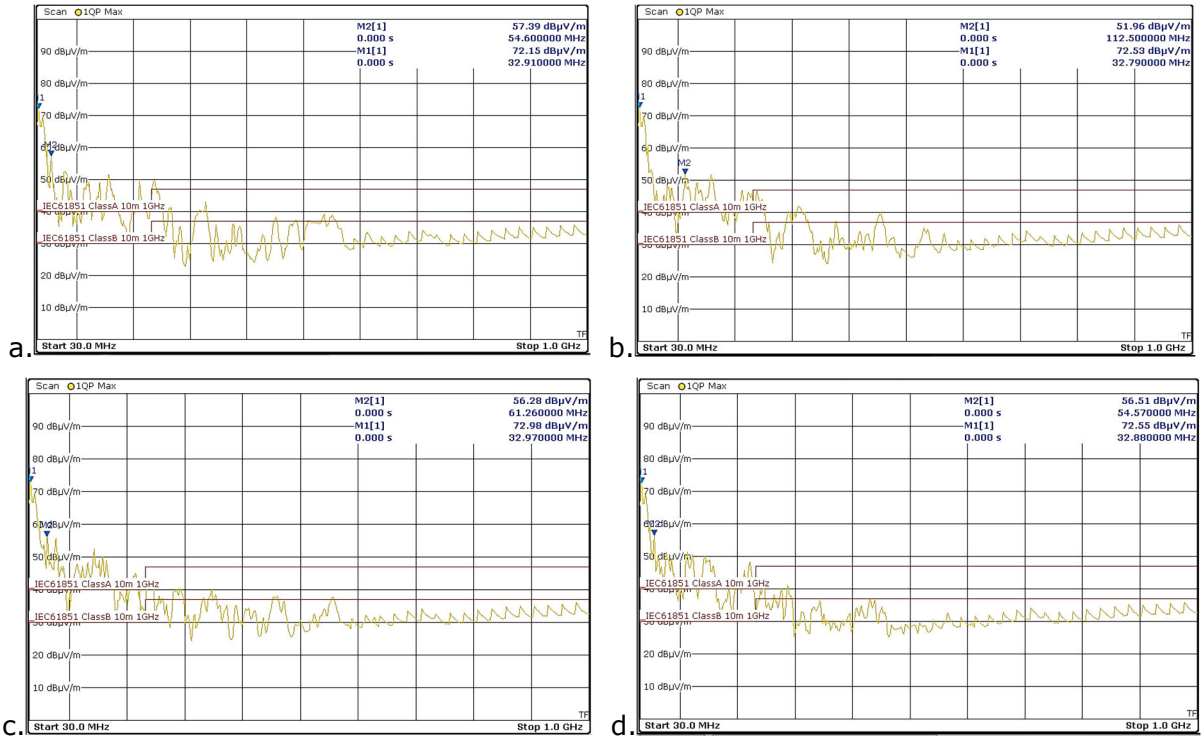

Figure 20: Charger 'B' H-pol, h=2.0m, (a) display, (b) right, (c) rear, (d) left

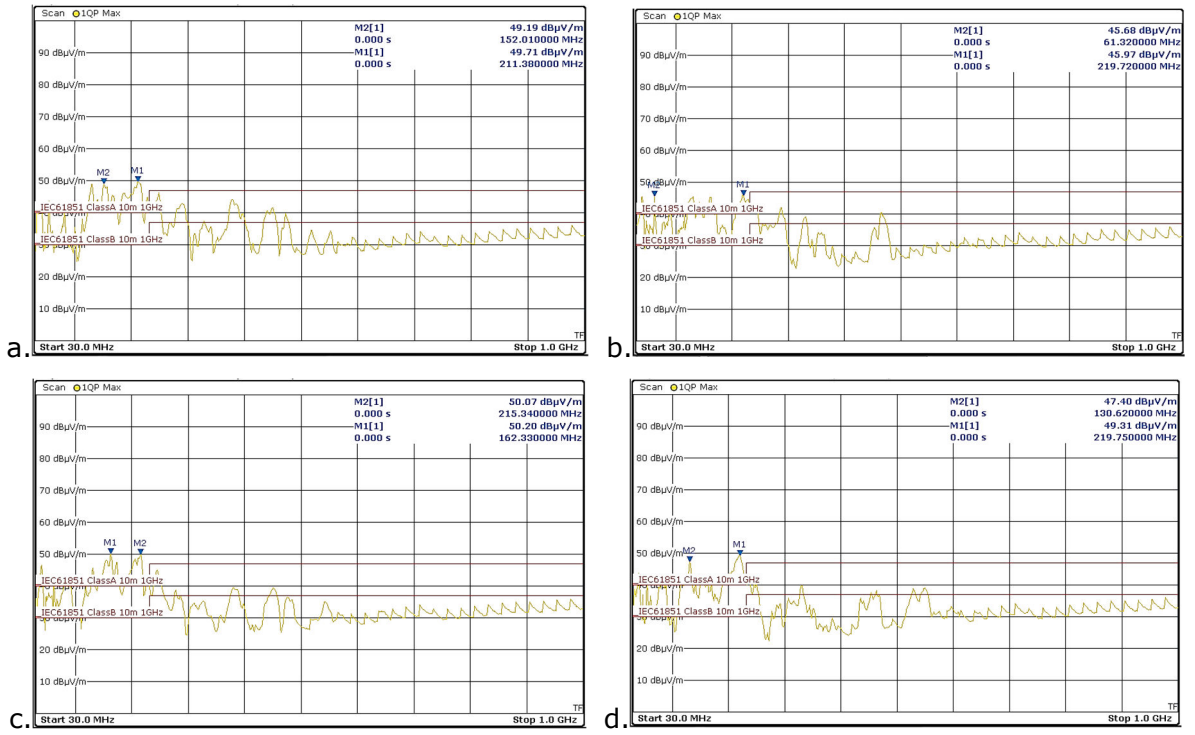

Figure 21: Charger 'B' V-pol, h=3.0m, (a) display, (b) right, (c) rear, (d) left

a.
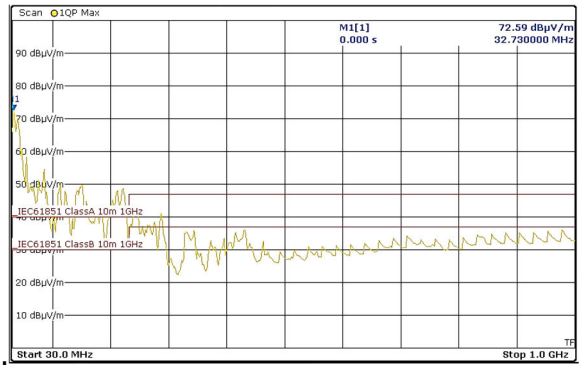

b.
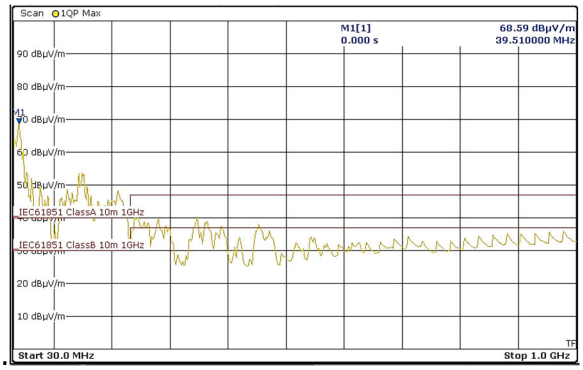

c.
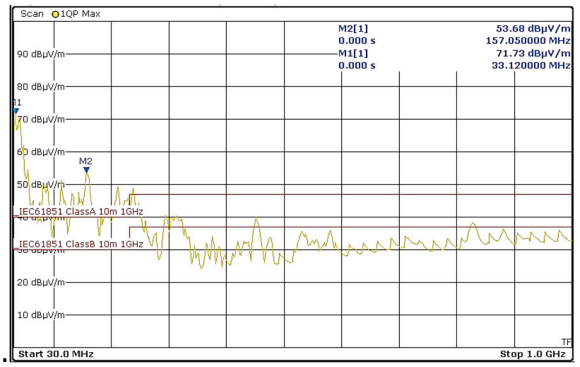

d.
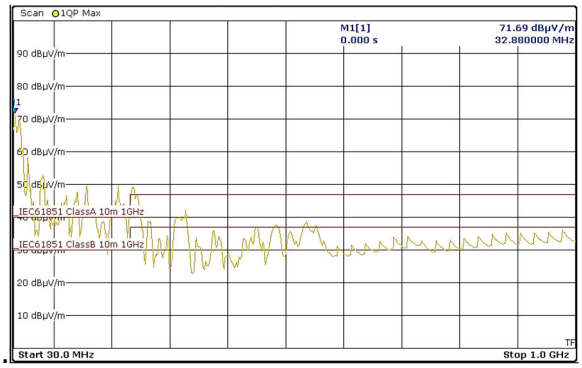

Figure 22: Charger 'B' H-pol, h=3.0m, (a) left, (b) rear, (c) right, (d) display

a.
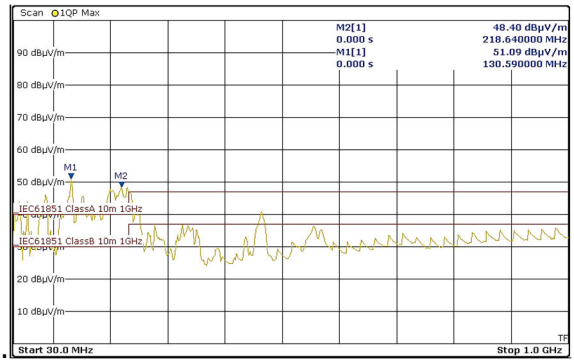

b.
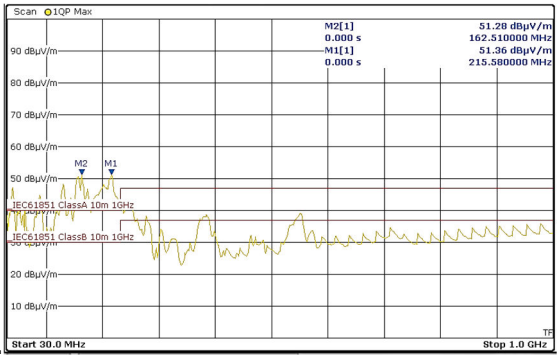

c.
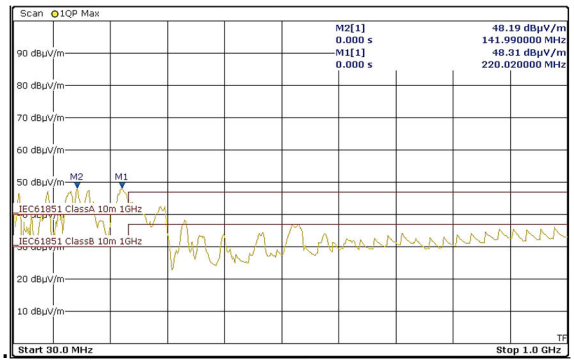

d.
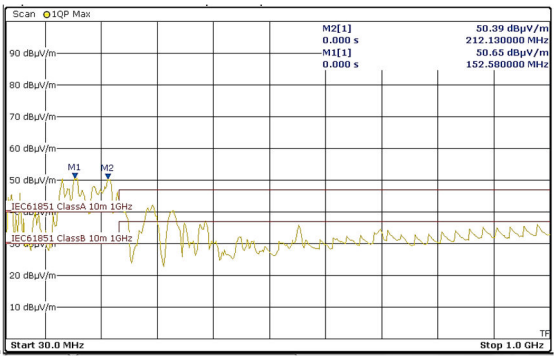

3.1.3 Radiated emissions for Charger 'C'

Figure 23: Charger 'C' V-pol, h=1.5m, (a) left, (b) rear, (c) right, (d) display

a.
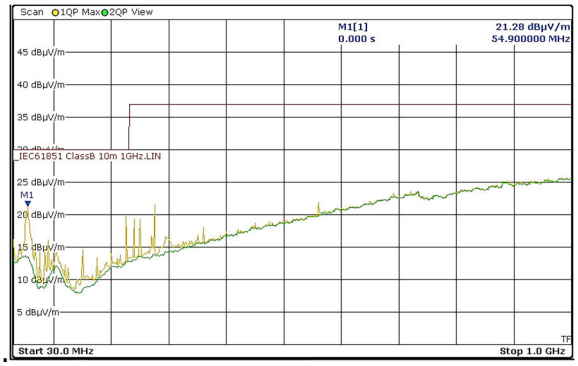

b.
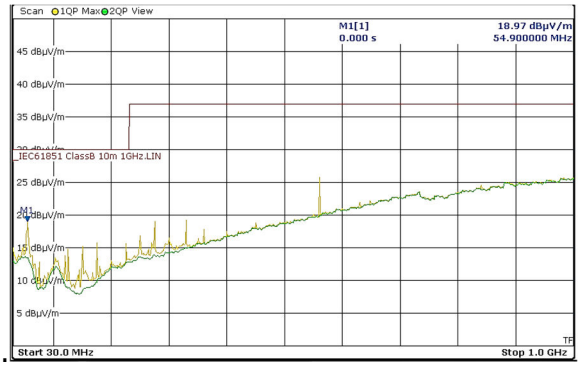

c.
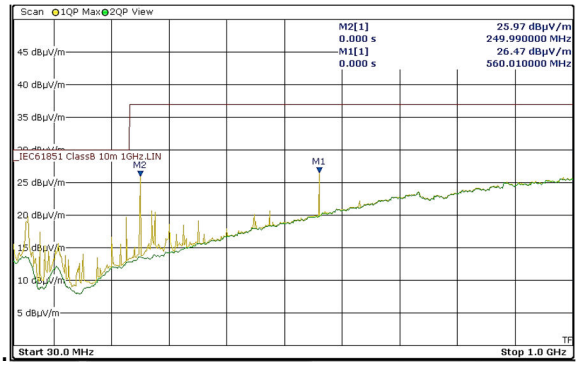

d.
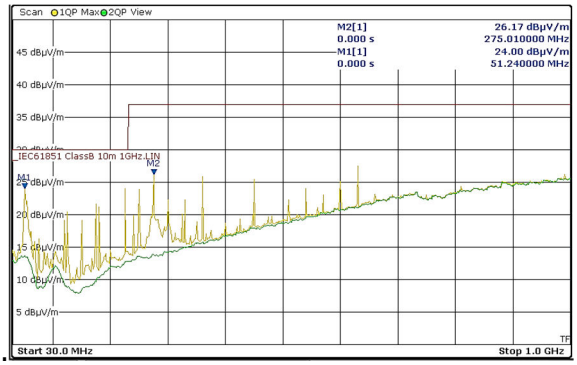

Figure 24: Charger 'C' H-pol, h=1.5m, (a) display, (b) right, (c) rear, (d) left

a.
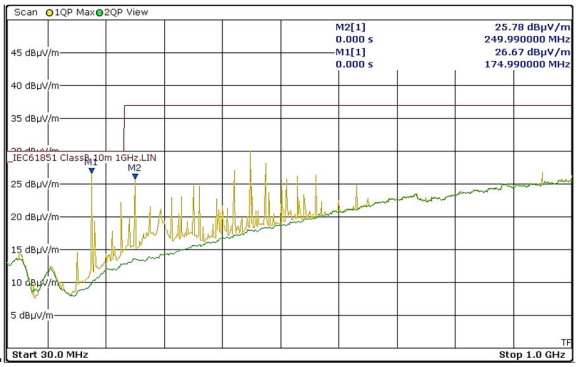

b.
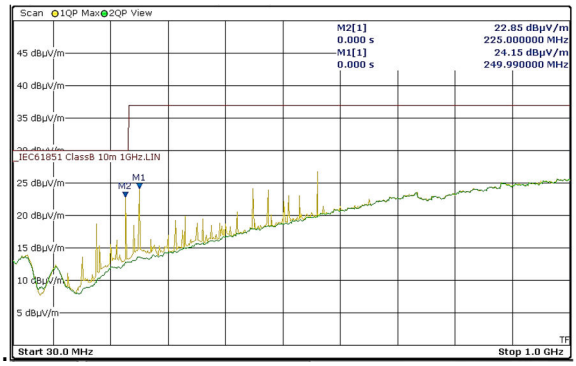

c.
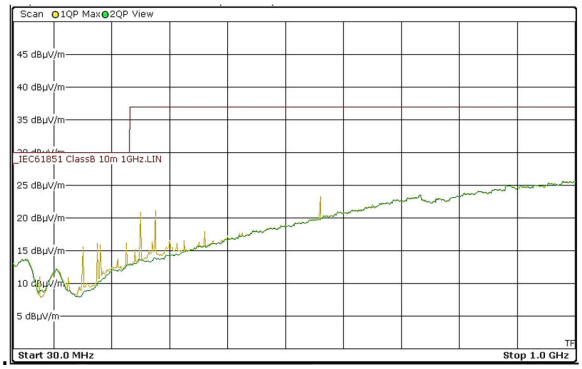

d.
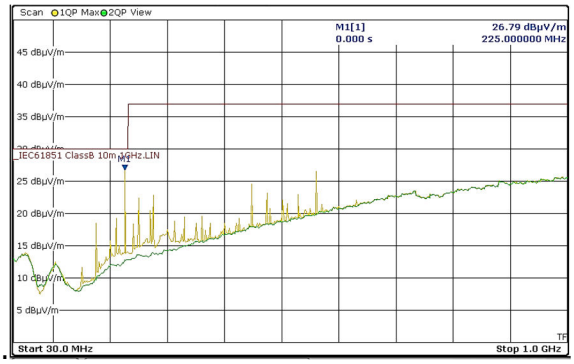

Figure 25: Charger 'C' V-pol, h=2.0m, (a) display, (b) right, (c) rear, (d) left

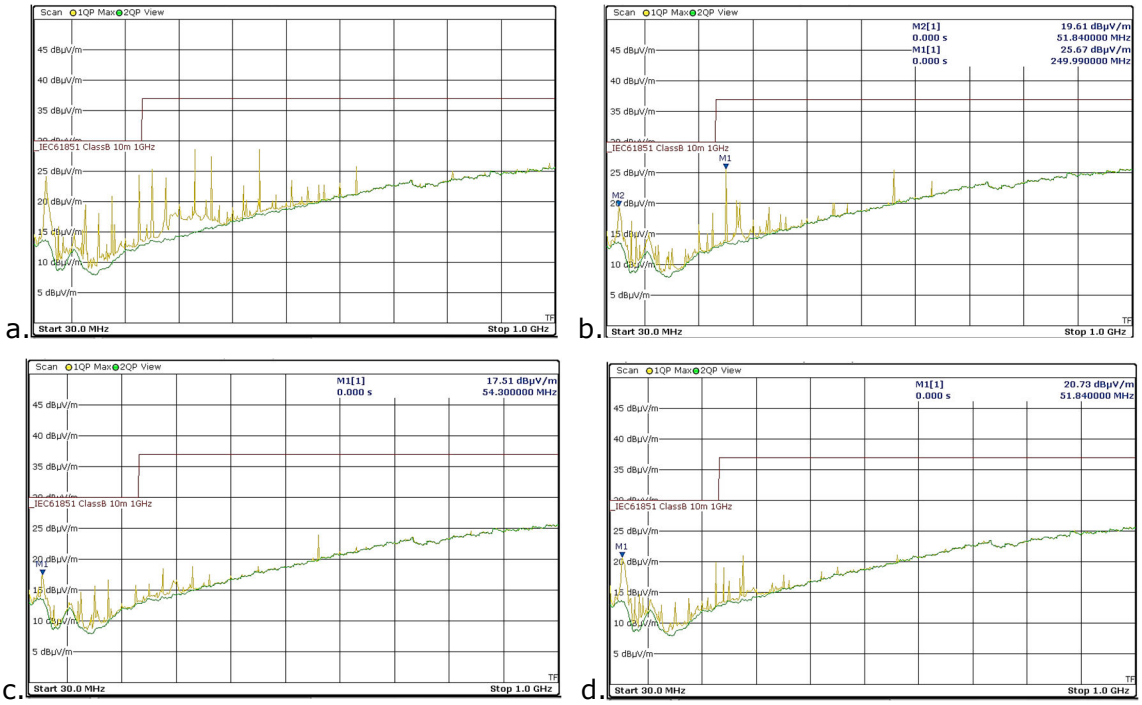

Figure 26: Charger 'C' H-pol, h=2.0m, (a) left, (b) rear, (c) right, (d) display

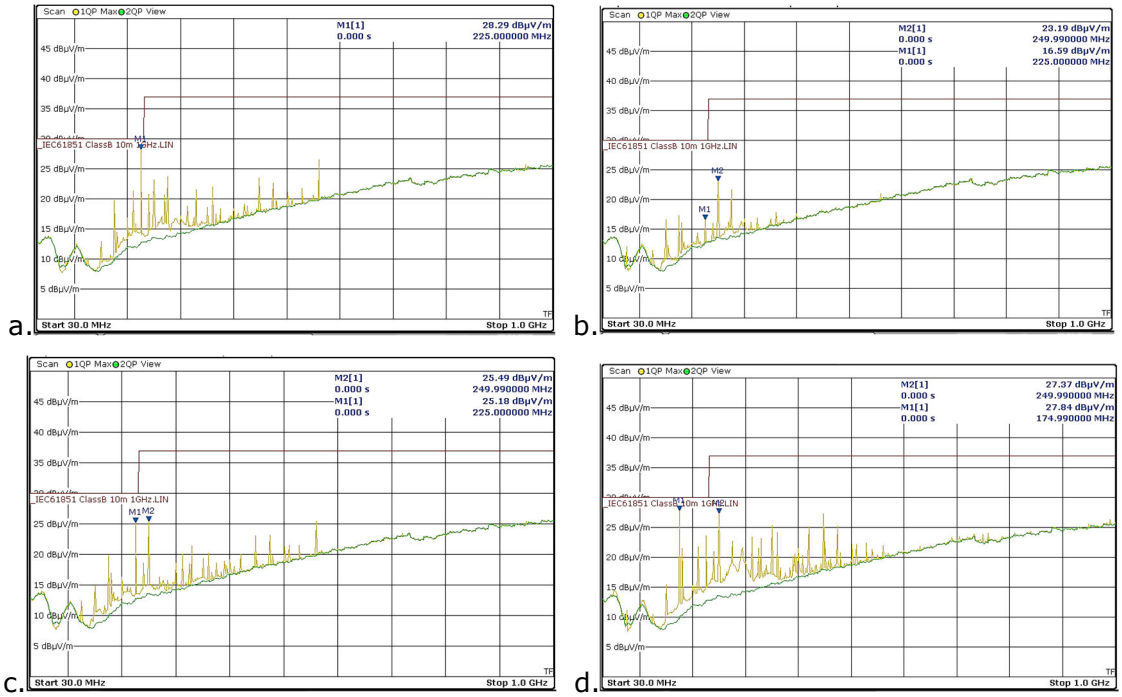

Figure 27: Charger 'C' V-pol, h=3.0m, (a) display, (b) right, (c) rear, (d) left

a.
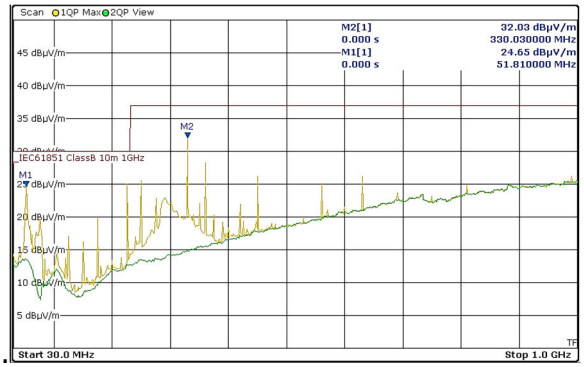

b.
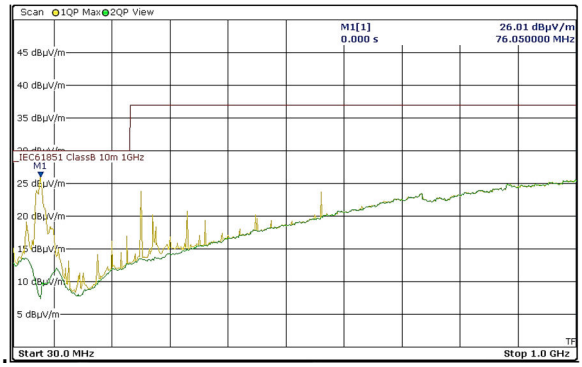

c.
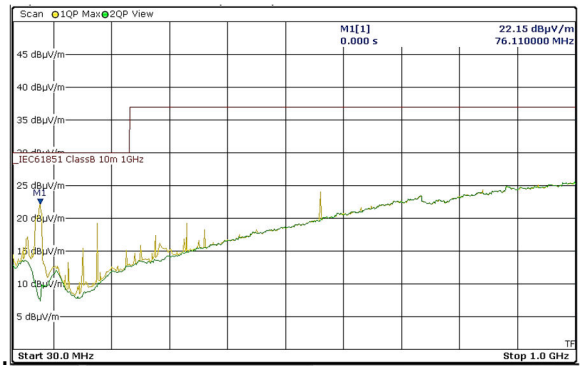

d.
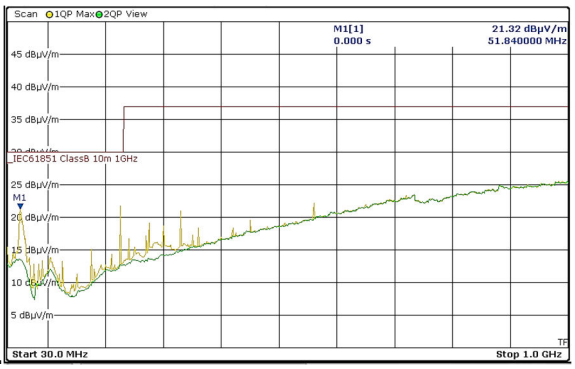

Figure 28: Charger 'C' H-pol, h=3.0m, (a) left, (b) rear, (c) right, (d) display

a.
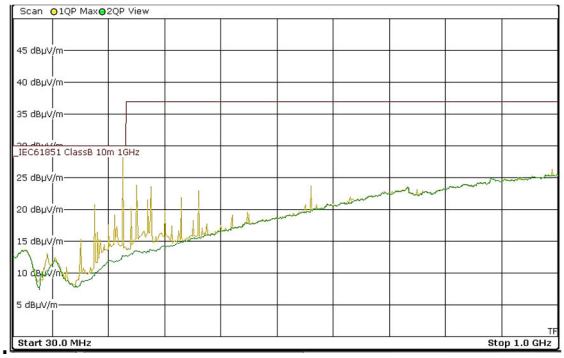

b.
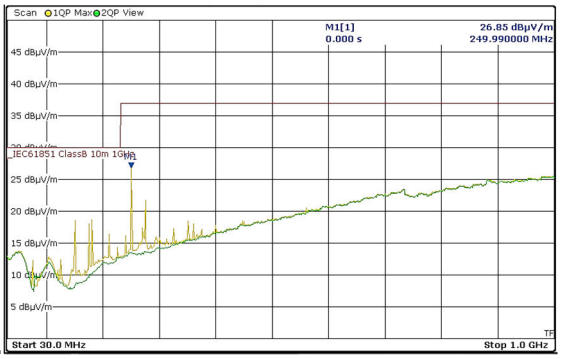

c.
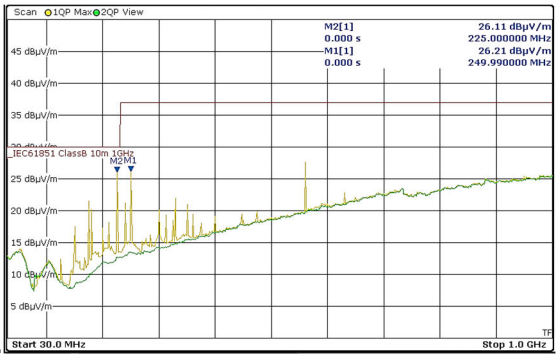

d.
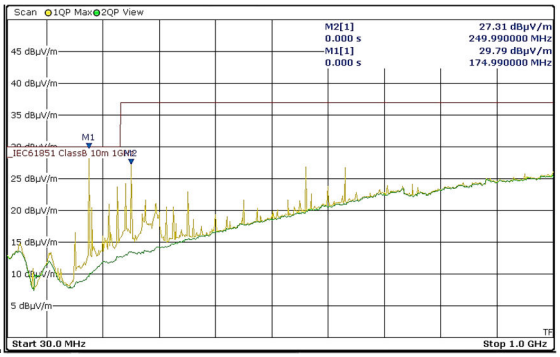

3.2 Radiated emissions 1 GHz to 6 GHz

3.2.1 Radiated emissions for Charger 'A'

Figure 29: Charger 'A' V-pol, h=1.5m, (a) right, (b) display, (c) left, (d) rear

a.
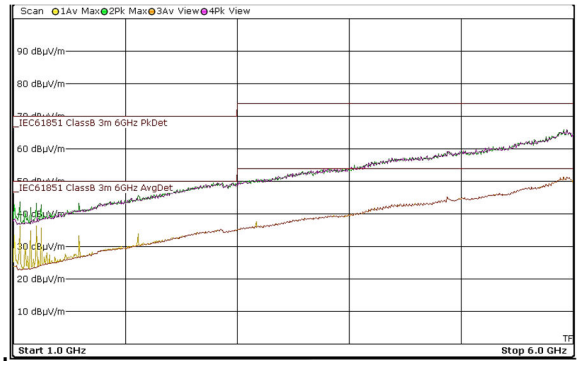

b.
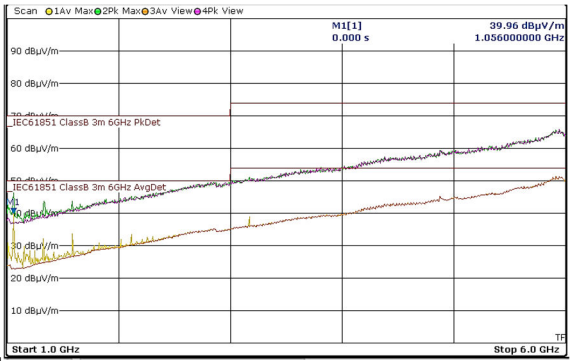

c.
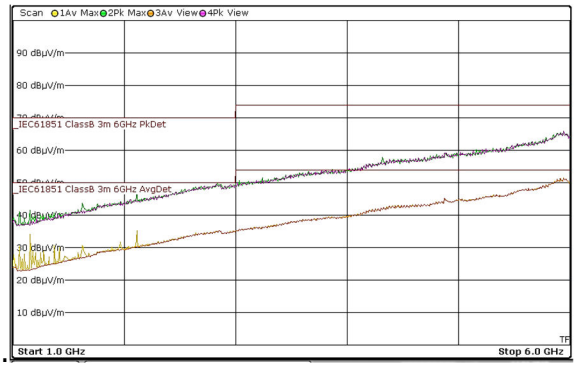

d.
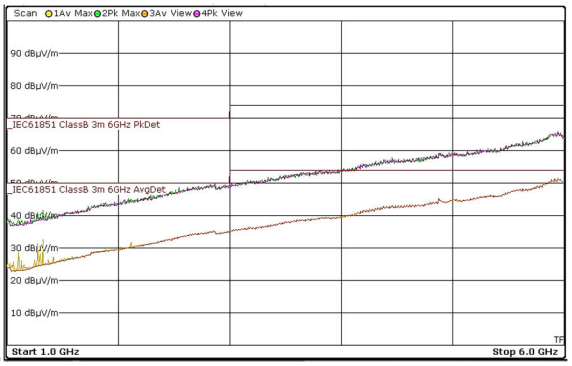

Figure 30: Charger 'A' H-pol, h=1.5m, (a) rear, (b) left, (c) display, (d) right

a.
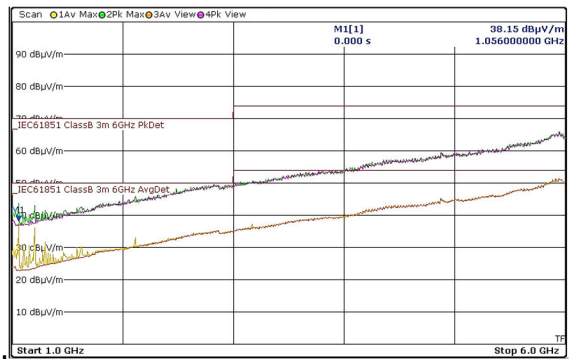

b.
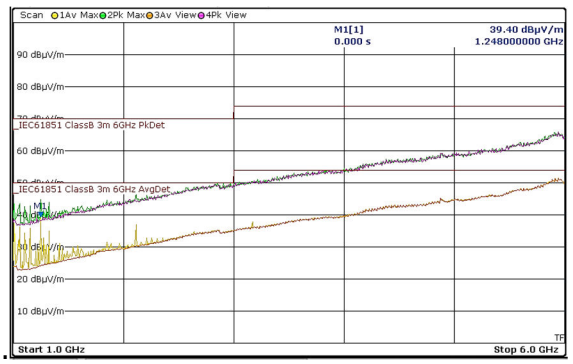

c.
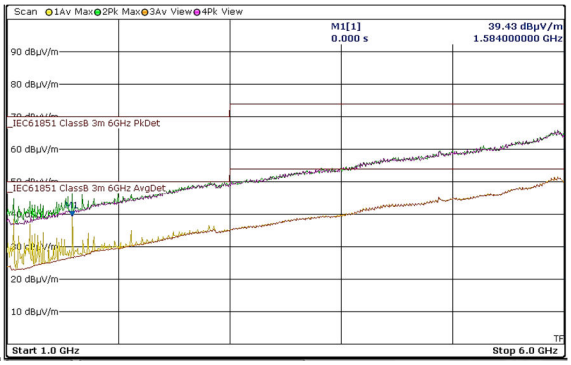

d.
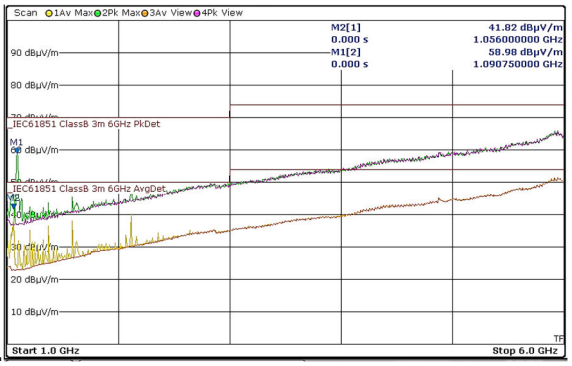

3.2.2 Radiated emissions for Charger ‘B’

Figure 31: Charger 'B' V-pol, h=1.5m, (a) display, (b) right, (c) rear, (d) left

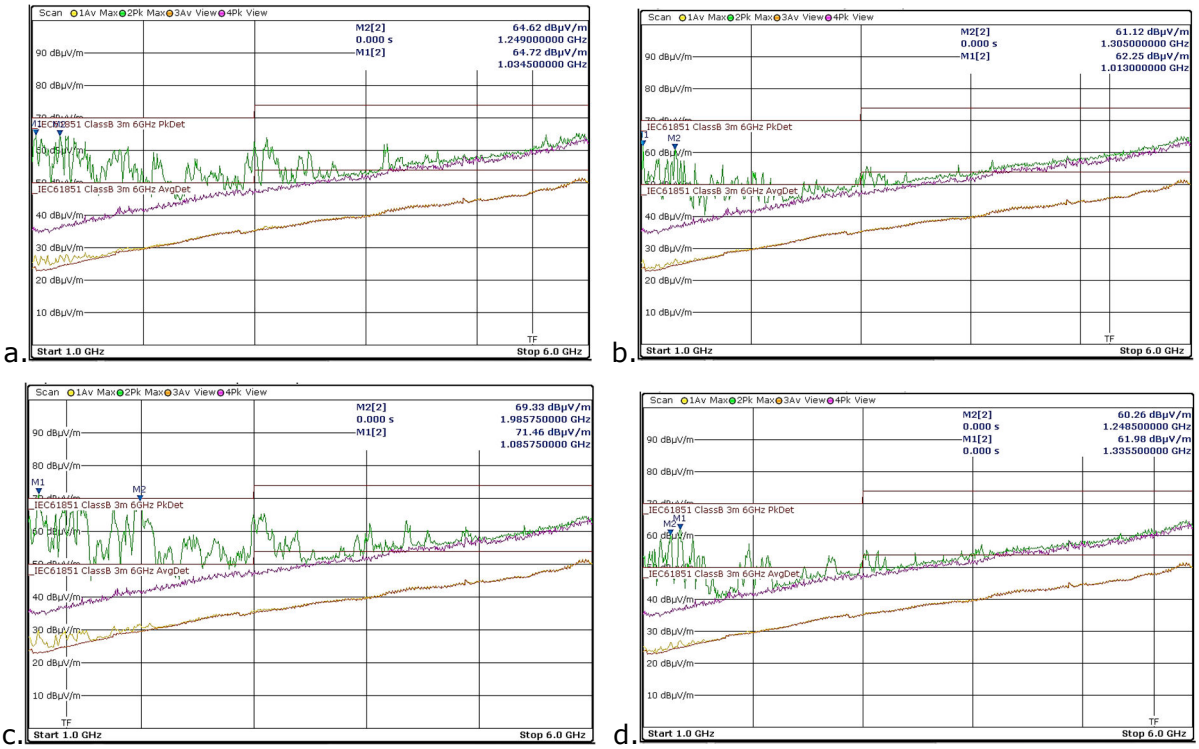

Figure 32: Charger 'B' H-pol, h=1.5m, (a) left, (b) rear, (c) right, (d) display

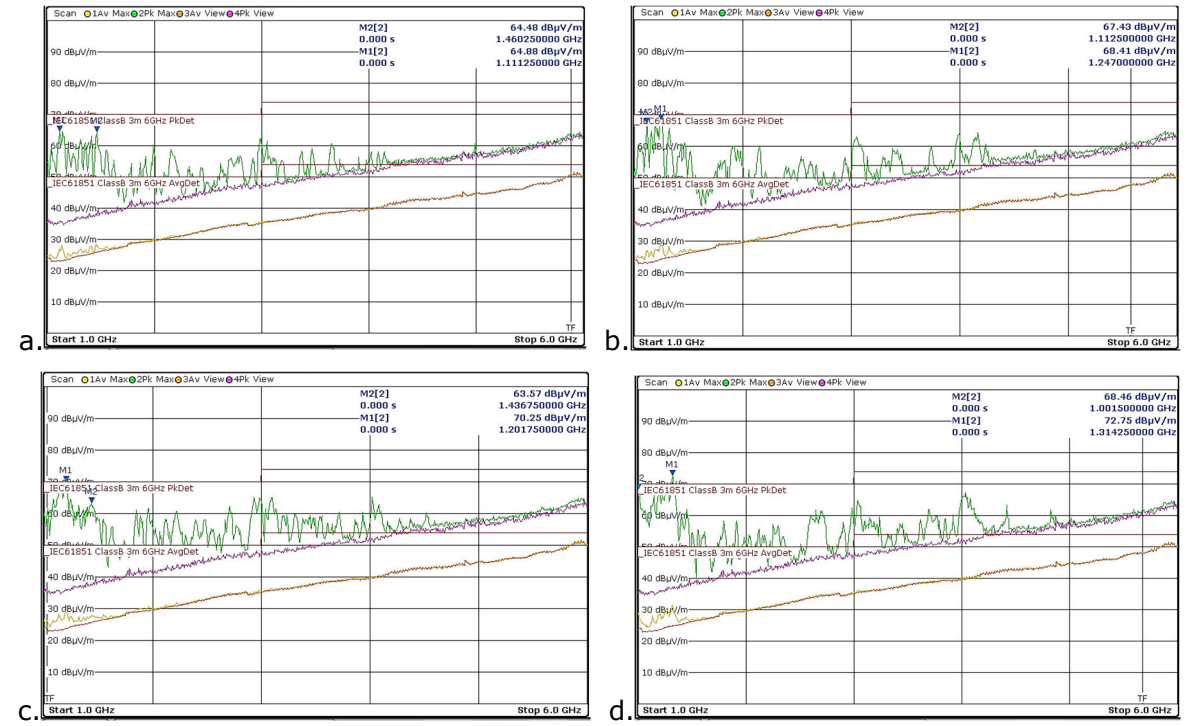

3.2.3 Radiated emissions for Charger ‘C’

Figure 33: Charger 'C' V-pol, h=1.5m, (a) display, (b) right, (c) rear, (d) left

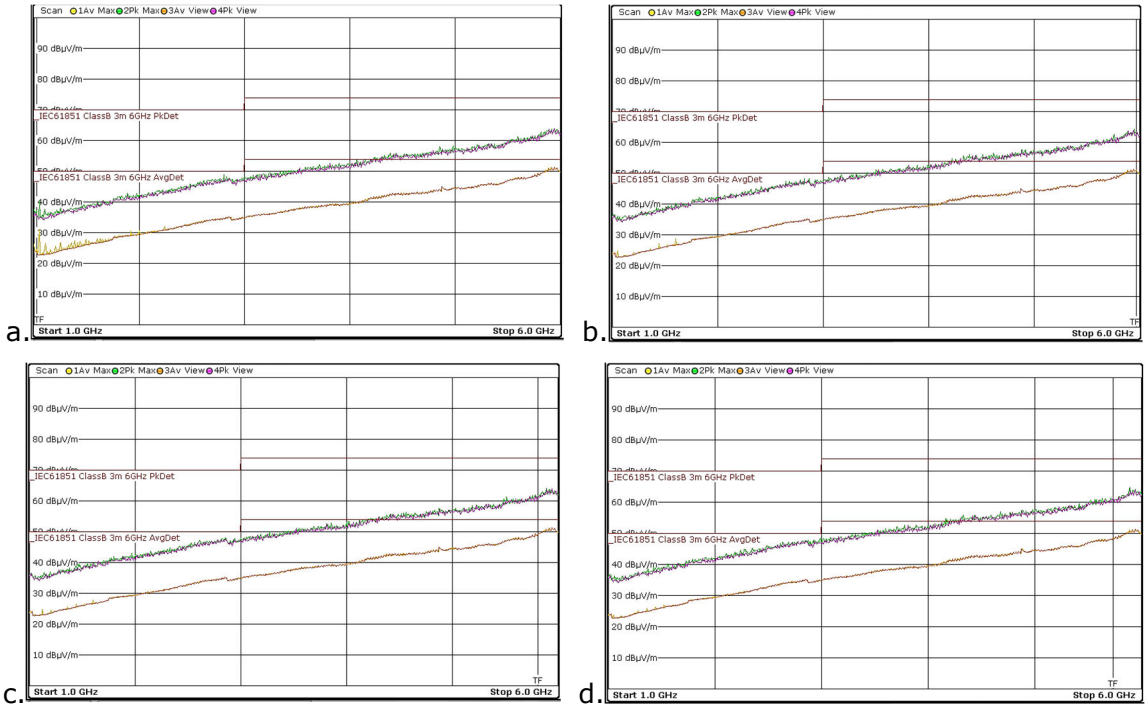

Figure 34: Charger 'C' H-pol, h=1.5m, (a) left, (b) rear, (c) right, (d) display

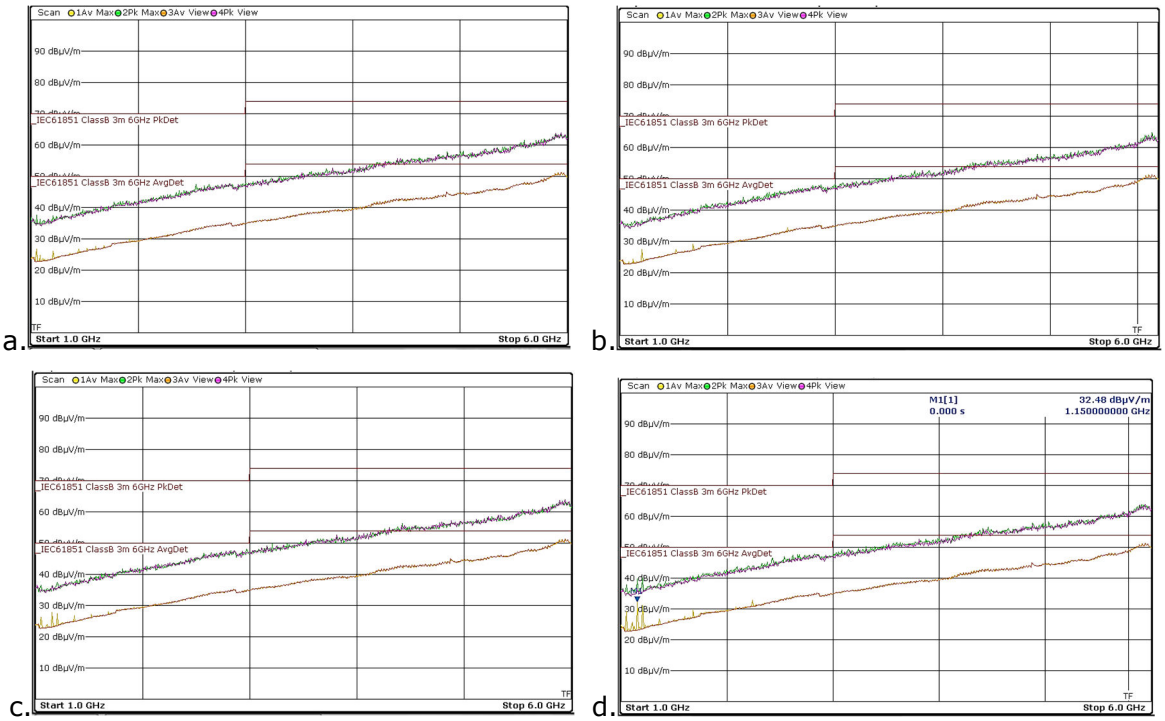

Figure 35: Charger 'C' V-pol, h=2.0m, (a) left, (b) rear, (c) right, (d) display

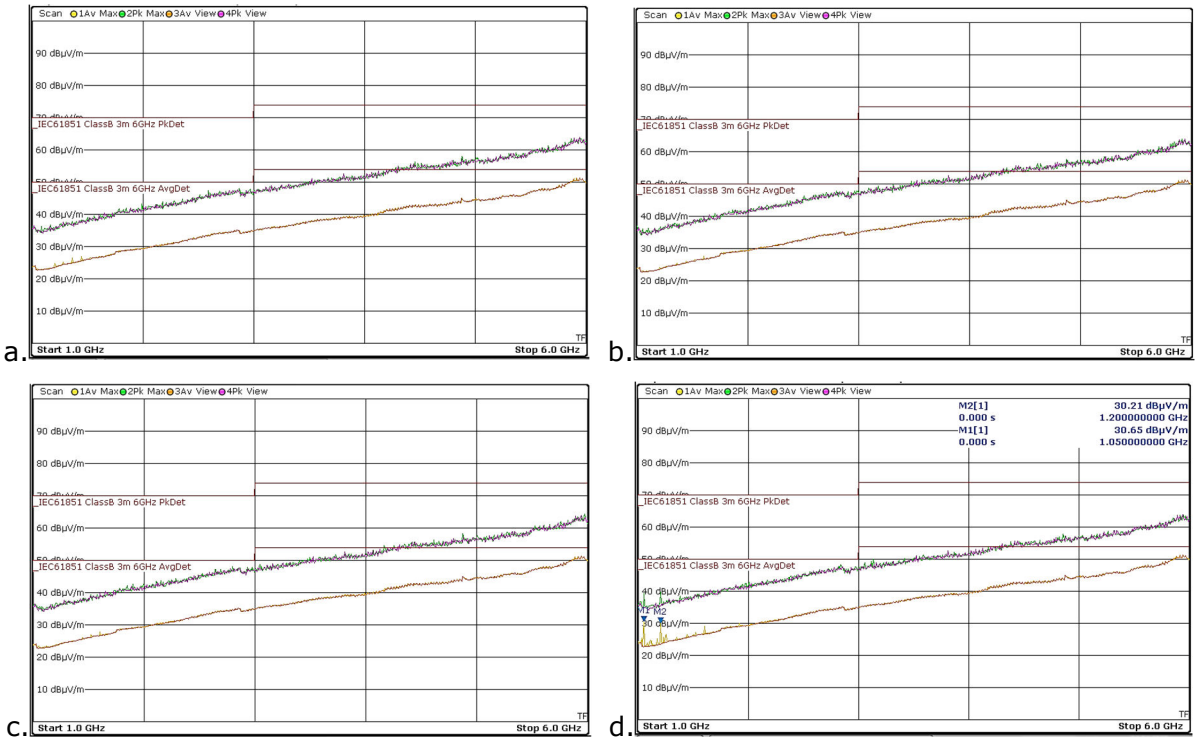

Figure 36: Charger 'C' H-pol, h=2.0m, (a) display, (b) right, (c) rear, (d) left

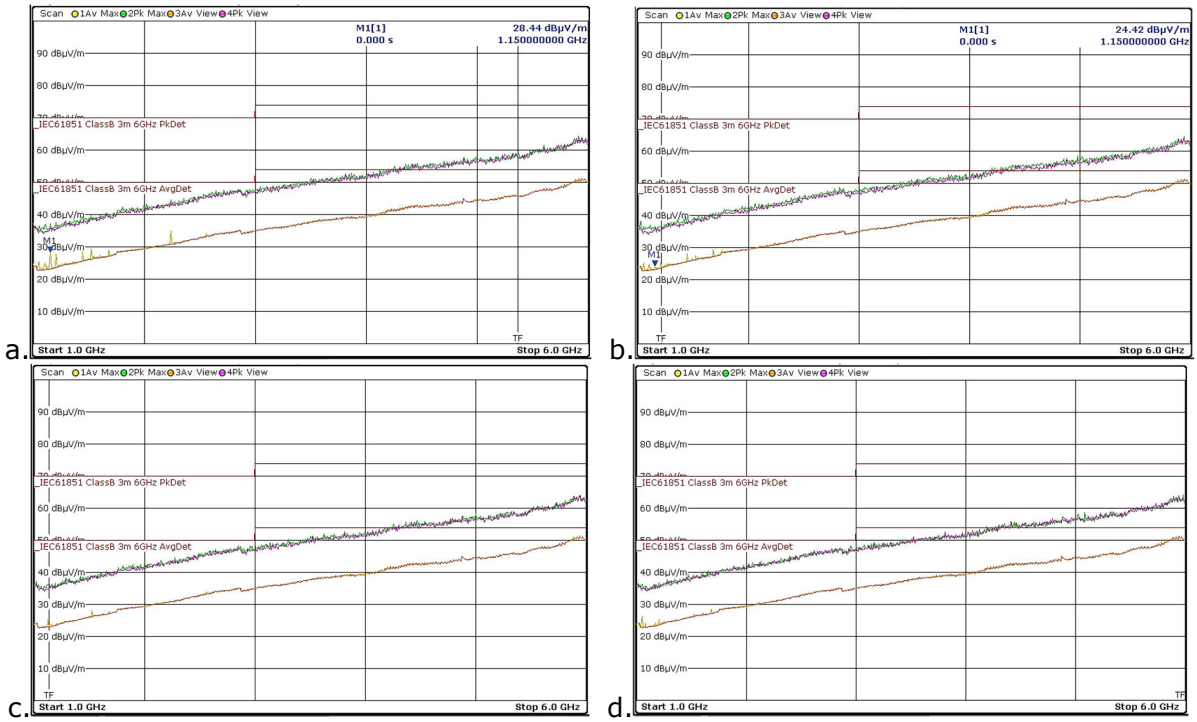

3.3 Discussion on radiated emissions results

3.3.1 Charger 'A'

The measured results of Charger 'A' between 30-1000 MHz, Fig. 11 to Fig. 16, indicated that the generated emissions were predominately narrowband in nature, which spanned all the way up to 1 GHz. For some setups, the levels of the emissions were extremely close or exceeded the limit, e.g. on the vertical polarisation for spot frequencies between 30 MHz to 200 MHz and on the horizontal polarisation for all antenna heights.

The results indicated as well than in general the horizontal polarisation picks up EMI, which was higher compared to the vertical polarisation. This could be due to the noise generated by the power line cable that lied in *parallel* to the floor and hence matched the antenna's polarisation (when horizontal).

The plots also illustrate that the interference was a combination of broadband and narrowband type interference. For instance, the rear side of the HPC, when the antenna was horizontally located 2m above the ground, Fig. 14(a), showed that the main broadband noise was centred close to 230 MHz, while multiple harmonics were also superimposed on the broadband envelope indicated by the 'needle' shape.

Furthermore, it was observed that on the vertical polarisation the display and left sides had in most cases more EMI than the rear and right side. This could be due to the noise pick-up from the display and/or the main charging cable (shown on Annex 1), which was vertically oriented on the left side of the column matching the polarisation of the antenna.

The placement of the HPC with the right side towards the antenna resulted in the lowest emissions, i.e. 'quiet' compared to the other setups: On this setup the AC power line cable, the RF ground cable and the charging cable were located furthest away compared to the other 3 different sides and this could be an explanation for the reduced emissions.

The radiated emissions of this charger in the 1-6 GHz band, Fig. 29-30, range were in general very close to the noise floor in the vertical polarisation. The horizontal polarisation identified some EMI close to 1.05 GHz and 1.09 GHz regions. However, above 2.5 GHz there was no deviation with respect to the noise floor. For these reasons, the tests on this frequency range were only carried out at 3m antenna height without any further investigation.

Based on the aforementioned measured results, the HPC has to improve the EMC aspect to fully satisfy Class B limits, and Class A limits with the suppression of the interference at 696 MHz. The worst emissions were noticed on the left side of the column, e.g. Fig. 12(b), 14(b), when the antenna was horizontally placed. It should also be noted that the cabinet material of the charger was *not conductive* and hence, there was no protection against any radiated interferences from within the unit.

The table below summarises the critical frequencies, i.e. those above or close to the limit, of Charger 'A':

Table 7: Charger 'A' critical radiated emission frequencies

Polarisation	**Critical frequencies (MHz)**
Vertical	39.57, 40.29, 52.98, 54.57, 132.87, 133.35, 192, 216
Horizontal	192, 216, 240, 264, 288, 336, 384, 432, 528, 552, 600, 624, 648, 672, 696, 792

The importance of the antenna height scan on this series of measurements was also evident by examining the critical frequency, for example, at 696 MHz, in the horizontal polarisation and on the left side of the HPC column, figures 12(b), 14(b) and 16(b). For an antenna height of h=1.5m the strength of this emission was at 46.71 dBμV/m, then at h=2m it reduced slightly to 46.22 dBμV/m, but when the antenna was placed at h=3m its level was only just above 35 dBμV/m. So, a *lower* antenna positioning managed to identify a *stronger* emission in this case for the frequency at 696 MHz.

3.3.2 Charger 'B'

From the measured results of charger 'B' between 30 MHz to 1 GHz, Fig. 17-22, we immediately observe that the level of EMI was significant and exceeded by far, especially in the vertical polarisation, both Class A and Class B limits. In the vertical polarisation the major interferer was centred at about 33 MHz and in the horizontal polarisation at 130 MHz, 152 MHz and 219 MHz. The maximum reference level on the vertical axis of the instrument's display was set to a higher value, i.e. 100 dBμV/m, compared to charger 'A' (50 dBμV/m), in order to fit entirely the maximum level of the emissions.

The strength of the electric field picked up by the EMI received required to turn OFF the internal pre-amplifier in order to avoid overloading the intermediate frequency (IF) stage. The worst case emission level was identified on the right side of the charger, which was more than 70 dBμV/m at frequencies close to 32.8 MHz for the vertical polarisation and h=1.5m above the SAC floor.

The measurements up to 6 GHz indicated that the EMI was still evident as seen from the deviations of the electric field with respect to the noise floor, Fig. 31, 32. At 1.08 GHz the emissions were just above the limit for the peak detector from the rear side of the column in the vertical polarisation and h=1.5m, Fig. 31(c). In the horizontal polarisation, the peak detector exceeded, as well, the maximum allowed limit when the antenna was viewing the right and the display side at frequencies 1.20 GHz, Fig. 32(c), and 1.314 GHz, Fig. 32(d). These disturbance frequencies above 1 GHz fall close to the satellite signals that some radio navigation devices are utilizing, as reported for example on [13].

The measurements at 1-6 GHz were carried out *with* the internal pre-amplifier of the EMI receiver, as this did not cause overloading of the IF section of the instrument. In general, the radiated emissions up to 4.5 GHz were evident all around the four sides of the charger at standby and for all antenna heights above the ground.

The table below summarises the critical frequencies, i.e. those above or close to the limit, of Charger 'B':

Table 8: Charger 'B' critical radiated emission frequencies

Polarisation	**Critical frequencies (MHz)**
Vertical	32.73, 54.6, 61.26, 63.99, 76.35, 112.5, 157, 1086, 1986
Horizontal	40.08, 61.32, 130.59, 142, 152.01, 162.51, 211.29, 215.18, 218.64, 220.02, 1001, 1112, 1202, 1247, 1314

3.3.3 Charger 'C'

The profile of charger 'C' in terms of its emissions was generally 'quiet' and did not show any particular EMC issues. Clearly, there were deviations of the response with respect to the noise floor, but these were mostly concentrated up to 500 MHz or so. Based on the measured plots, the EMI contained a mixture of discrete harmonics, caused perhaps by the digital/clock frequencies, superimposed with broadband type noise. This was seen for example on the display side, Fig. 27(a), on the vertical polarisation when h=3.0m. Broadband noise was observed at 51 MHz, 76MHz and about 300 MHz, next to interference due to harmonic components.

We also observe that the display side emitted in principle more RF noise than the other sides. On the horizontal polarisation, the HPC was challenged by a harmonic at 175 MHz (display side at h=3.0m, Fig. 28(d)) and 225 MHz (left h=3.0m, Fig. 28(a) and h=2.0m, Fig. 26(a)), which were extremely close, nevertheless below, the limit.

For the spectrum between 1 GHz and 6 GHz, Fig. 33-26, the deviation was very minor for all laboratory setups in consideration.

The table below summarises the critical frequencies, i.e. those above or close to the limit, of Charger 'C':

Table 9: Charger 'C' critical radiated emission frequencies

Polarisation	**Critical frequencies (MHz)**
Vertical	none
Horizontal	175, 225

4 Conducted Emissions Testing

The measured results of the conducted emissions for the three HPC columns are presented next.

4.1 Conducted emissions for Charger 'A'

Figure 37: Charger 'A' Conducted Emissions Quasi-peak detector (a) Phase, (b) Neutral lines

a.

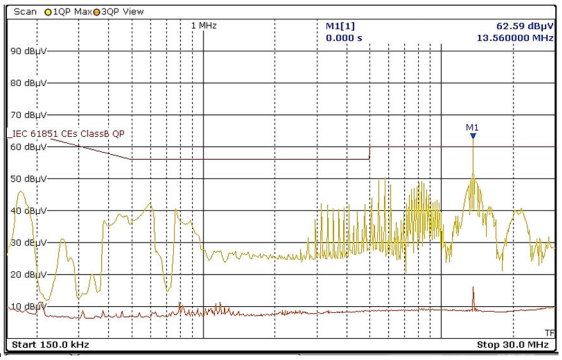

b.

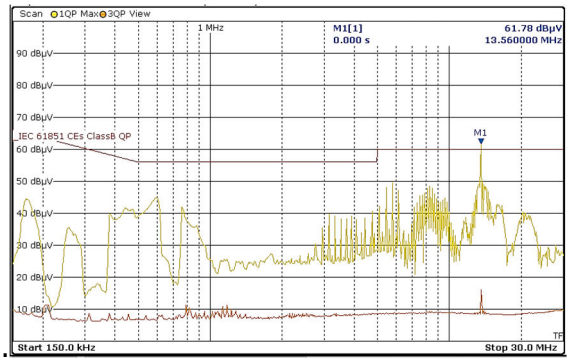

Figure 38: Charger 'A' Conducted Emissions Average detector (a) Phase, (b) Neutral lines

a.

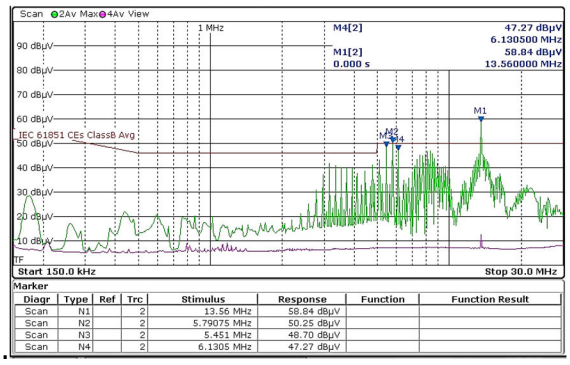

b.

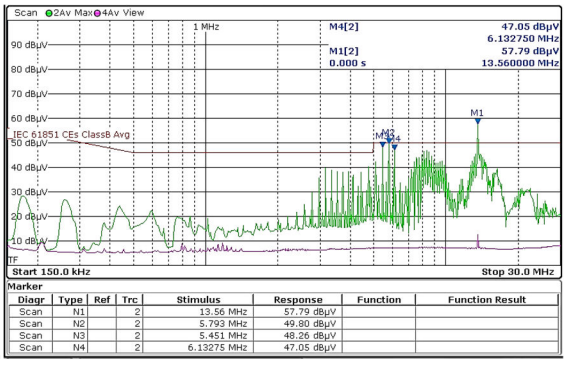

4.2 Conducted emissions for Charger 'B'

Figure 39: Charger 'B' conducted emissions (a) Quasi-peak detector, (b) Average detector, [Traces: 1. Phase, 2. Neutral, 3. Noise floor]

a.

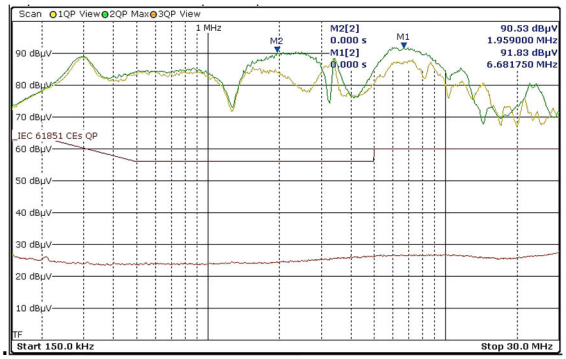

b.

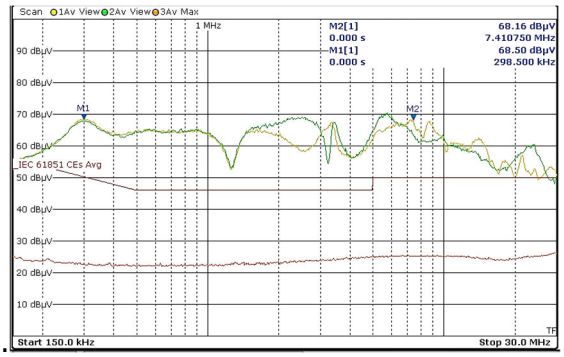

4.3 Conducted emissions for Charger 'C'

The connection of the three-phases to the main grid for the power supply of charger 'C' required the use of ENV4200 LISN, which had a 3-phase ports, instead of the LISN1600 which had connection for a 1-phase load. At the same time and during the execution of the measurements, the grid supply of VeLA 9 was installed with an earth safety switch, which would allow a leakage current (towards earth) up to 30mA before forcing a complete power shut-down.

The leakage current produced by the ENV4200 was around 150mA and for this reason it was necessary to provide power supply to the EUT through the ENV4200 using a separate and external to SAC main grid network that had an elevated leakage current of 300mA. This requirement introduced an additional safety concern though: The presence of *two separate grounds*, one from the SAC and the other one from the external grid, required to check that there was no differential voltage between them. For this reason, an electrical assessment was carried out and it was verified that that both grounds presented the same (zero) voltage potential.

In addition, after the connection of the two separate mains lines the noise floor was re-checked to ensure that no unwanted EMI was introduced into the receiver port of the LISN.

The results of the conducted emissions for Charger 'C' are depicted in Fig. 40.

Figure 40: Charger 'C' conducted emissions (a) Quasi-peak detector, (b) Average detector [Traces: 1.Line-1, 2.Line-2, 3. Line-3, 4. Noise floor]

a.

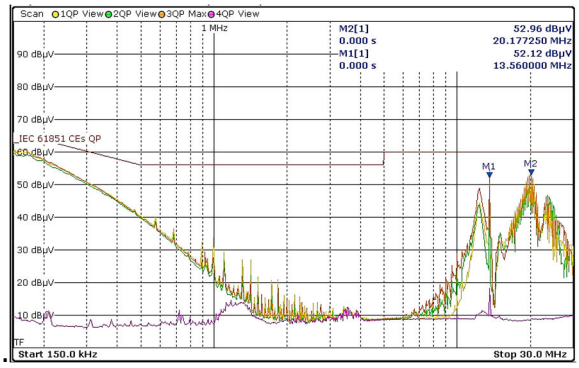

b.

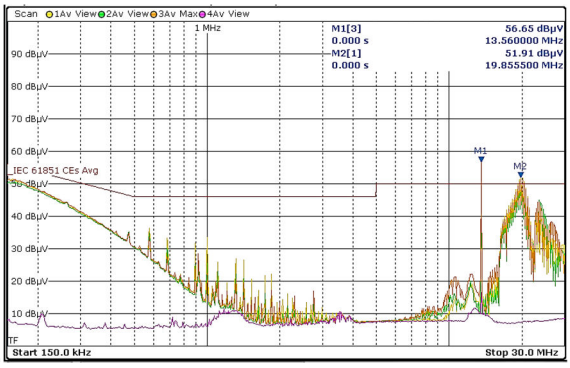

4.4 Discussion on conducted emission results

For the evaluation of the conducted emissions, the LISN was connected between the main grid and the input AC power port of the HPC. As discussed previously, Chargers 'A' and 'B' had one phase 230VAC line and so LISN 1600 was used, while charger 'C' a 3-phase 230VAC line, without neutral line, which the LISN ENV4200 could accommodate.

4.4.1 Charger 'A'

From Fig. 37, 38, Charger 'A' showed a spot frequency at 13.56 MHz, which exceeded the limit in all test setups, both on the Phase and Neutral wire and for both type of detectors (quasi-peak and average). The worst case level was 8.8 dB above the limit on the phase line with the average detector. In addition, both lines had emissions close to the limit, for the average detector measurements. These were located at 5.45 MHz, 5.79 MHz and 6.13 MHz, almost uniformly spaced by 35 MHz: This was an indication that these frequencies could be generated by digital clock harmonics. Such a uniform spacing pattern is particularly visible between 2 MHz and 10 MHz, noting the log-scale on the horizontal axis.

4.4.2 Charger 'B'

The conducted emission measurements of Charger 'B', Fig. 39, indicated that the emission levels were excessively above the limit both on the Phase and Neutral lines and all across the spectrum in consideration (150 kHz - 30 MHz). The measurements exceeded 90 dBμV with the quasi-peak detector and reached almost 80 dBμV with the average detector. As it will be shown later, providing a RF ground for this charger did not supress these high emissions.

4.4.3 Charger 'C'

The plots of the conducted emissions in Fig. 40, showed that Charger 'C' was below the limit with the quasi-peak detector, but it exceeded it with the average detector at 13.56 MHz and 19.85 MHz by 6.6 dB and 1.9 dB, respectively. Among these frequencies, the first one (13.56 MHz) appeared to be caused by an oscillator/resonator operation indicated by its narrowband response [this frequency was also captured on the conducted emissions of Charger 'A']. On the other hand, the emission at 19.85 MHz contained multiple near-spaced harmonics, which could be an indication of non-linearity caused by digital clock signals.

It is interesting to note that the response for both type of detectors showed a decreasing 'slope' starting from 150 kHz towards 2 MHz. Such a behaviour points to an EMI source, which could be generated by the high-frequency switching signals managed by a rectifier or a power supply unit, or by the harmonics of the 50 Hz fundamental frequency.

5 Radiated Immunity (susceptibility) testing and discussion

The radiated immunity tests were performed by observing the functionality of the display when the HPC column was exposed to an electric field from the same direction.

During the exposure, the display of Charger 'A' started to flick at around 840 MHz in the vertical polarisation, while a 10 V_{rms}/m 80% AM-modulated field strength was applied. However, the display managed to restore itself after the removal of the externally applied electric field. In the horizontal polarisation, the condition on the display did not change under the presence of any level of electric field all across the frequencies in consideration.

As an additional test to susceptibility for Charger 'A', the antenna tip moved close to d=1m away from charger facing the display side and a height of h=1.5m above the SAC floor. Based on the manufacturer's antenna datasheet [11] and for an input power of 25W, the electric field strength generated at 1m distance exceeds 50V/m. On this scenario, it was noticed that the display remained OFF (i.e. 'black' screen) completely throughout the exposure at frequencies between 816 MHz and 883 MHz in the vertical polarisation. A similar result was observed at 840 MHz in the horizontal polarisation. The situation is visualised in figure 41. The display was restored though after the removal of the external electric field without requiring intervention e.g. restarting the charger.

Figure 41: Charger 'A' immunity tests. Photo on the left shows the user-display in the ON state without any external electric field applied. Right photo: The display goes OFF when the column is exposed to an electric field for frequencies between 816 MHz and 883 MHz. On this setup the antenna was placed 1m away from display and 1.5m above the ground.

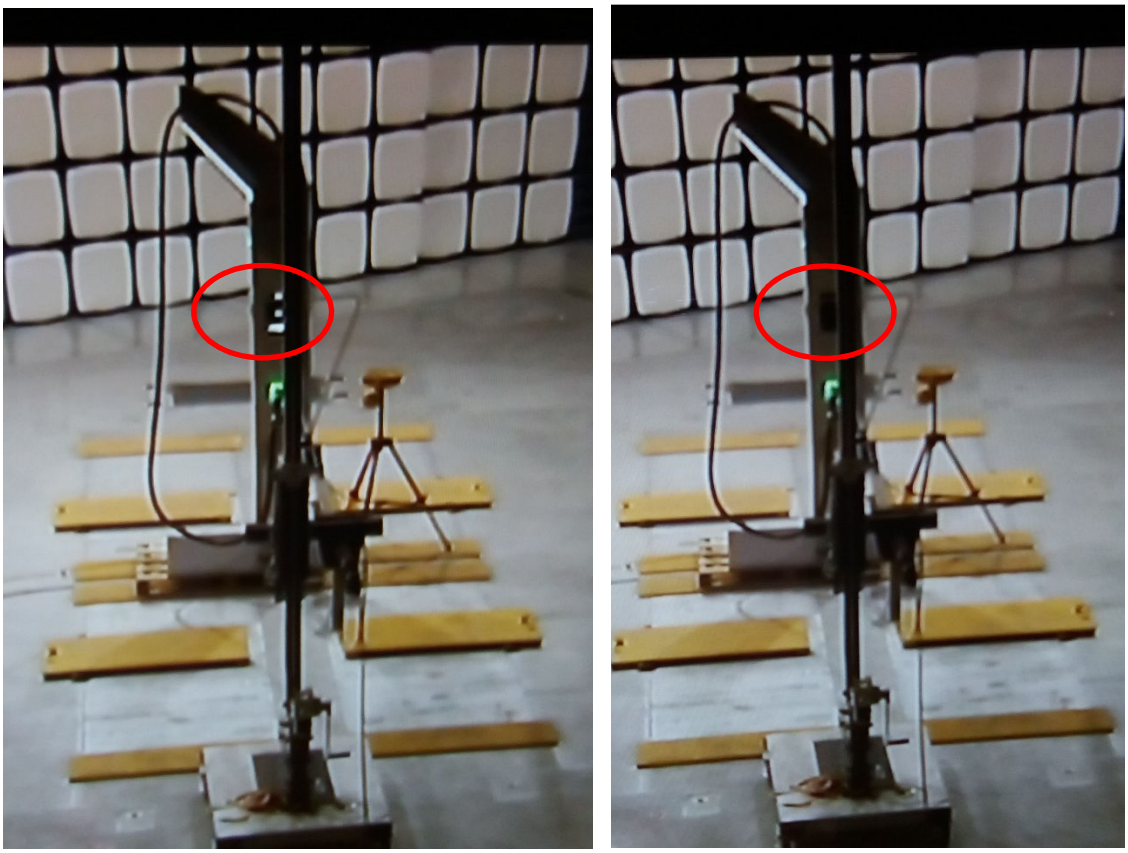

Charger 'B' was found to be susceptible to 810MHz in the vertical polarisation. On this setup, the display was 'flickering' throughout the presence of the electric field, however it restored itself after the termination of the exposure to this field. In all other conditions, the indication on the display was as expected.

Charger 'C' did not show any deviation of its condition during the immunity testing either in the horizontal or vertical polarisation and for all frequencies in consideration.

5.1 Conclusions on immunity testing

The measurements inside the SAC indicated that two of the three chargers presented an immunity issue on the display side during electric field exposure. More specifically, their displays flickered at frequencies close to 840 MHz and 810 MHz, respectively for the chargers 'A' and 'B'.

The aforementioned finding could introduce a potential situation for an EMI issue as some mobile phone services rely on the 800 MHz bands [13, 14] for the communication, which fall close to the critical frequencies on the immunity testing. To make this clear, let us consider a simple example of the electric field level that is generated by a mobile phone handset. The electric field equation [7] is expressed by:

$$E = \frac{1}{r} \times \sqrt{30 \times Pt \times Gant} \text{ V/m}$$

where,

E is the electric field strength (V/m)

r is the distance from the transmit source

Pt is the transmitted power and

Gant is the antenna gain (linear)

Taking as an example a typical cell phone transmit power of Pt=0.5W and an antenna gain of Gante=0.5 ('lossy' antenna), at a distance of r=0.05m the established electric field is 54V/m. Of course, the presence of the user, e.g. his/her hand, can greatly affect the actual field strength, i.e. reduce it due to the losses introduced by the obstruction. We see from this theoretical calculation though that a cell phone is able generate field levels that are comparable to the field strengths of the laboratory immunity tests at close distances.

6 EMC troubleshooting

This section provides a brief description of practical EMC remedies that were applied to selected laboratory setups in order to supress critical emissions.

6.1 EMI remedies for Charger 'B'

6.1.1 Impact of internal cooling fan system

The excessive EMI levels generated by Charger 'B' were a clear indication that the EMC aspect of the HPC required improvements. For the operation of the charger at 230VAC in standby mode, the manufacturer indicated that specific wires should be bridged in order to allow operation of the internal cooling fan system (ventilator). This connection is shown in Fig. 42.

Figure 42: Connection requirement (red wire) for the operation of the internal fan system of charger 'B' (blue and brown wires coming from the HPC enclosure)

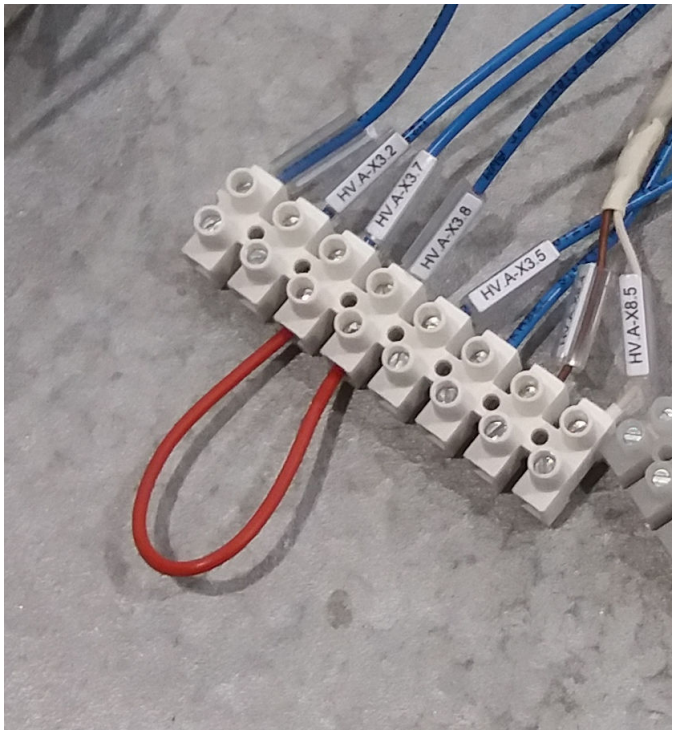

An experiment was carried out to understand whether the fan system was contributing, in any way, to the excessive EMI on the radiated and conducted emissions. For this purpose, the shunt (red wire in Fig. 42) was removed in order to isolate, i.e. de-activate the fan system completely and then, the emission measurements for specific setups were repeated. The results, firstly for the radiated emissions, are shown on the next four figures, for 30-1000 MHz (Fig. 43, 44) and 1-6 GHz (Fig. 45, 46) respectively, both in the vertical and horizontal polarisations.

Figure 43: Charger 'B' radiated emissions (vertical polarisation, d=10m, h=3m) with cooling fan system OFF (a) display, (b) right, (c) rear, (d) left

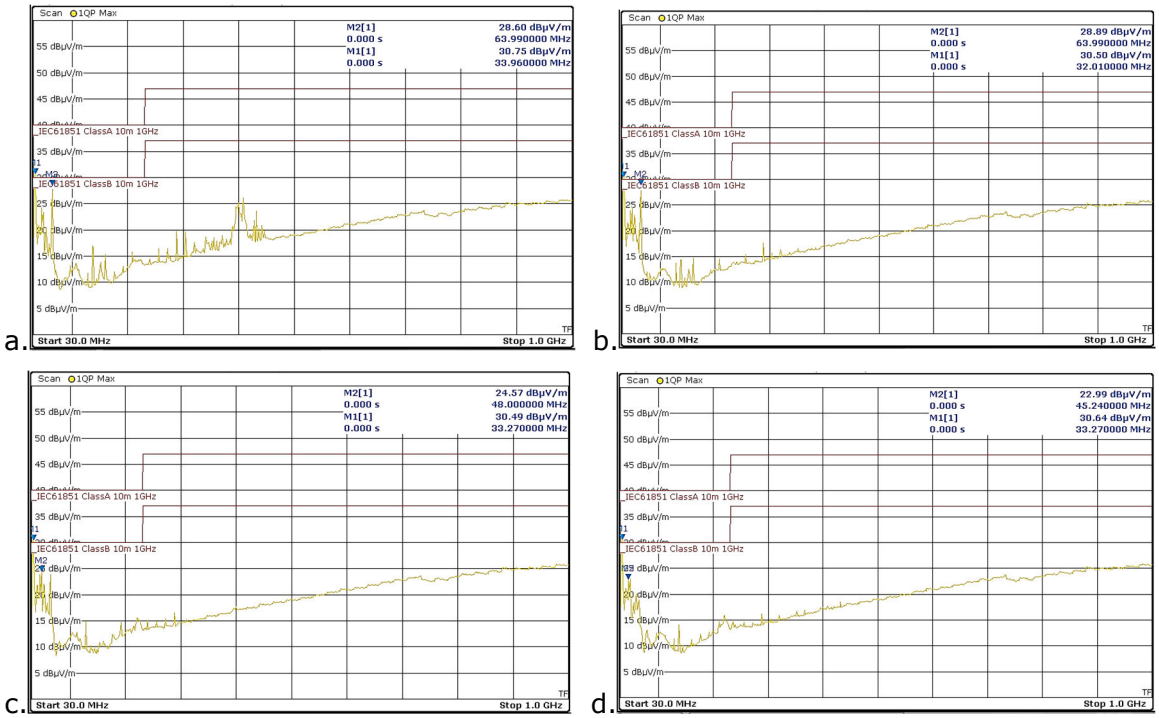

Figure 44: Charger 'B' radiated emissions (horizontal polarisation, d=10m, h=3m) with cooling fan system OFF (a) left, (b) rear, (c) right, (d) display

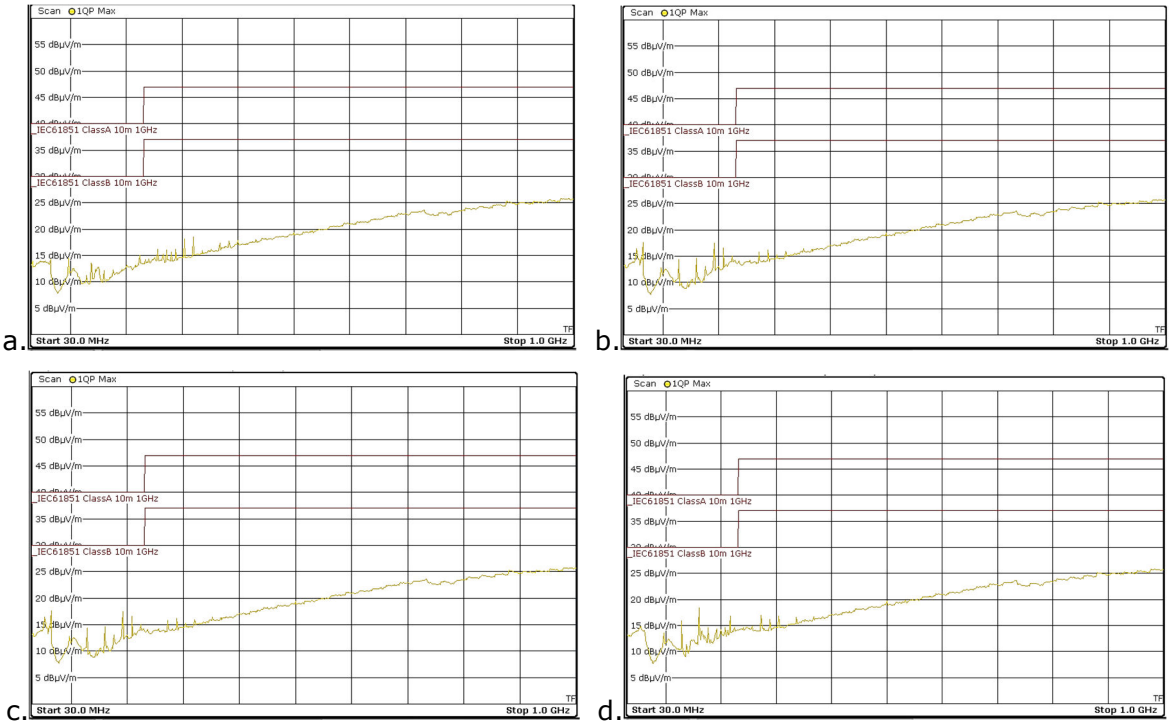

Figure 45: Charger 'B' radiated emissions (vertical polarisation, d=3m, h=1.5m) with cooling fan system OFF (a) display, (b) right, (c) rear, (d) left

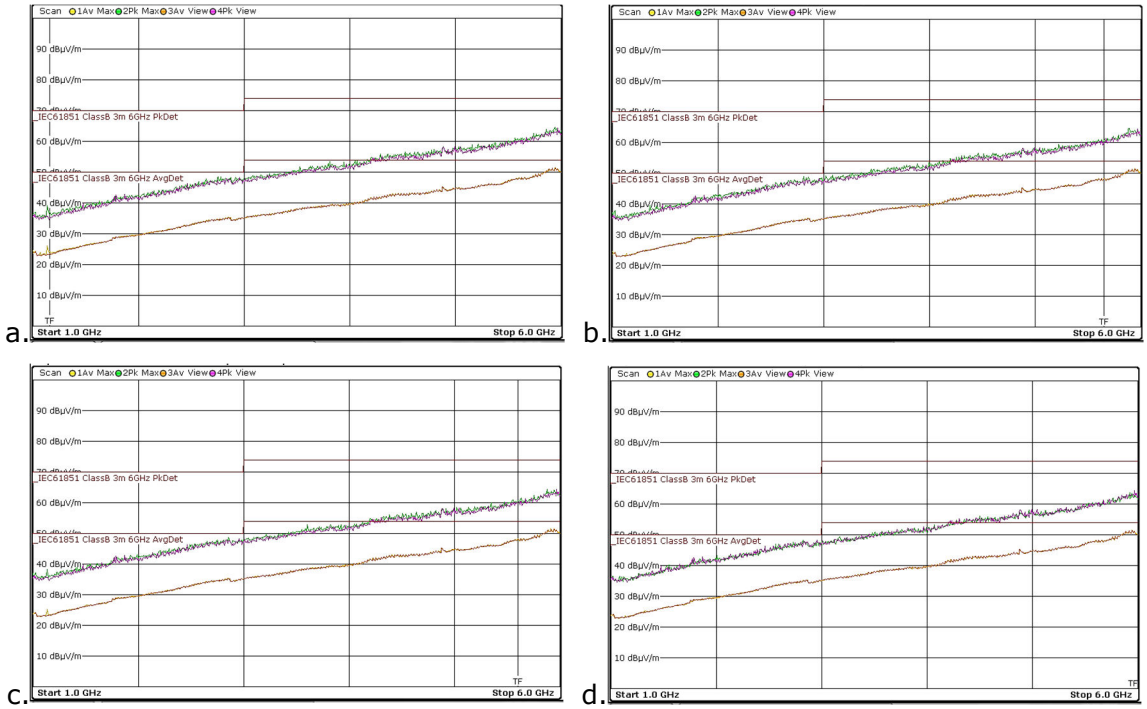

Figure 46: Charger 'B' radiated emissions (horizontal polarisation, d=3m, h=1.5m) with cooling fan system OFF (a) left, (b) rear, (c) right, (d) display

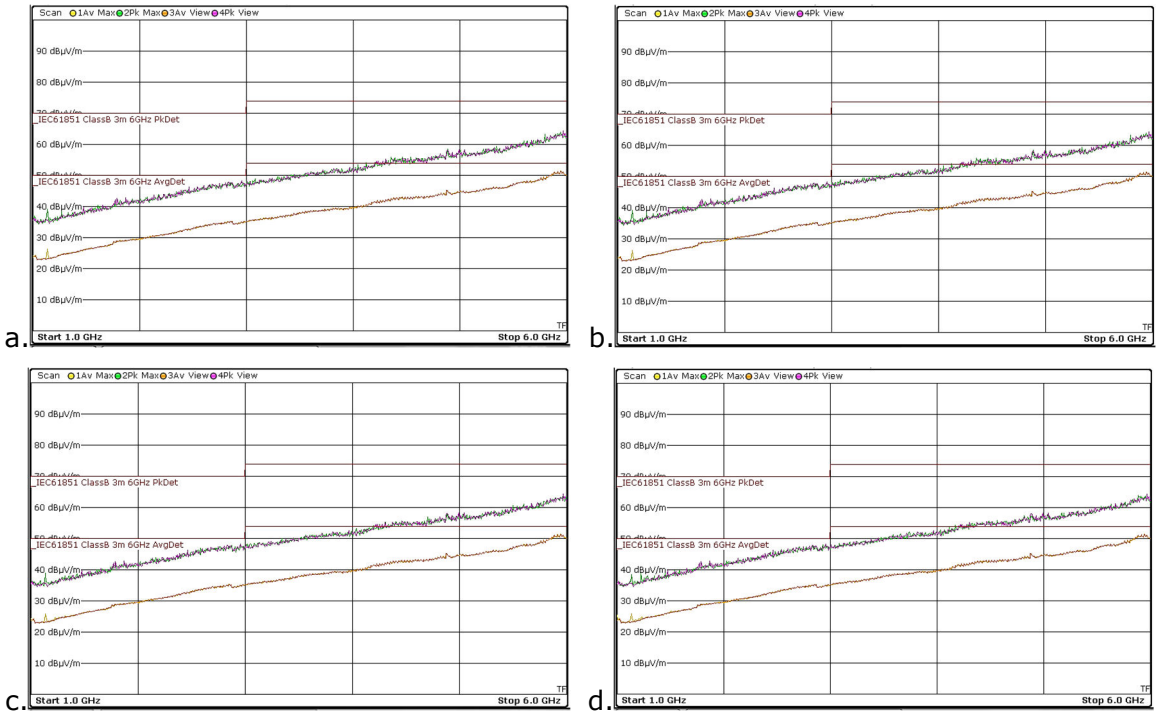

The measured responses, Fig. 43-46, illustrate that the radiated EMI levels were substantially lower after the removal of the red wire in Fig. 42. From this finding, it was immediately evident that the main cause of the above-the-limit radiated emissions discussed on previous section, Fig. 17-22, was the fan system. With the fan system isolated, the emissions of the charger were within the Class A limits and as well satisfied (marginally) the Class B limits too, with the exception of the emissions at 34 MHz and 64 MHz, which were challenging the 30 dBμV/m limit line. For the frequencies between 1-6 GHz, the HPC column showed almost no deviation with respect to the noise floor, contrary to the severe deviations that were identified before the modification, Fig. 31 and 32.

In a similar analogy, the conducted emissions were also repeated for Charger 'B' with the cooling fan system de-activated. The results are shown in Fig. 47.

Figure 47: Charger 'B' conducted emissions with fan system OFF (a) quasi-peak and (b) average detector [Trace: 1.Phase line, 2.Neutral line, 3. Noise floor]

a.

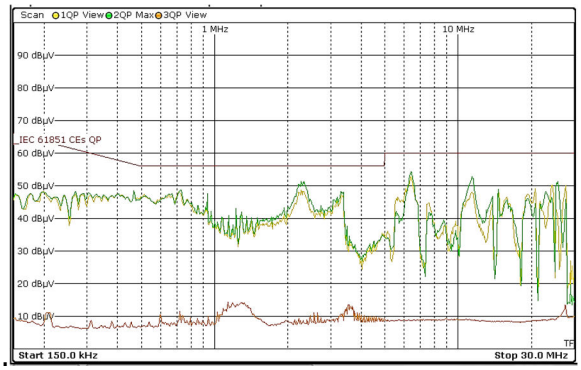

b.

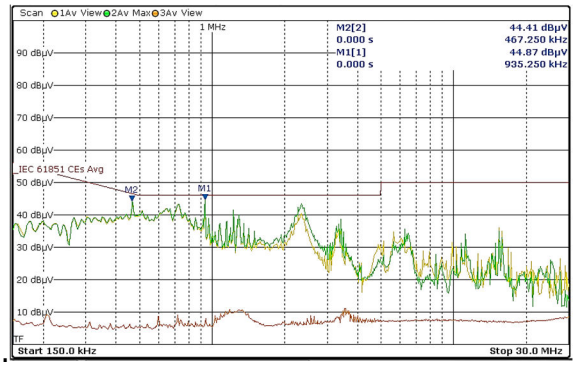

The response of the conducted emissions, both phase and neutral lines, showed now that the level of EMI reduced drastically (compare Fig. 47 with the responses on Fig. 39) when the fan system was not active. There were two critical frequencies captured with the average detector at 467 kHz and 935 kHz, which were extremely close to the limit, however the disturbances were in general significantly lower than before.

In conclusion, the strong interferences observed on Charger 'B' both on the radiated and the conducted emissions were largely affected by its internal fan system. It is believed that the cause of the problem was not be the *fan alone*: While the fan system was active, it was observed that the fan started to spin about 10 minutes after HPC was switched-ON, however no deviation on the EMI levels were observed during this event. Hence, it was understood that the excessive EMI was caused by the *fan system*, which could include the electrical and electronic boards and components that were controlling the fan, e.g. the temperature sensor units, switching relays, power supplies or other submodules, which were responsible for the control of the fan. Details of the internal circuitry, the schematics or the wire connections of the HPC were not provided to us in order to identify physically the part within the HPC that was attributing to this EMI issue.

6.1.2 Effect of RF grounding on EMI

In order to examine the effect of the RF ground on the EMI profile of the HPC (Charger 'B') the main chassis was grounded to the ground surface of the SAC using a very short cable.

Representative setups of the radiated emissions were carried out with the receive antenna viewing the display side of the HPC. The measured results of this setup are shown in Fig. 48.

Figure 48: Radiated emissions charger 'B' (display side) with RF ground between its main chassis and the SAC ground d=10m, h=3m (a) vertical, (b) horizontal polarisation

a. 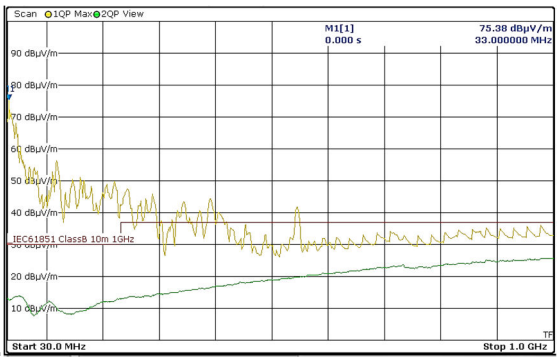

b. 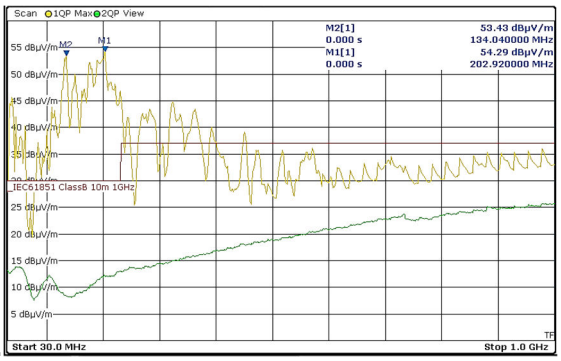

It was seen that the installation of the RF ground did not provide any improvement whatsoever on the EMI profile generated by charger 'B' during standby. The opposite happened actually, since the maximum radiated emissions *increased* almost by 5 dB as is shown in Fig. 48(b) above in the horizontal polarisation, with respect to the case when no RF ground, Fig. 22(d), was installed. In addition, the emissions close to 30 MHz, 250 MHz and 350 MHz were also increased when then HPC chassis was grounded.

6.2 Charger 'C'

6.2.1 Effect of display on EMI

For charger 'C' a simple modification was applied to examine the contribution of the display to the EMI emissions. For this setup, the display of the HPC was completely covered with an aluminium foil and as the paint applied to the enclosure of the HPC was not conductive, the aluminium foil was then grounded to the HPC ground by applying a copper tape 'path' to the system ground around the main chassis door, as shown in Fig. 49.

Figure 49: Investigating the contribution of the display to the overall EMI. The aluminium foil (in silver colour) completely covered the HPC display and was fixed with adhesive copper tape. Then the foil was connected to the HPC ground by using an additional copper tape towards the (right side on the photo) HPC conductive enclosure behind the main door.

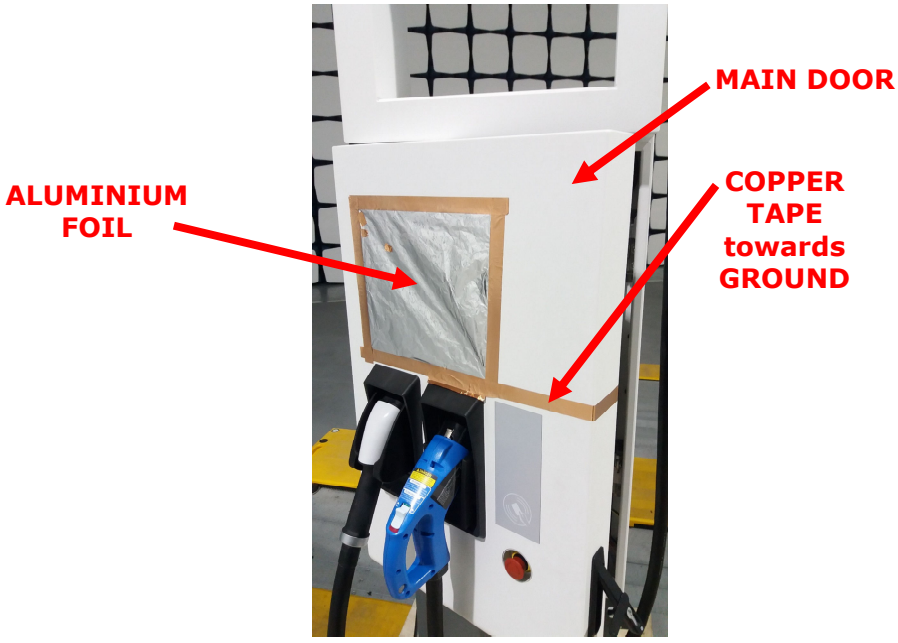

Figure 50: Charger 'C' radiated emissions (horizontal polarisation, d=10m, h=3m) display side, main trace with the quasi-peak detector in yellow colour, green trace: noise floor, others used for reference. Major interference at 175MHz (red circle) reduced when the display was fully covered with aluminium foil.

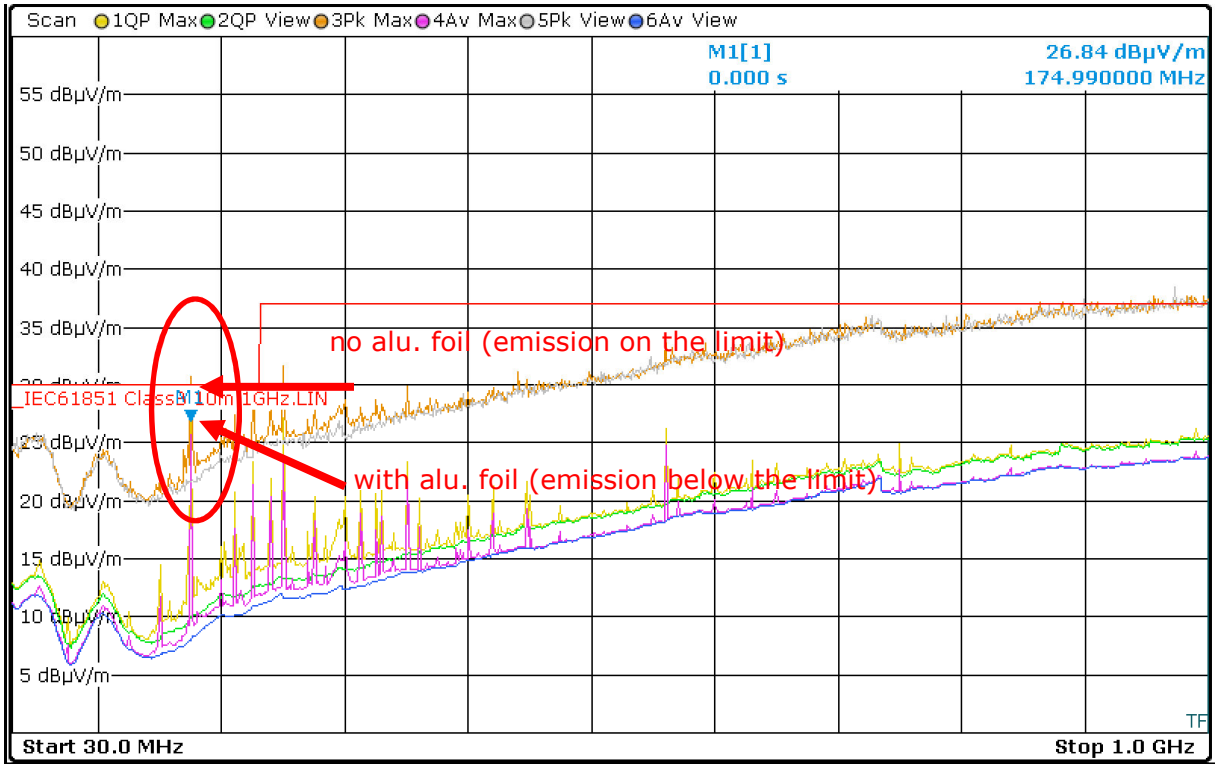

The measured results of the radiated emission when the display was covered completely with an aluminium foil are presented in Fig. 50 (above). It is seen that the aluminium cover provided a reduction of the spot emission at 175 MHz by about 2.5 dB with respect to the level shown in Fig. 28(d) when the display was exposed to the antenna. However, it is believed that the EMI could have improved further on this experiment should the cabinet was painted with a conductive material, instead of providing a 'long' (and perhaps not very efficient) ground all around the front door of the HPC towards the inside of the enclosure.

6.2.2 Impact of RF filtering with ferrites on the conducted emissions

A simple test was carried out in order to investigate the effectiveness of commercial clamp-on ferrites on the suppression of the conducted emissions. The ferrites selected for this purpose were by FAIR-RITE (#0431177081) [15], which corresponded to manufacturer's material No. 43. The reason for selecting this specific type of ferrite material was because it was effective in supressing EMI from 1 MHz up to 300 MHz. From the conducted emission measurements that we presented before, we have seen that indeed the majority of the critical interferences were concentrated on this frequency band and hence there was a good match between the interference frequencies and the specifications of the ferrite material. The ferrite units were installed on each phase wire close to the LISN ports, as is shown on the next figure.

Figure 51: Charger 'C' installation of clamp-on ferrites to investigate their effectiveness on the suppression of the conducted emissions. Thick wires go towards the HPC column.

The measured response of the conducted emissions on each phase with the introduction of the ferrites, is presented on Fig. 52.

Figure 52: Charger 'C' conducted emissions (average detector)
[Traces: 1. Phase-1, 2. Phase-2, 3. Phase-3, 4. Noise floor]

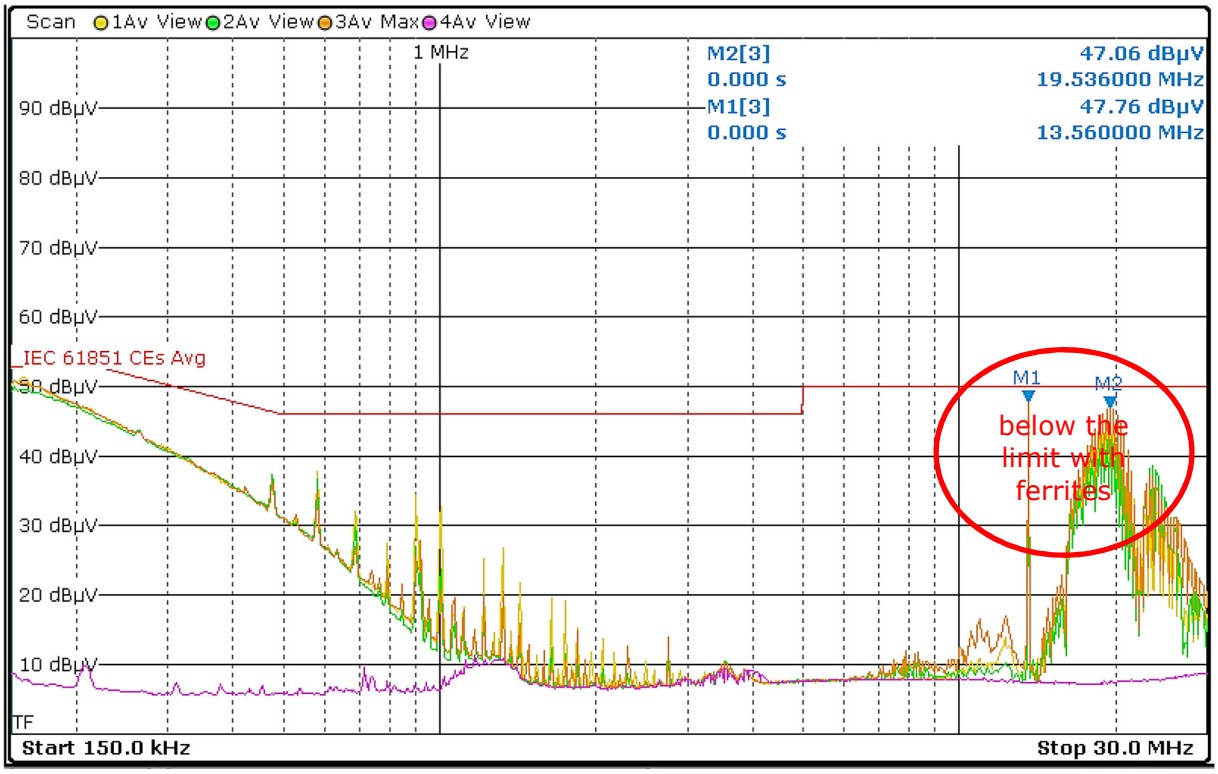

As seen from the responses in Fig. 52, the narrow-band harmonics, which exceeded the limits at 13.56 MHz and 19.5 MHz, Fig. 40(b), were reduced below the limit with the insertion of the aforementioned ferrites on each phase line. The ferrites were installed on each wire individually and hence this type of installation was effective for the suppression of differential-mode conducted noise. Having one ferrite encircling at once *all* 3 wires would have provided an effectiveness against the common-mode interference [2].

7 Measurement considerations

The quasi-peak detector, compared to a peak detector, as defined on IEC 61851-21-2 for the radiated emissions between 30-1000 MHz and the conducted emissions, is less responsive, i.e. in terms of its ability to identify the maximum level of a short in duration emission [2]. This is due to the fact that this type of detector is based on long charge time constant, which is 1ms on ESR7 EMI receiver [12]. Furthermore, interferences that have low repetition rates require longer MT in order to ensure that the receiver spends sufficient time at each frequency for capturing the signals.

The aforementioned fact was considered for Charger 'A' as it was noticed that some RF disturbances were not continuous, but rather they presented a short in duration ON-OFF periodic pattern. Under such situations it was necessary to increase the MT in order to capture the interferer. For this reason, the MT for the quasi-peak detector of Charger 'A' was set to MT=10secs (from MT=1sec) for 30-1000 MHz, MT=5sec for 1-6 GHz (from MT=1sec), while the MT for the measurement of the conducted emissions with the average detector was set to 1sec (from MT=50msec). One frequency, for example, that presented such a repetitive pattern on Charger 'A' was identified at 13.56 MHz (during the conducted emissions).

The increase of the MT time resulted however longer test times. A *single* sweep with the quasi-peak detector across 30-1000 MHz needed about 8 minutes with MT=10secs, while it would take about 50secs with MT=1sec. On the 1-6 GHz band, a single sweep took almost 15 minutes to complete with MT=5secs using the peak or the average detector.

For these reasons, it is important that the manufacturers supply the EMC test laboratories with the relevant information about the state of operation of the various electrical and electronic modules as these can affect the level of the measured emissions during the product EMC pre-compliance phase. For example, a sub-system, responsible for some radiated emissions within the HPC, could be turned OFF by the power management unit after a period of standby in order to reduce the power consumption. EMC tests should be carried out under worst case operational situations in order not to miss a potential EMI scenario.

8 Exploratory test activities beyond IEC 61851-21-2

8.1 Analysis of exploratory test methodologies

IEC 61851-21-2 standard allows both antenna height scan and all sides of the EUT to be tested for the radiated emissions between 30 MHz to 6 GHz. The measured results presented on this work showed that the chargers emitted significant disturbances under certain setups and conditions. It would make sense then to investigate emissions all around the EUT for the critical frequencies, which exceed or are close to the limit. In addition, exploring the spectrum below the existing 30 MHz low frequency bound set by IEC 61851-21-2 could potentially reveal additional information into the RF disturbances generated by the HPCs.

More specifically, the radiation pattern (azimuth scan) of some chargers was assessed inside V*e*LA 9 by rotating the turntable at a constant angular speed. Such a procedure allows to identify, which angle(s) is/are responsible for the worst case emissions from the EUT and provide as well a better understanding of the EMI causes.

For the plot of the radiation pattern, the EMI receiver was set to monitor a fixed frequency, which corresponded to the critical frequency observed on the frequency domain sweeps. For this measurement, the turntable performed one complete 360 degrees rotation at constant angular speed (1 degree/sec), while the receiver was monitoring the emissions in the time domain. This allowed then to relate the time information of the receiver's raw data with the observation angle of the EUT and plot a two-dimensional pattern of the response that was relating the electric field against the turntable angle. The measurement time was set to 1 second, while the peak, quasi-peak and average detectors were monitoring in parallel the electric field during the rotation of the turntable.

For the assessment of the *radiated* emissions at frequencies *below* 30 MHz, an active monopole antenna was used, Fig. 4, while the EMI receiver was configured to capture frequencies between 150 kHz and 30 MHz. The base of the monopole rod element was fixed on a tripod stand and was placed 10m away from the display side and 1.4m above the SAC floor.

8.2 Radiation Pattern (charger 'A' and 'C')

As an example and in order to demonstrate the generation of a plot of the radiation pattern, the critical frequency at 216 MHz for Charger 'A' was examined when the antenna was in the horizontal polarisation and h=3.0m. The plotted results of the electric field around the EUT at this frequency, both with the use of quasi-peak and peak detectors, are shown in Fig. 53.

Figure 53: Electric field strength around Charger 'A' at 216 MHz (H-pol, h=3m)
[display side faces +25 degrees]

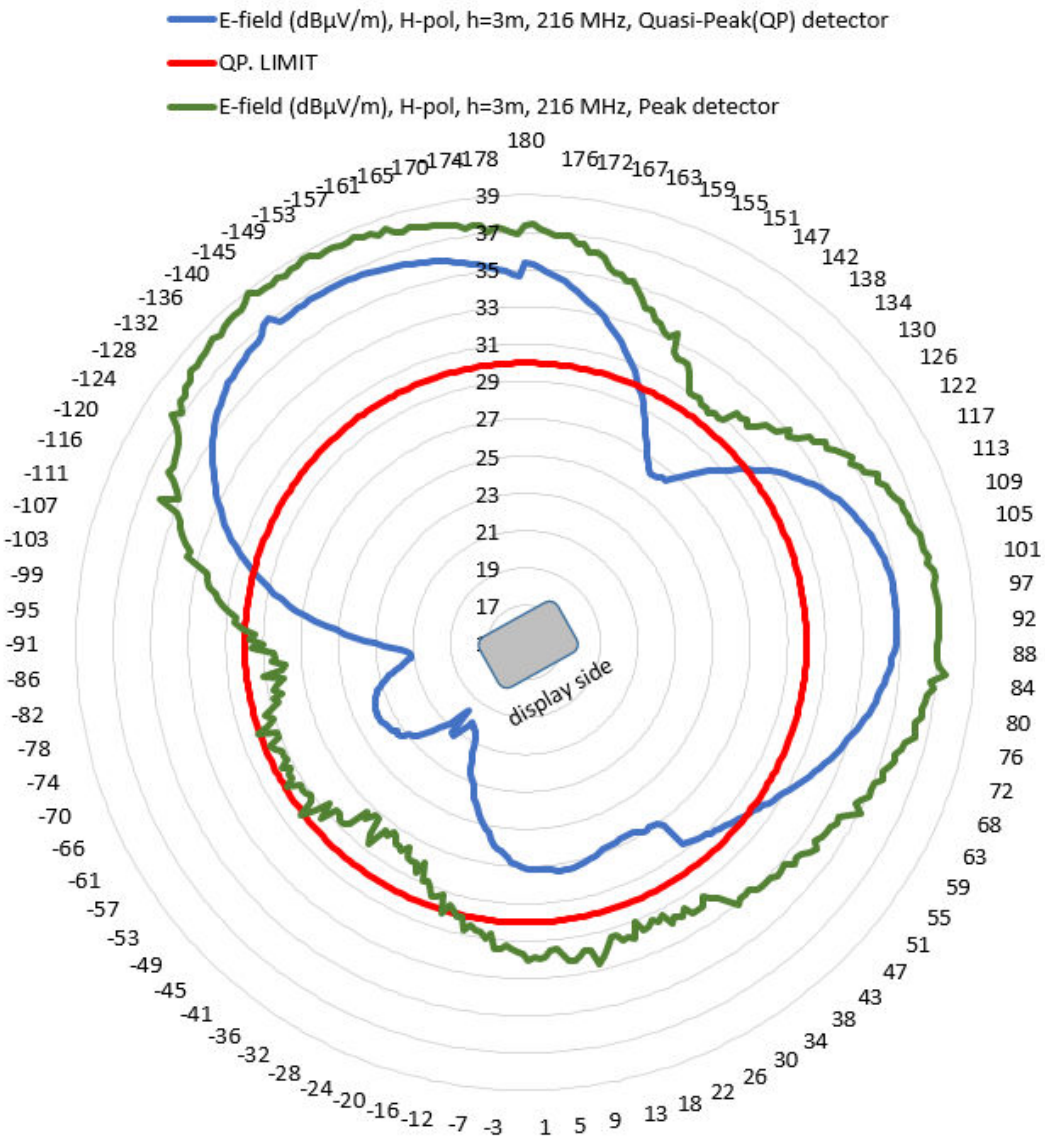

The plot, Fig. 53, shows that the level of the radiated emissions (with the QP detector) exceeded the limit on the rear side (-155 degrees on the figure) and towards the display-right side of the charger. This plot was also crossed verified by the frequency domain measurements of the setup on Fig. 16, (Charger 'A', H-pol, h=3m), as the emissions were indeed strong on the rear, display and right side for the spot frequency at 216 MHz.

An additional information that we extract from Fig. 53 is that the strong emission at around +97 degrees was higher than the values that we received when the emissions were measured either on the display (+25 degrees) or right side (+115 degrees). Such a result indicates that one strong emission could have missed (i.e. falls into a 'blind' spot) should a 360 degrees had not been carried out. In this situation, we observe that the display and the right side were pretty close to the limit, while in between them the emissions exceeded the limit by 5 dB. It could be argued though that four observation angles (left, right, rear, display) are minimising the possibility that such strong emissions could be missed or, if there is one, it should be not very much higher above the worst case values that the 4 angles identify.

Furthermore, the above figure shows that the peak detector identified the actual levels of the electric field strength, which were higher than the quasi-peak [this was expected, but it is plotted on the graph to illustrate this clearly]. However, for frequency measurements below 1 GHz, IEC 61851-21-2 foresees the use of the quasi-peak detector only (although the peak detector is defined for radiated measurements between 1-6 GHz).

In an similar analogy, the radiated emissions around Charger 'C' at 175 MHz and 225 MHz were extracted in the horizontal and vertical polarisation, respectively, for h=3m. The results are depicted in Fig. 54.

Figure 54: Charger 'C' radiation pattern at 175 MHz and 225 MHz (display side faces at -155 degrees)

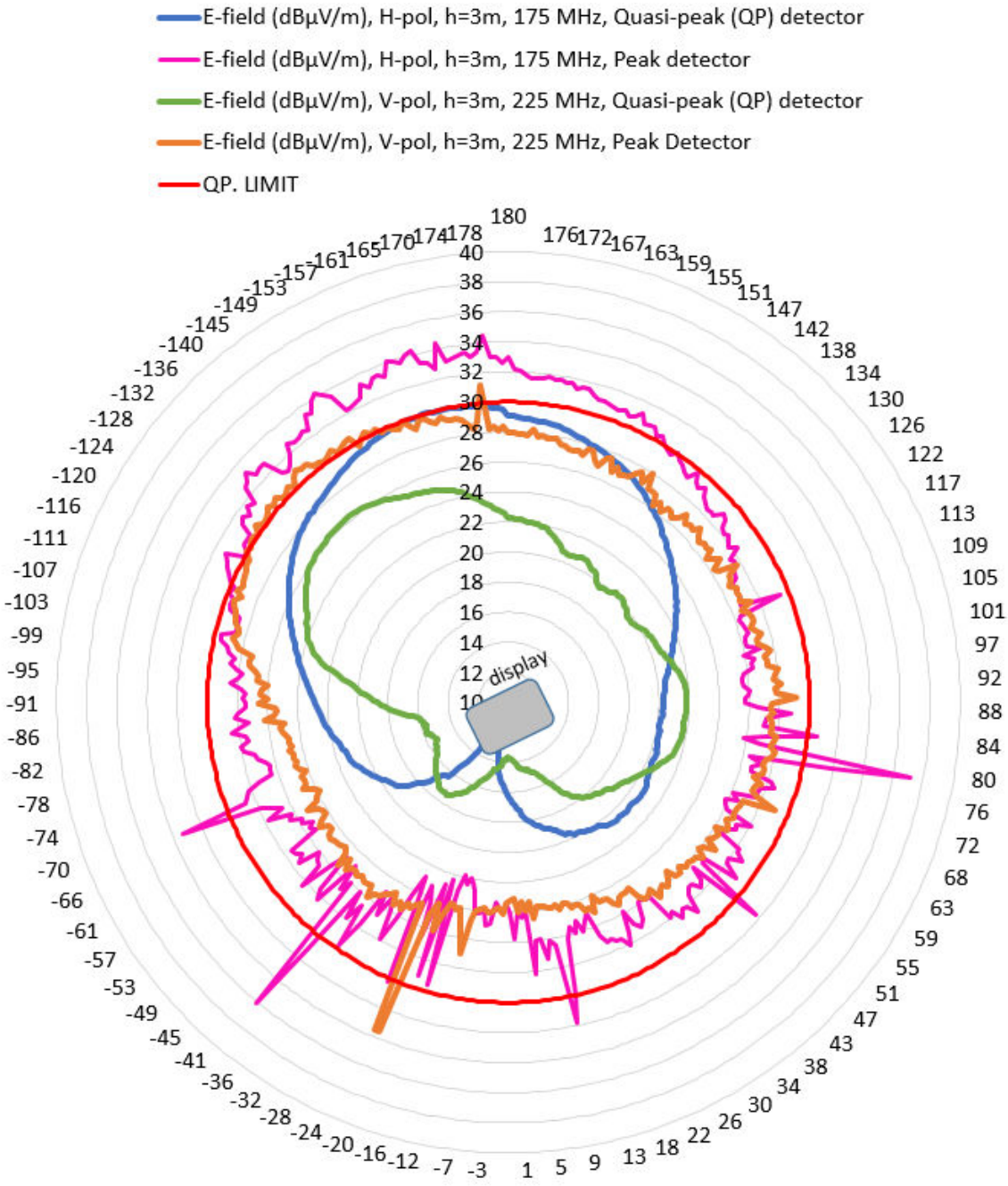

From the plots it was verified that the display side area showed elevated field strength compared to other viewing angles. In addition, it was observed that the field levels captured by the peak detector deviated significantly from these of the quasi-peak detector. For the example, the rear side (+25 degrees) of the HPC column at 225 MHz had a field strength of about 16 dBµV/m with the QP detector, while the peak detector identified it at 24 dBµV/m.

8.3 Radiated emissions 150 kHz – 30 MHz (Charger 'B' and 'C')

For the exploration of the radiated emissions below 30 MHz, Charger 'B' was used as EUT. The internal pre-amplifier of the scanning receiver was set to OFF, while its resolution bandwidth (RBW) was set to 9 kHz. During the receiver sweep, a scan was performed around the HPC (Charger 'B') inside V*e*LA 9 by executing a full 360 degrees

rotation with the turntable. In this way, effectively the frequency plot on the receiver's display captured the maximum level of the emissions around the HPC. Based on this, the results, using quasi-peak and peak detectors are shown in Fig. 55.

Figure 55: Charger 'B' maximum *radiated* emissions from 150kHz-30MHz (monopole antenna) around its enclosure using quasi-peak (Trace 1) and peak detectors (Trace 3) (MT=1sec, RBW=9kHz)

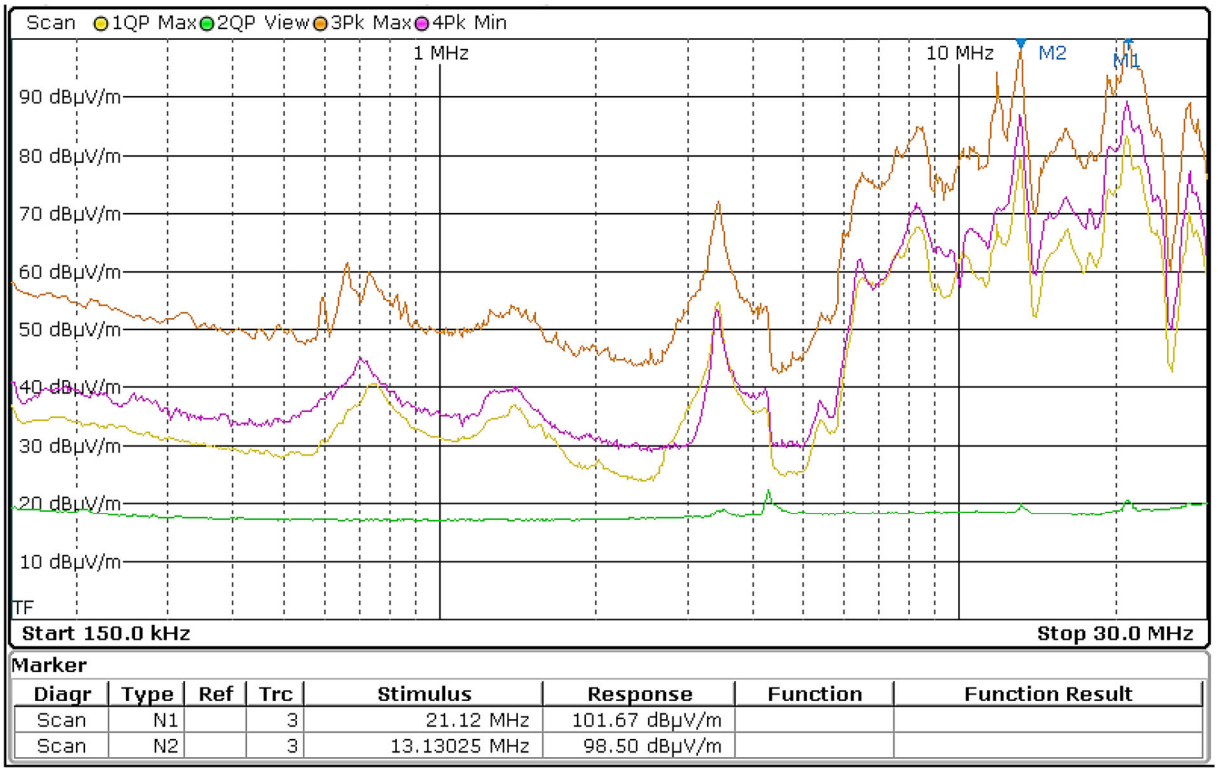

Marker

Diagr	Type	Ref	Trc	Stimulus	Response	Function	Function Result
Scan	N1		3	21.12 MHz	101.67 dBµV/m		
Scan	N2		3	13.13025 MHz	98.50 dBµV/m		

As IEC 61851-21-2 does not require to carry out radiated emission measurements below 30 MHz and so, no limit line could be defined on this plot. Observing the quasi-peak detector response (yellow trace) with respect to its deviation from the noise floor (green trace), it is evident that the HPC generated significant RF noise even below 30 MHz, which extended all the way down to 150 kHz. The highest emission was close to 21.2 MHz and it exceeded 80 dBµV/m, while the next maximum emission was at 13.1 MHz, just below 80 dBµV/m.

The response of the peak detector (orange trace) indicated that the actual emissions were way above the emissions captured with the quasi-peak detector. This gives an additional information into the peak instantaneous emissions that the EUT generated, as the quasi-peak detector provides only an indication of the 'annoyance' factor [2] and is less sensitive to fast transients.

In a similar manner, a radiated emissions test for frequencies below 30 MHz was also carried out for charger 'C' with the measured response shown in Fig. 56.

Figure 56: Charger 'C' maximum radiated emissions from 150kHz-30MHz (monopole antenna) around its enclosure using quasi-peak (Trace 1) and average detectors (Trace) (MT=1sec, RBW=9kHz)

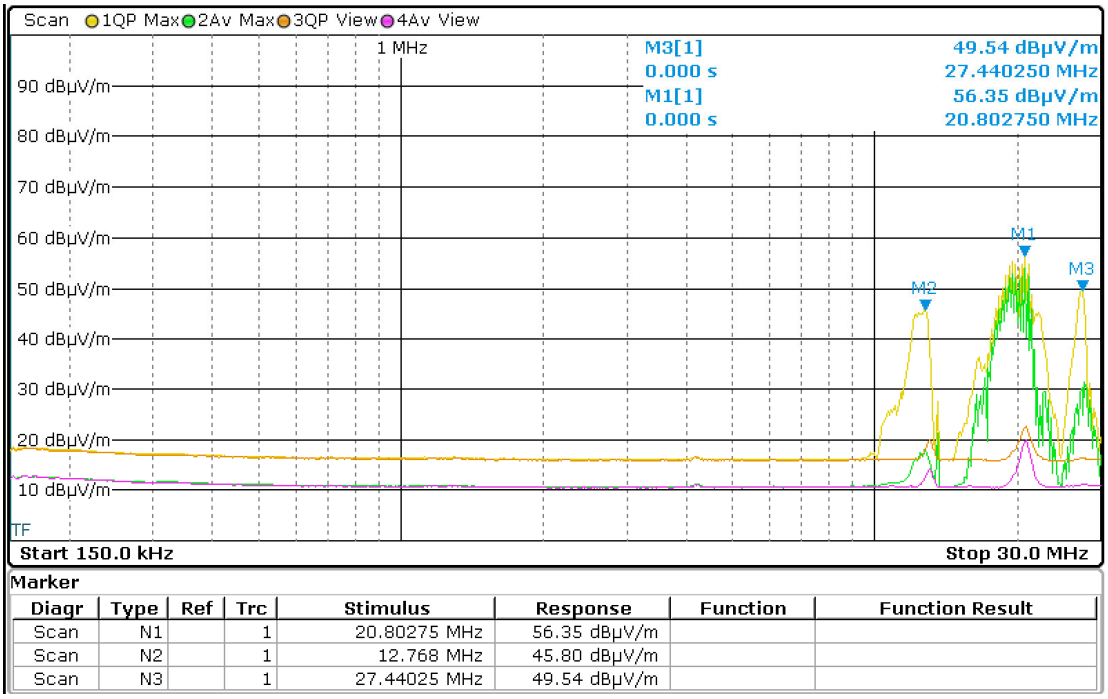

Marker

Diagr	Type	Ref	Trc	Stimulus	Response	Function	Function Result
Scan	N1		1	20.80275 MHz	56.35 dBµV/m		
Scan	N2		1	12.768 MHz	45.80 dBµV/m		
Scan	N3		1	27.44025 MHz	49.54 dBµV/m		

The plots on the above figure showed that Charger 'C' presented radiated disturbances, which were restricted between 10 MHz and 30 MHz. In addition, each of the four sides of Charger 'C' were, as well, assessed for their emissions with the monopole antenna (Fig. 57).

Figure 57: Charger 'C' radiated emissions 150kHz-30MHz (monopole antenna) (a) display, (b) left, (c) rear, (d) right

a.

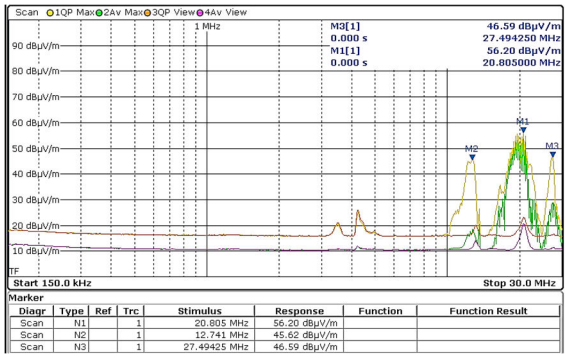

Marker

Diagr	Type	Ref	Trc	Stimulus	Response	Function	Function Result
Scan	N1		1	20.805 MHz	56.20 dBµV/m		
Scan	N2		1	12.741 MHz	45.62 dBµV/m		
Scan	N3		1	27.49425 MHz	46.59 dBµV/m		

b.

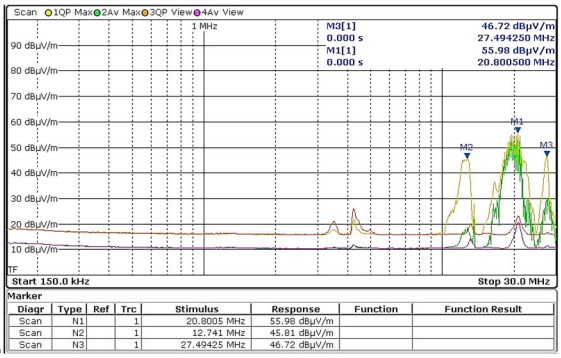

Marker

Diagr	Type	Ref	Trc	Stimulus	Response	Function	Function Result
Scan	N1		1	20.8005 MHz	55.98 dBµV/m		
Scan	N2		1	12.741 MHz	45.81 dBµV/m		
Scan	N3		1	27.49425 MHz	46.72 dBµV/m		

c.

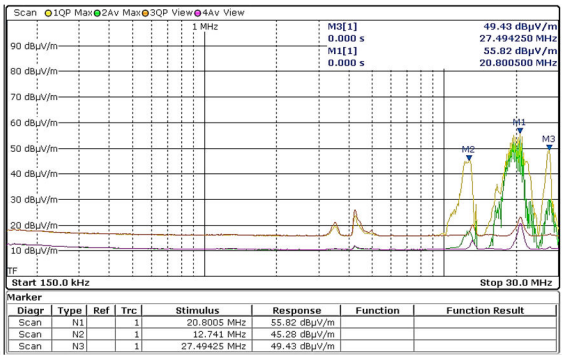

Marker

Diagr	Type	Ref	Trc	Stimulus	Response	Function	Function Result
Scan	N1		1	20.8005 MHz	55.82 dBµV/m		
Scan	N2		1	12.741 MHz	45.28 dBµV/m		
Scan	N3		1	27.49425 MHz	49.43 dBµV/m		

d.

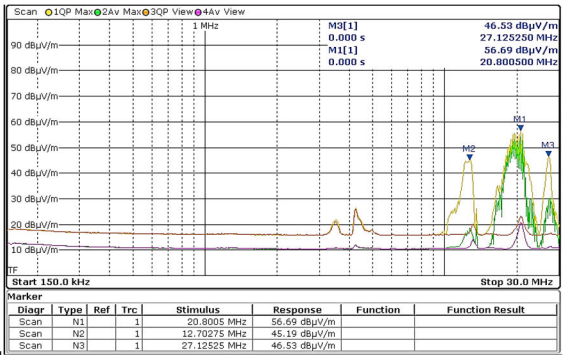

Marker

Diagr	Type	Ref	Trc	Stimulus	Response	Function	Function Result
Scan	N1		1	20.8005 MHz	56.69 dBµV/m		
Scan	N2		1	12.70275 MHz	45.19 dBµV/m		
Scan	N3		1	27.12525 MHz	46.53 dBµV/m		

We observe that the radiated emissions were present in all four sides around the EUT and had a very similar response among them.

8.4 On the conducted emissions of main grid inter-connected HPCs (Charger 'B' and 'C')

The conducted emissions on the AC power line assess the amount of EMI that a load generates towards the grid. This is an important aspect on the EMC design process, as one RF 'noisy' device could cause interference to another device through a common conductive path. For example, a 'noisy' microprocessor module could generate EMI towards the power supply, which in turn could affect the operation of an analogue circuit connected to the same power supply.

On this regard, an exploratory activity on the conducted emissions was setup with chargers 'B' and 'C', in order to explore the effect that one 'noisy' system imposes towards a more 'quiet' system. From the previous measurements on the conducted emissions, we showed that charger 'B' generated excessive EMI, while charger 'C' was less 'noisy' with the exception of some narrowband 'spot' frequencies above the limit. On the new setup, Charger 'B' and Charger 'C' were connected on the *same* AC power supply line and their combined effect on the conducted emissions was measured using LISN ENV 4200, which monitored 3-phases and the neutral line.

More specifically, charger 'B was connected to line-1 and neutral, while charger 'C' was connected to line-1, line-2 and line-3 (Charger 'C' had no neutral connection and it required a 3-phase AC supply). This setup is illustrated on the diagram below (Fig. 58), while Annex 3 shows the laboratory setup of the interconnections.

Figure 58: Electrical connection diagram of Charger 'B' and Charger 'C' on a common AC power line for the measurement of their combined conducted emissions

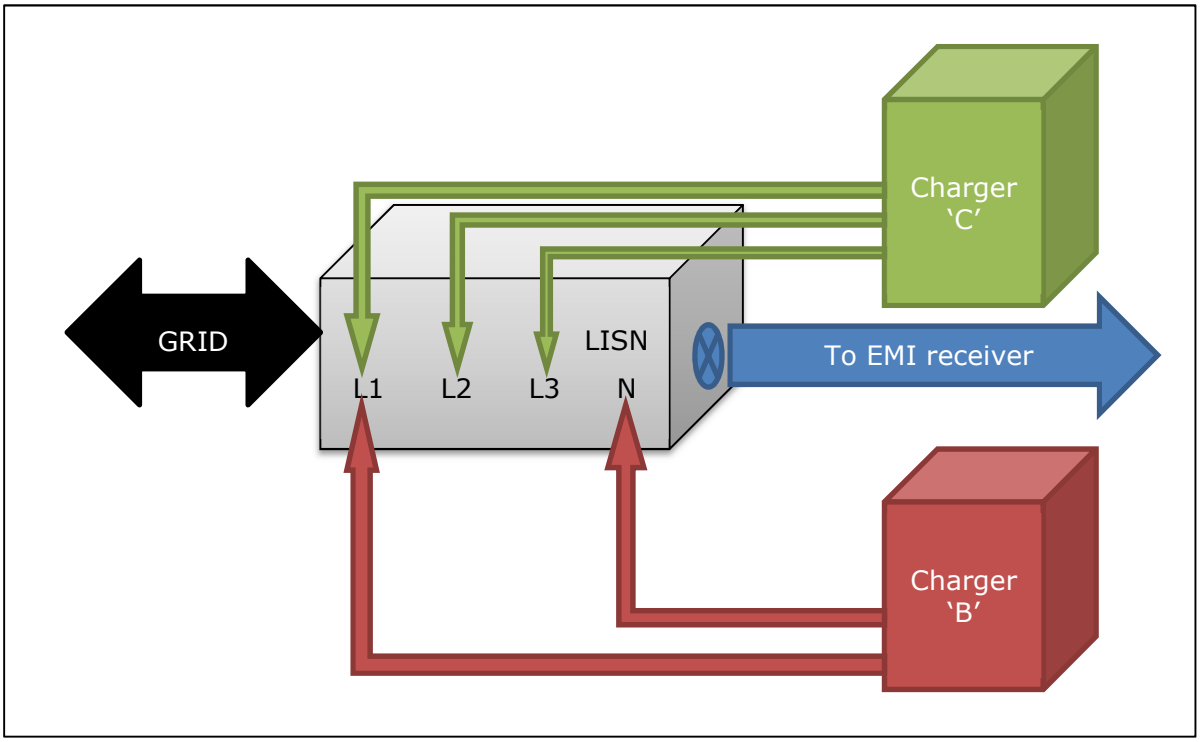

The conducted emissions of the above setup were measured under two situations, when the cooling fan system of Charger 'B' was (i) active and (ii) inactive. The measured results are shown in figures 59 and 60, respectively.

Figure 59: Conducted emissions of Charger 'B' and Charger 'C' connected on the same AC power supply line. On this setup the cooling fan system of Charger 'B' was *active*. (a) Quasi-peak, (b) Average detector results. [Traces: 1. Line-1, 2. Line-2, 3. Line-3, 4. Neutral, 6. Noise floor]

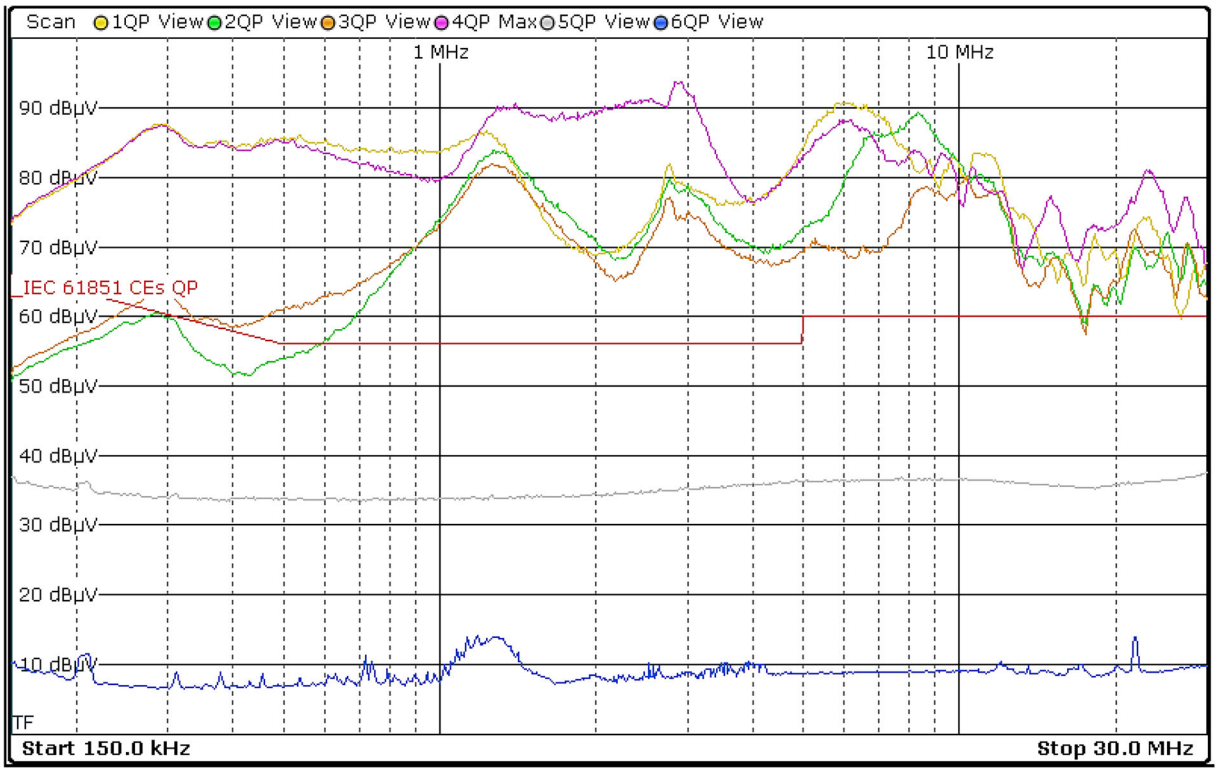

(a)

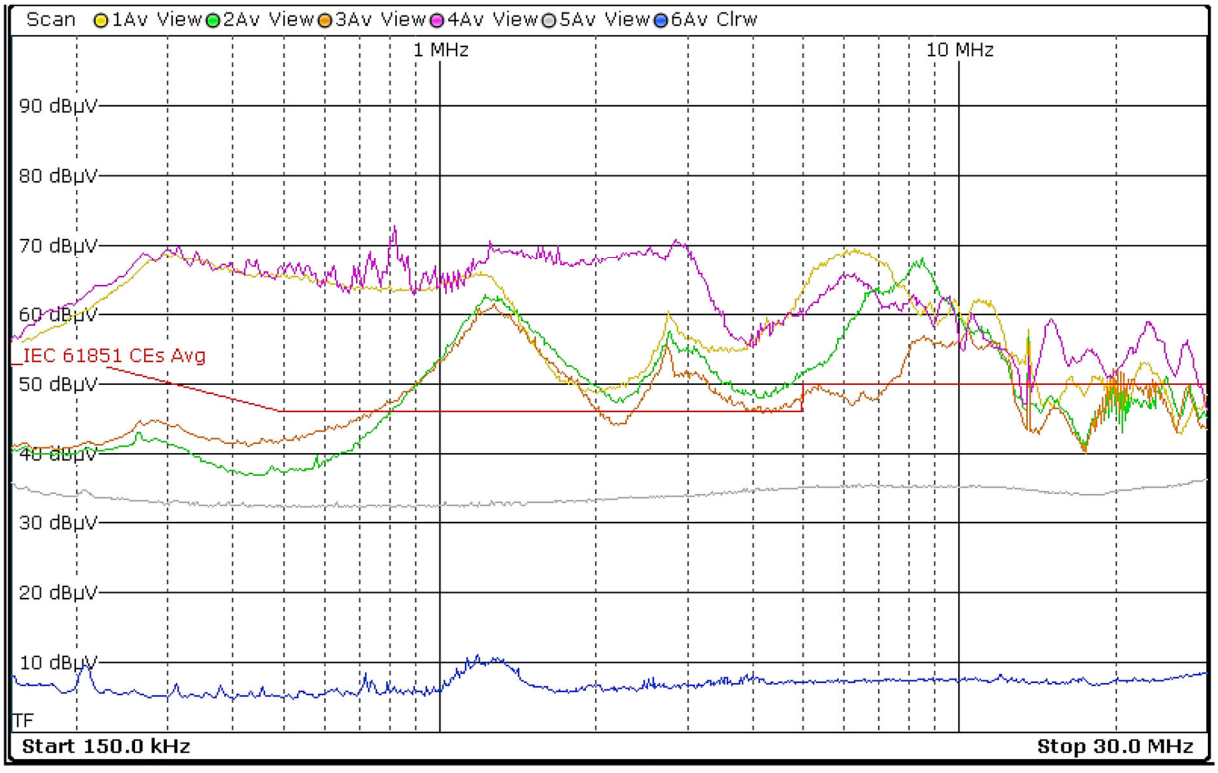

(b)

Figure 60: Conducted emissions of Charger 'B' and Charger 'C' connected on the same AC power supply line. On this setup the cooling fan system of Charger 'B' was *inactive*. (a) Quasi-peak, (b) Average detector results. [Traces: 1. Line-1, 2. Line-2, 3. Line-3, 4. Neutral, 6. Noise floor]

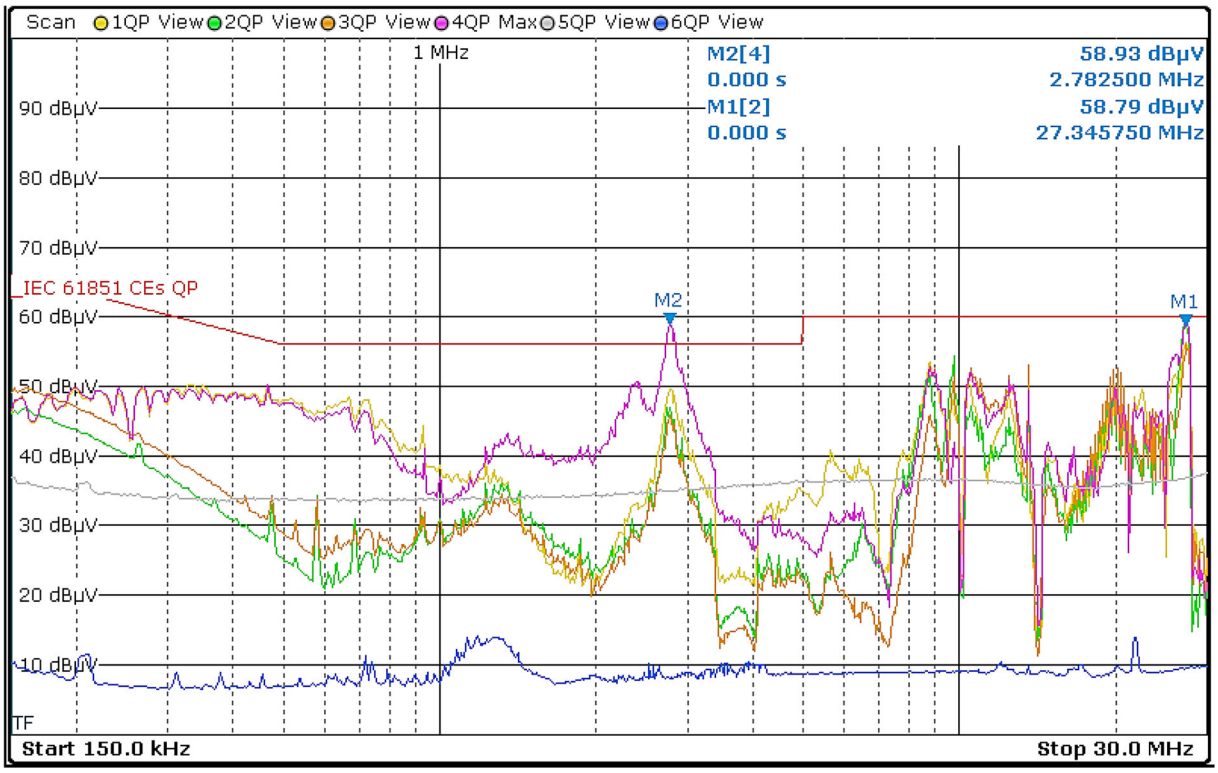

(a)

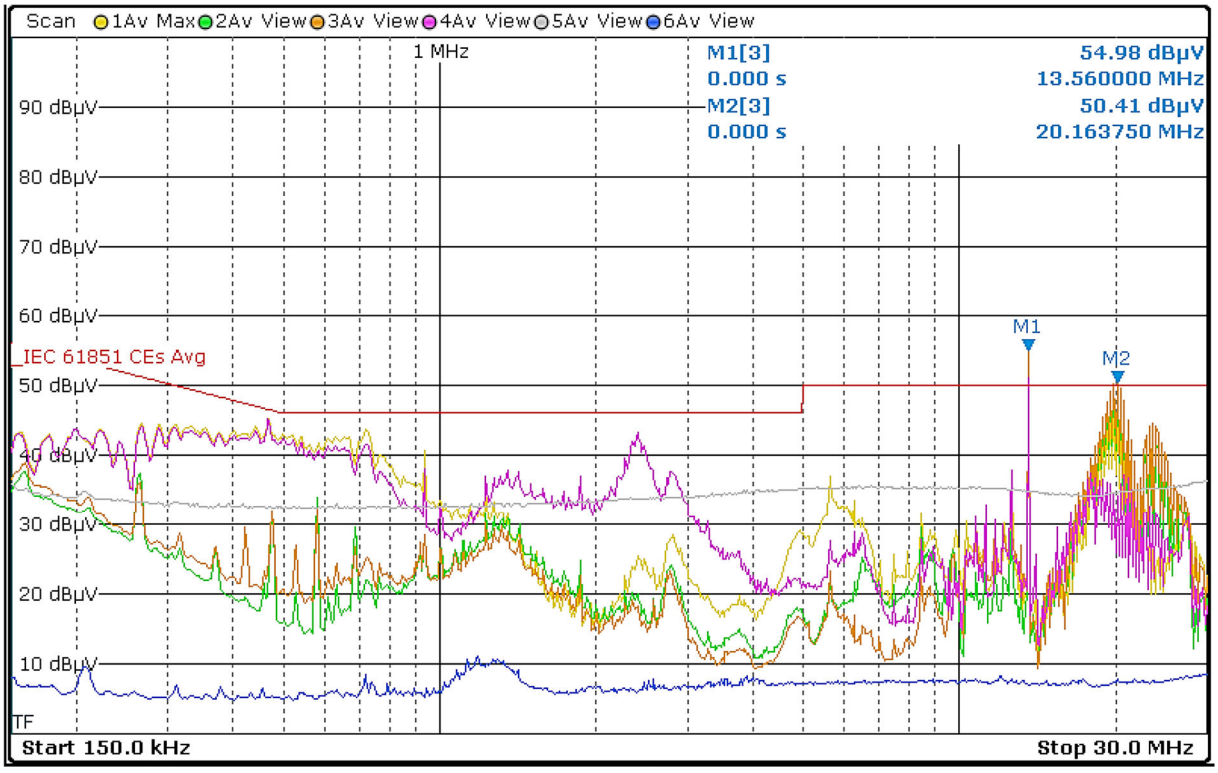

(b)

From the above figures 59 and 60, we extract a number of important findings. Examination on Fig. 59, shows that Charger 'B' generated excessive interference on Line-1 and Neutral (due to the operation of the cooling fan system as investigated before), which was spread all across the measured spectrum. Like before, both type of detectors, QP and average, identified that EMI was well above the limit.

However, there is an additional implication coming out from this result. From the previous measurements, we showed that Charger 'C' possessed a response on the

conducted emissions, which was below the limit with the quasi-peak detector, and with only 2 spot frequencies on line-3 above the limit with the average detector, Fig. 40. What is depicted though now from Fig. 59 is completely different. More specifically, line-2 and line-3 of Charger 'C' were now well above the limit across the band, although line-2 and line-3 were not connected to the 'noisy' Charger 'B'.

Most probably the explanation for this degradation on the EMC performance of Charger 'C' could be justified like this: RF noise from line-1 of Charger 'B' was coupled conductively into line-1 of Charger 'C' (see, figure 58). This RF noise was then spread further down to line-2 and line-3, internally to Charger 'C' and then propagated back to the LISN, which the EMI receiver then captured.

The measured response of the conducted emissions when the cooling fan system of Charger 'B' was isolated, i.e. was inactive, is shown in Fig. 60. On this setup, we observe that the quasi-peak detector, Fig. 60(a), identified only one interfere above the limit at 2.78 MHz, which was present on the *neutral* line coming from Charger 'B'. Furthermore, the average detector, Fig. 60 (b), showed that there were 2 spot critical frequencies at 13.56 MHz and 20.16 MHz on *line-3 (of Charger 'C')*, which were generated by Charger 'C'. We also observe from Fig. 60(b) that the spot frequency at 13.56 MHz from Charger 'C' was coupled also back to the neutral line of Charger 'B', so in effect Charger 'C' affected the line of Charger 'B'.

8.5 Conclusions on the results of the exploratory testing

The exploratory measurement methods presented on this work provide an additional tool during the debugging of EMC issues on the EUT. EMC test laboratories, which have a SAC with turntable can apply a 360 scan around EUT to identify the critical areas around the HPC enclosure, as prescribed for instance in other EMC standards e.g. CISPR 32.

Laboratory assessment of the radiated emissions for frequencies between 150 kHz and 30 MHz showed that the HPCs generated interferences way *below* the 30 MHz lower bound of IEC 61851-21-2. One explanation for these low frequency emissions could be due to the presence of the mains line cables, which were needed to supply the electric power to the HPCs. These can become effective antennas at frequencies where the length of the cable approaches that of a half wavelength, i.e. $\lambda/2$. In addition, the presence of high-speed fast-changing digital signals or pulse type signals that are utilised during the operation of the HPCs, or the switching mode power supplies introduced on modern apparatus, have the potential to generate harmonics, which can attribute to the generation of radiated emissions. Numerous wireless services, e.g. AM broadcast receivers, aeronautical communications, radio astronomy services, amateur and CB radios, military systems and so on, rely for their operation on frequency bands below 30 MHz [13], so it is sensible to consider this type of interference scenario.

We also briefly demonstrated that the use of the peak detector, next to the quasi-peak detector provided an additional tool for the identification of the actual level of the emissions.

Finally, results of the conducted emissions when Charger 'B' and 'C' were connected on the same AC power supply line were presented. On this setup, it was found that a RF noisy system 'pollutes' a 'quiet' system through the common wire connections.

9 Conclusions and suggestions for future work

The EMC profile of three different prototype HPCs columns was evaluated and analysed on V*e*LA 9 SAC of the Joint Research Centre of the European Commission, based on IEC 61851-21-2 standard. Analytical test results for radiated emissions, conducted emissions and radiated immunity were presented and discussed.

On the radiated emissions, it was identified that the display side was the major contributor to the EMI levels with respect to the other sides. However, the presence of the external cabling, including the HV DC-charging cable and the mains power line cable were found to influence the levels of the radiated emissions too.

Both broadband and narrowband type interference was generated by the HPCs, as it was observed on some results. The use of the peak detector identified disturbances, which otherwise the 'slower' quasi-peak detector could not capture. This implies that it would be sensible to 'harmonise' the type of detectors defined on the test protocol of the radiated emissions on IEC 61851-21-2 between the 30-1000 MHz and the 1-6 GHz bands.

One out of three columns presented significant EMI from 150 kHz up to about 2.5 GHz, which was well above Class A and Class B limits both on the conducted and radiated emissions. For this 'critical' column, EMC troubleshooting was successfully applied and it was discovered that the strong EM emissions were caused by the HPC's cooling fan (ventilation) system. The other two chargers, which also exceeded the limits on some setups, presented predominately narrowband type disturbances at a few spot frequencies.

We showed that with basic EMC troubleshooting practices it was possible to successfully reduce the level of narrowband conducted emissions using the appropriate type of ferrite material. On this aspect, the out-of-limit conducted emissions for one charger were supressed below the limit by inserting ferrite filters on the main line wires.

On the aspect of the immunity testing, it was identified that some HPCs had susceptibility issues at frequencies close to the 800 MHz region. This finding is important to consider, because there are wireless devices and services, e.g. carrier frequencies of mobile service operators and handsets alike that operate on bands close to these critical frequencies. This situation could pose a risk, under certain conditions, to the normal operation of the HPCs should e.g. an active handset unit is brought close to the HPC enclosure.

We also carried out novel exploratory measurement methods, which showed that *radiated* emissions appear *below* the current 30 MHz lower bound of the existing IEC 61851-21-2 standard. Such a situation could introduce the potential situation that HPCs interfere with other wireless services that utilise these lower frequencies. It is suggested that the results on this report around this aspect are considered on the future versions or updates of the IEC 61851-21-2 standard.

In addition, 360 degree (azimuth) scans around the HPC identified peak emissions, which could be missed if only the four sides of the EUT were considered. Nevertheless, such higher emissions should not deviate significantly with respect to the EMI levels that the 4-sides assessment of the EUT can identify.

Exploratory work was also carried out on the conducted emissions, when two HPCs were connected on the *same* AC mains grid. The results of the measurements showed that a well EMC designed system was affected by another system generating significant EMI. What was also found was that a single phase HPC, which generated EMI on the wires of the AC supply affected all 3-phases of a 'quiet' system connected to the same mains grid. This was an important finding, as it verified that conducted emissions have the potential to spread across the grid network and affect several other interconnected devices and systems.

A complete HPC system consists of AC to DC rectifiers and high-power control modules, which rely on fast changing switching signals and pulse width modulations for the control of the internal electronic modules. Some HPC systems require, as well, the use high-power step-up AC to AC transformers and so on. All these components introduce additional constrains and challenges on the EMC design phase. For this reason, having a

HPC column free from any EMI at the very start of the prototyping process simplifies the EMC procedure when the complete HPC system is considered for testing at a later stage.

It is very important that the manufacturers apply proper and methodological EMC practices into the early phase of the product design in order to minimise EMC pre-compliance issues and accelerate the penetration time to the market. At a more general implementation level, electric vehicle technology and systems are in strong need to have a reliable and safe charging infrastructure in place. EMC constitutes a key parameter for this success, as it ensures that the risk of dysfunctions, error states and interoperability problems, caused by EMI, are minimised. In addition, management and control of the EM emissions from the HPCs reduces the exposure of the population to high frequency radiation, a concern which is increasingly discussed in the literature.

Manufacturers can assist the EMC testing laboratories to follow the right troubleshooting procedures by providing basic technical documentation of the internal functionalities of their products (whenever possible). For example, a radiated interference at 175 MHz could be related to a digital signal utilised by the display circuitry, while a conducted noise at 13.56 MHz could be related to the operation of an resonator/oscillator component for the synchronisation of a digital microprocessor. Knowledge of such facts can quickly assist the identification of a problematic EMI source and apply correction methods (e.g. shutting down the power supply of the main display could give a clue as to whether it is responsible for the EMI levels that the column generates).

The results of the laboratory measurements and the findings presented on this report can become a source of reference information to the EMC pre-compliance test services and assist the manufacturers and the involved parties to the further development of the HPC technology. In addition, this material can contribute, as well, to the future policy-making of IEC 61851-21-2 standard applicable to electric vehicle charging systems.

Future activities on VeLA 9 will extend towards the EMC aspect of the HPC systems (50kW upwards) under charging conditions, when both the entire charging system, i.e. HPC column and the rectifiers are placed next to an electric vehicle for charging, as it happens in real situations. The current version of IEC 61851-21-2 standard considers EMC pre-compliance test methods for either the charging system or the vehicle alone, but not their combined setup.

The results from this exploratory study showed that the application of EMC to a product is a challenging process. At the same time, the implications, from the EMI point of view, to the environment and to the systems from the mass-release and large-scale deployment of high power chargers for electric vehicles on the market are still unknown. This indicates that it is more than necessary to research further the EMC aspect of the HPC systems and their corresponding infrastructure.

References

[1] Henry Ott, "Electromagnetic Compatibility Engineering", Wiley Publishing, 2009

[2] Mark I. Montorose, Edward M. Nakauchi "Testing for EMC Compliance: Approached and Techniques", IEEE 2004

[3] Xue Wenyan, Chen Xiao, Ma Xikui, "Analysis and reduction of conducted EMI from an AC/DC high power converter", 2005 IEEE International Symposium on Microwave, Antenna, Propagation and EMC Technologies for Wireless Communications

[4] Qing Chen, "Electromagnetic interference (EMI) design considerations for a high power AC/DC converter", PESC 98 Record. 29th Annual IEEE Power Electronics Specialists Conference, 22-22 May 1998

[5] E.T. Arntzen, R.F. Kubichek, J.W. Pierre, S. Ula, "Initial findings in electromagnetic emissions above 30 MHz from power inverters and variable speed motor controllers", IEEE 1997, EMC, Austin Style. IEEE 1997 International Symposium on Electromagnetic Compatibility.

[6] Surajit Midya, Rajeev Thottappillil, "An overview of electromagnetic compatibility challenges in European Rail Traffic Management System", ELSEVIER, Transportation Research Part C: Emerging Technologies, Volume 16, Issue 5, October 2008, Pages 515-534

[7] Williams T. "EMC for Product Designers", 4th edition, Newnes, 2007

[8] Christos Christopoulos "Principles and Techniques of Electromagnetic Compatibility", 2nd edition, CRC Press, 2007

[9] IEC 61851-21-2 Ed. 1.0: Electric vehicle charging system – Part 21-2: EMC requirements for OFF board electric vehicle charging systems

[10] CISPR 16-1-4:2010 + AMD1:2012 + AMD2:2017 CSV Consolidated version, Specification for radio disturbance and immunity measuring apparatus and methods - Part 1-4: Radio disturbance and immunity measuring apparatus - Antennas and test sites for radiated disturbance measurements

[11] SCHWARZBECK MESS – ELEKTRONIK, VULB 9162 Generating Defined Field-strength datasheet, available online at (last accessed Nov.2018): http://www.schwarzbeck.de/en/antennas/hybrid-antenna/375-vulb-9162-trilog-broadband-antenna.html

[12] Rohde and Schwarz, ESR EMI Test Receiver User Manual, 2017 (#1171.0000.42 – 09), available from: www.rohde-schwarz.com

[13] Electronic Communications Committee (ECC) within the European Conference of Postal and Telecommunications Administrations (CEPT), THE EUROPEAN TABLE OF FREQUENCY ALLOCATIONS AND APPLICATIONS IN THE FREQUENCY RANGE 8.3 kHz to 3000 GHz (ECA TABLE), Approved October 2018

[14] GSM frequency bands, wikipedia internet source: https://en.wikipedia.org/wiki/GSM_frequency_bands#cite_note-t-gsm-1 (last accessed: Nov. 2018)

[15] Fair-Rite Product Corps (2014), 31 SPLIT ROUND CABLE ASSEMBLY, Part Number: 0431177081,

[16] IEC 61000-4-3, Electromagnetic compatibility (EMC) – Part 4-3: Testing and measurement techniques – Radiated, radio-frequency, electromagnetic field immunity test

List of abbreviations and definitions

AC	Alternative Current
BB	Broadband (emissions)
CW	Continuous Wave
DC	Direct Current
EM	Electromagnetic
EMI	Electromagnetic Interference
EUT	Equipment Under Test
HPC	High Power Charger (for vehicles)
JRC	Joint Research Centre of the European Commission
MT	Measurement Time
NB	Narrowband (emissions)
QP	Quasi-peak (detector)
RBW	Resolution bandwidth
RF	Radio Frequency
SAC	Semi Anechoic Chamber
V*e*LA	Vehicle Electric Laboratory

List of figures

List of tables

Annexes

Annex 1. Laboratory setup of High-Power-Chargers inside the VeLA9 EMC SAC

Figure 61: Charger 'A' (a) radiated emissions and (b) radiated immunity setup

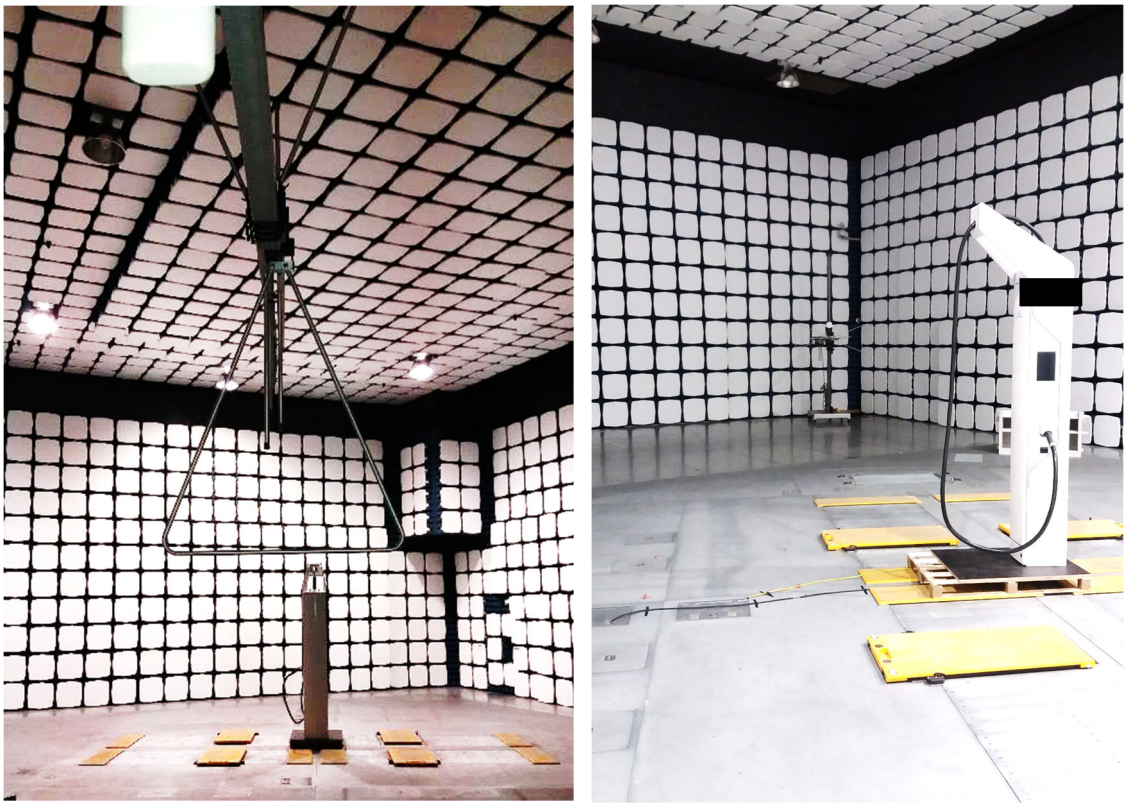

(a)

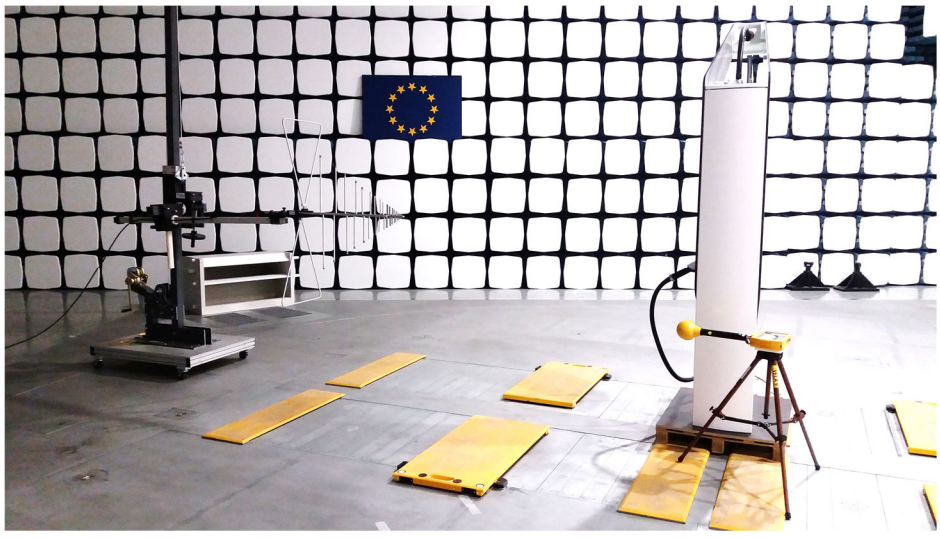

(b)

Figure 62: Charger 'B' (a) radiated emissions, (b) conducted emissions and (c) radiated immunity setup

(a)

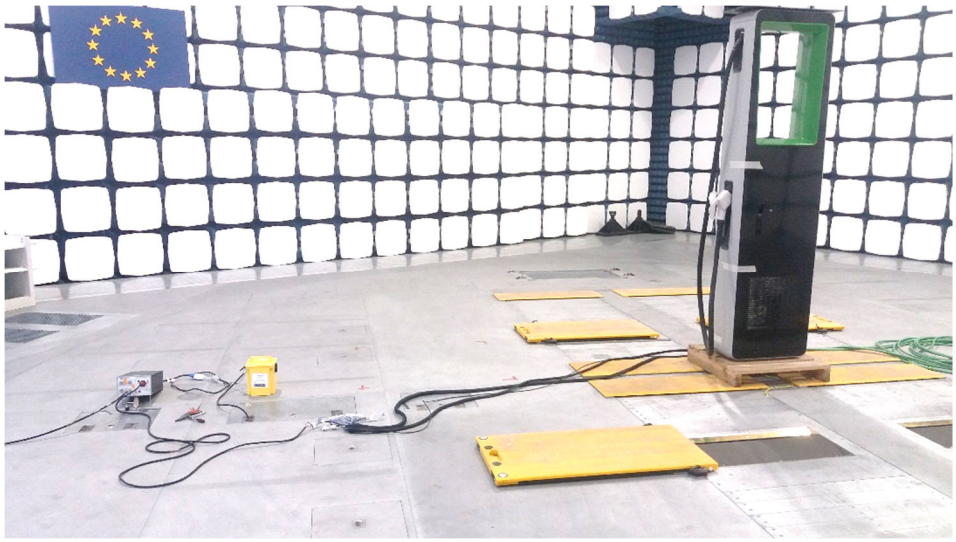

(b)

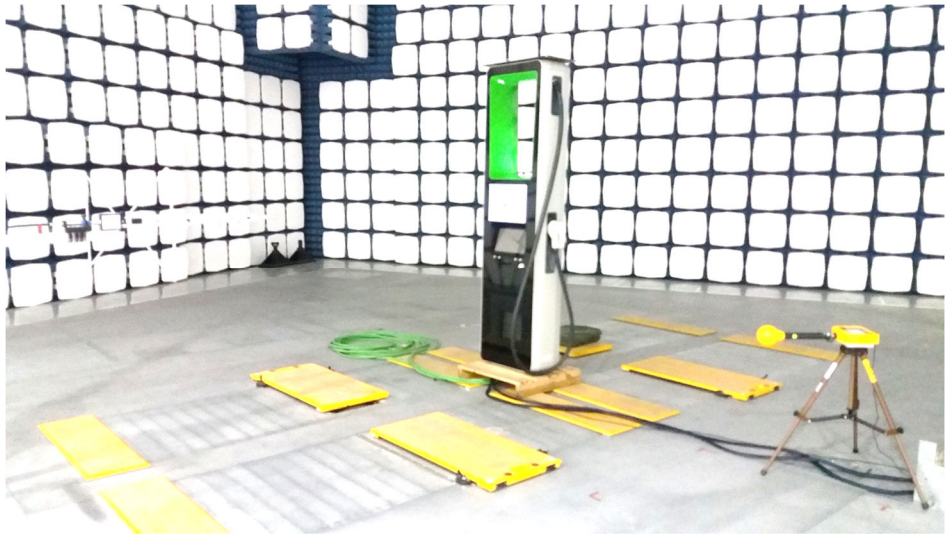

(c)

Figure 63: Charger 'C' (a) radiated emissions, (b) conducted emissions and (c) radiated immunity setup

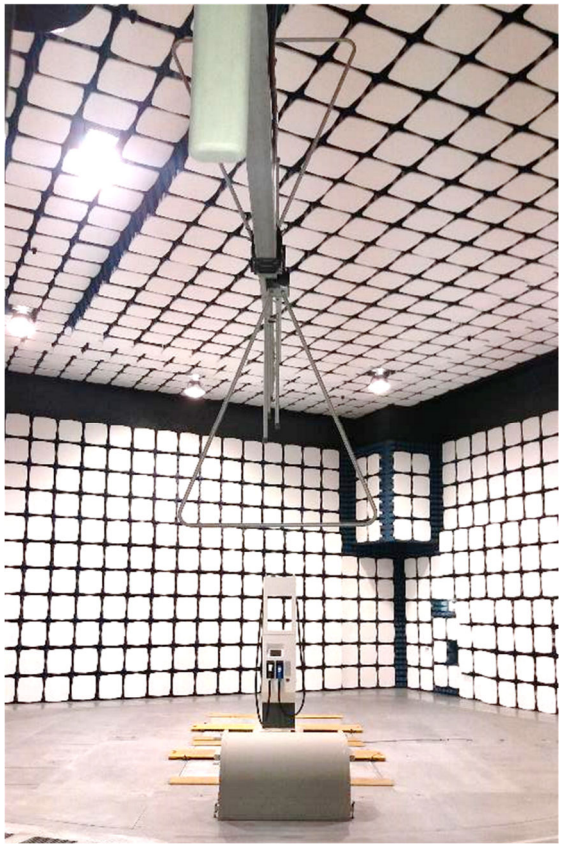

(a)

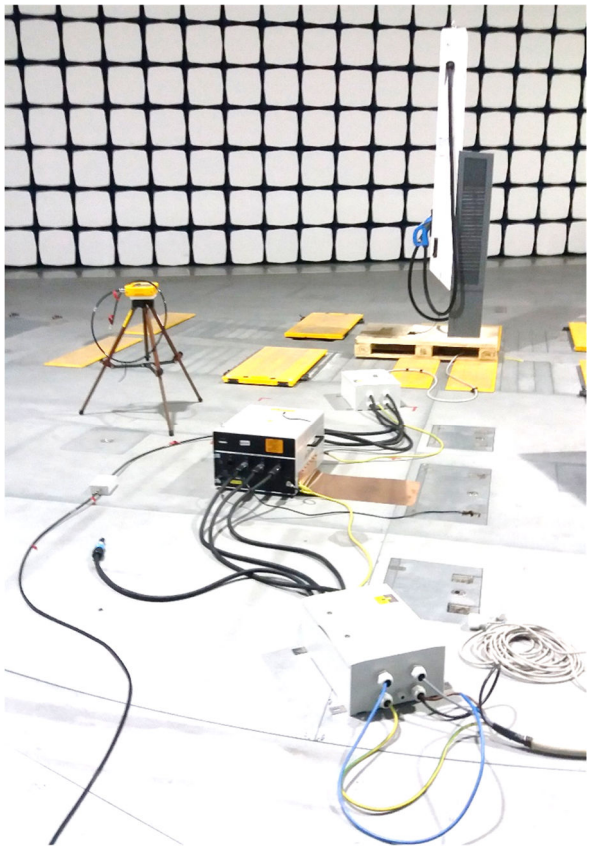

(b)

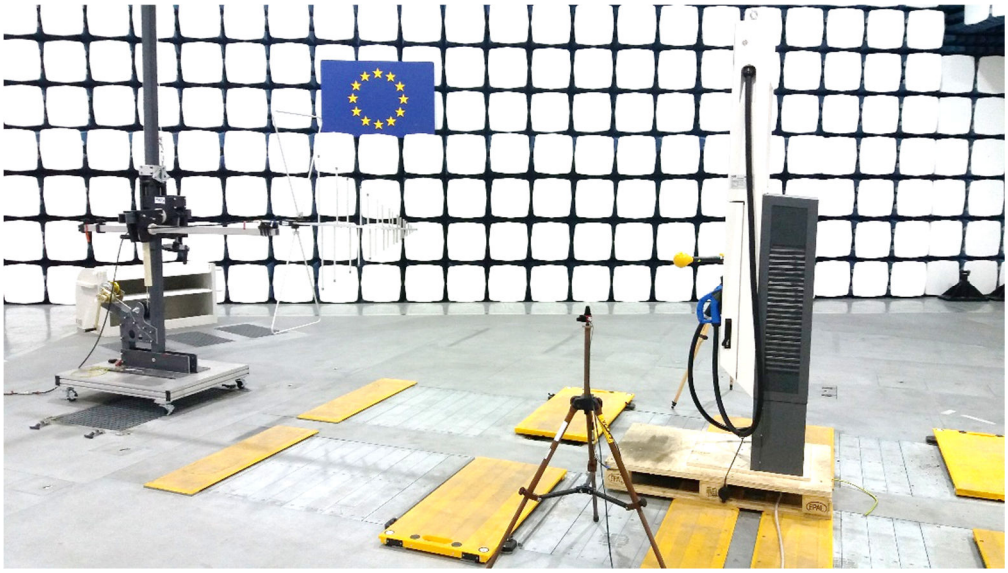

(c)

Annex 2: Screenshot of the field-strength computer application used with ETS-Lindgren field sensors during the immunity testing and field-probe on tripod used for immunity testing.

Figure 64: Monitoring of the field-sensor reading during the radiated immunity testing (Probe Z-axis=vertical polarisation)

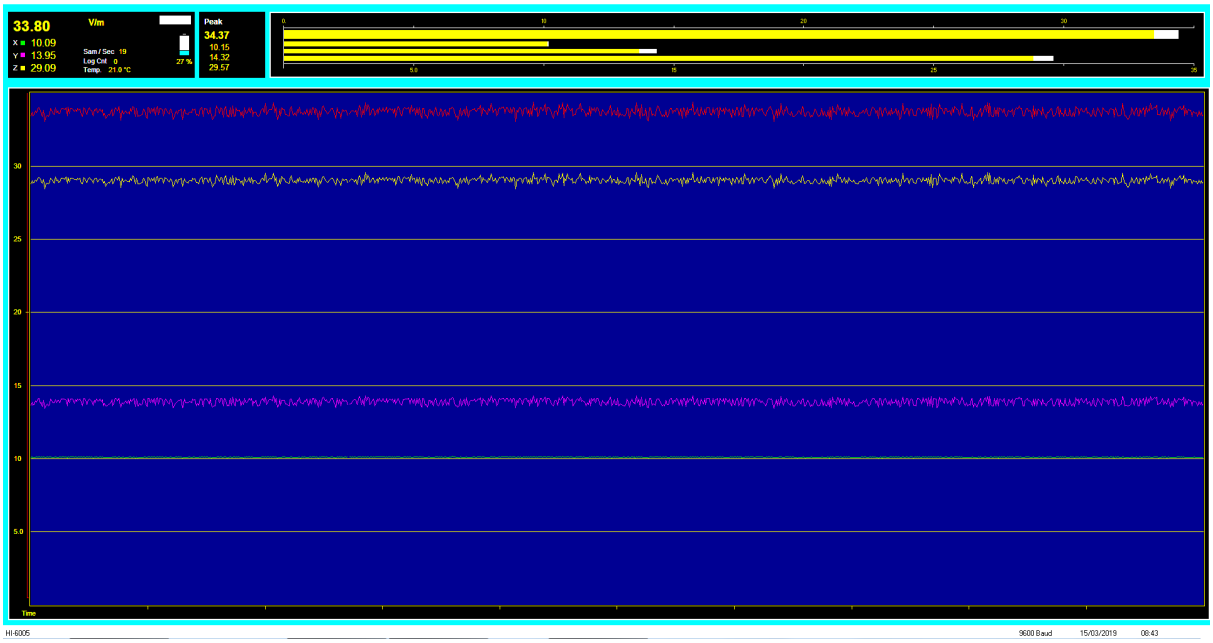

Figure 65: Field-sensor on tripod mast

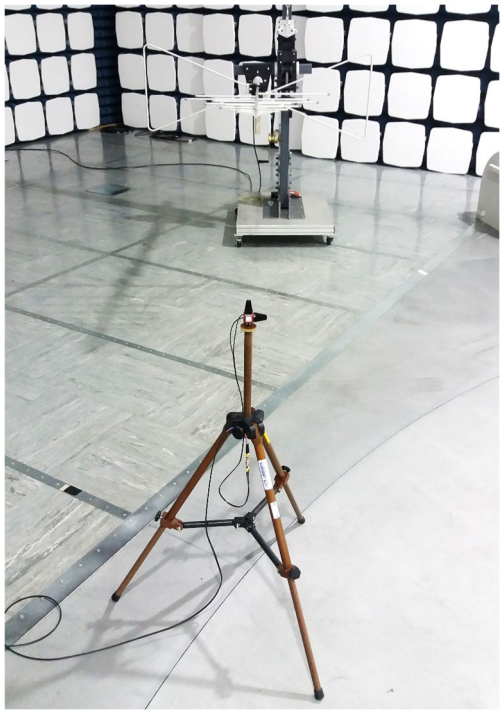

Annex 3: Laboratory setup for the conducted emissions of Chargers ‘B’ and ‘C’

Figure 66: Laboratory setup for the measurement of the conducted emissions, when Charger 'B' and Charger 'C' were connected to the same AC power line

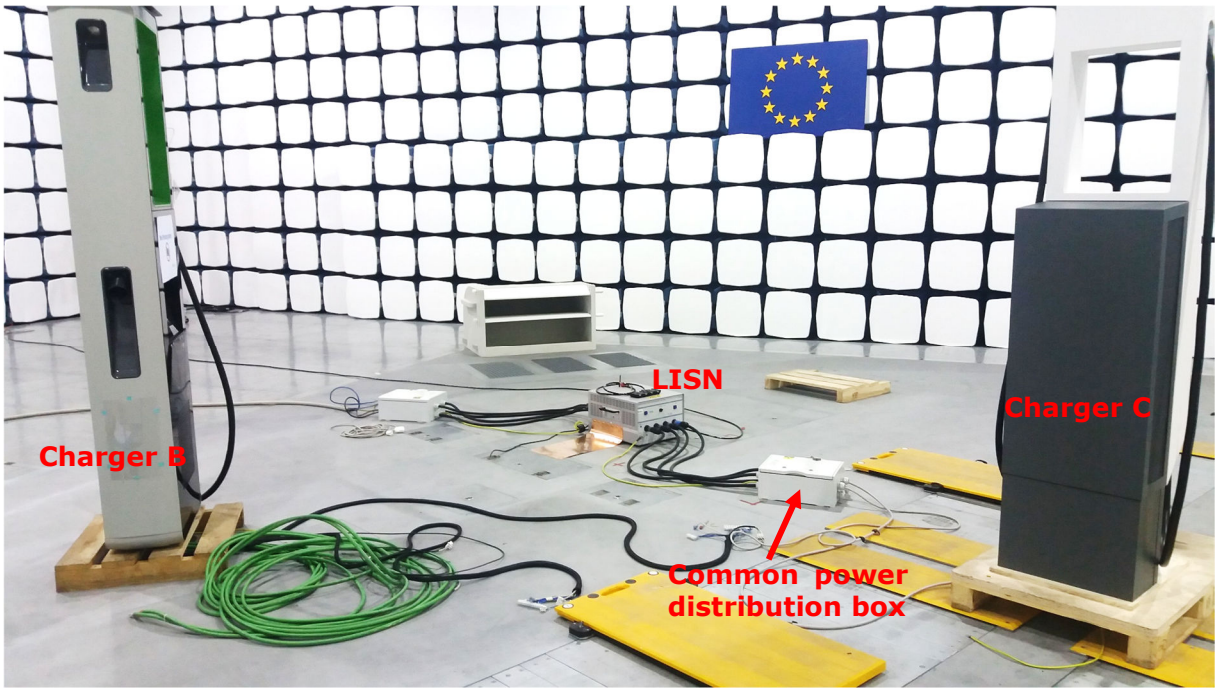

GETTING IN TOUCH WITH THE EU

In person

All over the European Union there are hundreds of Europe Direct information centres. You can find the address of the centre nearest you at: https://europa.eu/european-union/contact_en

On the phone or by email

Europe Direct is a service that answers your questions about the European Union. You can contact this service:

- by freephone: 00 800 6 7 8 9 10 11 (certain operators may charge for these calls),

- at the following standard number: +32 22999696, or

- by electronic mail via: https://europa.eu/european-union/contact_en

FINDING INFORMATION ABOUT THE EU

Online

Information about the European Union in all the official languages of the EU is available on the Europa website at: https://europa.eu/european-union/index_en

EU publications
You can download or order free and priced EU publications from EU Bookshop at: https://publications.europa.eu/en/publications. Multiple copies of free publications may be obtained by contacting Europe Direct or your local information centre (see https://europa.eu/european-union/contact_en).

KJ-NA-29704-EN-N

The European Commission's science and knowledge service

Joint Research Centre

JRC Mission

As the science and knowledge service of the European Commission, the Joint Research Centre's mission is to support EU policies with independent evidence throughout the whole policy cycle.

EU Science Hub

ec.europa.eu/jrc

@EU_ScienceHub

EU Science Hub - Joint Research Centre

Joint Research Centre

EU Science Hub

Publications Office

doi:10.2760/08750

ISBN 978-92-76-01440-9